Analysis of Harmonic Distortion in an Integrated Power System for Naval Applications
by
Edward G. West
B.S.E., Electrical Engineering
The Citadel, 1999

Submitted to the Department of Ocean Engineering and the Department of Electrical Engineering and Computer Science in Partial Fulfillment of the Requirements for the Degrees of

Naval Engineer

and

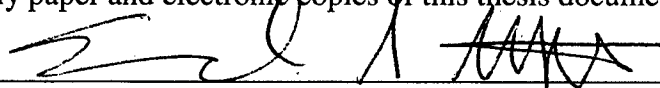Master of Science in Electrical Engineering and Computer Science

at the
Massachusetts Institute of Technology

June 2005
© 2005 Edward G. West. All rights reserved.

The author hereby grants to MIT and the United States Government permission to reproduce and to distribute publicly paper and electronic copies of this thesis document in whole or in part.
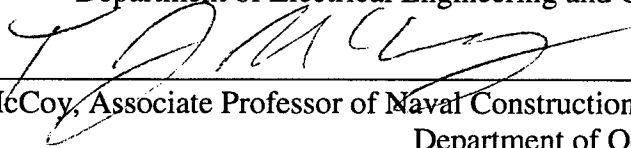
Signature of Author_____
Department of Ocean Engineering and the
Department of Electrical Engineering and Computer Science
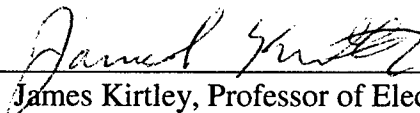May 12, 2005

Certified by _____
Timothy J. McCoy, Associate Professor of Naval Construction and Engineering
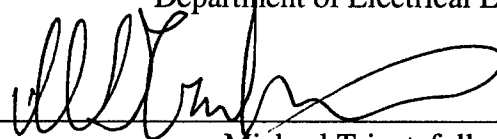Department of Ocean Engineering
Thesis Supervisor

Certified by _____
James Kirtley, Professor of Electrical Engineering and Computer Science
Department of Electrical Engineering and Computer Science
Thesis Reader

Accepted by _____
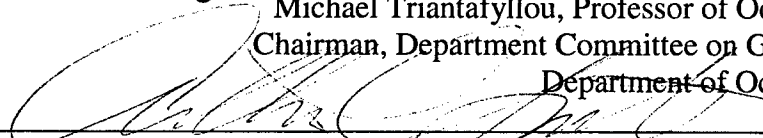Michael Triantafyllou, Professor of Ocean Engineering
Chairman, Department Committee on Graduate Students
Department of Ocean Engineering

Accepted by _____
Arthur C. Smith, Professor of Electrical Engineering and Computer Science
Chairman, Department Committee on Graduate Students
Department of Electrical Engineering and Computer Science

20060516058

Page Intentionally Left Blank

Analysis of Harmonic Distortion in an Integrated Power System for Naval Applications
by
Edward G. West

Submitted to the Department of Ocean Engineering and the Department of Electrical Engineering and Computer Science in Partial Fulfillment of the Requirements for the Degrees of

Naval Engineer

and

Master of Science in Electrical Engineering and Computer Science

ABSTRACT

This research quantifies the voltage distortion over the broad range of operating conditions experienced by a Naval warship. A steady state model of an Integrated Power System (IPS) was developed in a commercially available power system simulation tool. The system chosen for this study was a three-phase, 4160 VAC, 80 MW power system with a 450 VAC bus to supply traditional ship service loads. Sensitive loads, such as combat systems equipment, are isolated from the harmonic content of the 450 volt bus via solid state inverters. Power generation for this system included two 30 MW and two 10 MW generators. The sizing of these generators was based on operating configurations that would result in the best fuel efficiency under the most common loading conditions. Model components were simulated and compared to data recorded for the U.S. Navy's Full Scale Advanced Development (FSAD) test system for the IPS at the Philadelphia Land Based Engineering Site (LBES). The propulsion motor used in the simulations was developed based on the advanced induction motor installed at LBES. Various loading conditions, including battle, cruise and anchor were simulated for both 10°F and 90°F ambient design conditions and with propulsion loads ranging from 0% to 100%. Numerous system configuration changes were implemented to determine their impact on system harmonics. These included operating the propulsion converter front end rectifiers in both controlled (varying commutation angle) and uncontrolled (diode bridge) configurations; implementation of both twelve and six pulse rectification; and installation of a tuned passive 5th harmonic filter. The simulation results are compared to both IEEE Std 519-1992 and Mil-Std 1399.

Thesis Supervisor: Timothy McCoy
Title: Associate Professor of Ocean Engineering

Thesis Reader: James Kirtley
Title: Professor of Electrical Engineering and Computer Science

Page Intentionally Left Blank

Table of Contents

List of Figures

List of Tables

This page intentionally left blank.

Chapter 1 Introduction

1.1 Purpose

The purpose of this thesis is to develop accurate models of power electronic devices that will be installed on future naval warships. These models will be used to analyze the harmonic distortion on the main electrical busses under a variety of operating conditions. The impact of harmonic mitigation techniques on an Integrated Propulsion System will also be analyzed.

1.2 Problem

The Navy envisions a significantly greater role of electrically powered systems in future naval warships. This is represented by the commitment to an Integrated Power System (IPS) for the next generation warship.[1] A ship configured with IPS uses an electrical motor to drive the speed of the propeller, eliminating the need for a reduction gear and long shaft. A common electrical bus provides the ships electrical power and propulsion power. A traditional non-IPS surface combatant dedicates over two thirds of its power generation capability to turning its propellers. This generation capacity is not available for anything other than propulsion and is typically represented by four prime movers. Additional prime movers are required for generation of electricity for ship loads. Some of the advantages of an IPS arrangement are listed below.[2]

- Increased fuel economy due to the efficient operation of prime mover
- Arrangement flexibility due to the elimination of large mechanical shaft components and the reduction of total prime movers
- Availability of a large amount of electrical power for non-propulsion use
- Ability to accommodate the electrical power needs of future military systems
- Reduced manning requirements due to high levels of automation and control

The successful implementation of IPS is only possible due to advances in high voltage, high power semiconductor switching devices. These advances in power electronics have made propulsion systems utilizing variable speed AC motor drives cost competitive with traditional mechanical drive plants. [1][2] Additionally, weapons systems and high power radars are expected to have a similar power electronic interface with the main bus distribution systems.

The installation of these power electronic devices will have a negative impact on main bus power quality. The deleterious effect is due to the fact that these loads do not draw purely sinusoidal current. The non linear circuit elements in these circuits distort the current waveform and result in harmonics of the fundamental frequency. In this paper the terms non-linear and harmonic will be used when describing loads exhibiting these characteristics. The power supply for these loads usually requires use of a bridge rectifier at the front end. The bridge rectifier draws current at harmonics of the fundamental frequency from the distribution system. When these currents propagate through the distribution system they develop voltage across the impedance of the source. This leads to distortion of the voltage waveform seen by all loads in the distribution system. Distortion of supply voltage can lead to improper operation of sensitive electronic equipment and overheating of certain elements in the power system such as motors, transformers, and cables.

Interest in power system harmonics dates to the early 1930's when utilities first noticed distorted voltage and current waveforms on overhead transmission lines. At the time, their interest was primarily in the effect on electric machines, telephone interference, and power capacitor failure.[6] Over the last twenty years the proliferation of electronic switching into power electronics devices has caused renewed interest in power system harmonic studies. Concerns over the increase in non-linear loads have shown the need for harmonic studies as a standard component of power system analysis and design. [7]

A navy ship with IPS can be regarded as a small scale, autonomous, industrial type power system sharing the same power quality concerns as the utilities. The modern warship, like the continental grid, has experienced the same proliferation of power electronics and shares the need for analysis of power system harmonics. However, there are several differences between a land based distribution system and ship based system. [8] They are:

- The ships power system is completely autonomous. Reliability is essential for safety of the ship and crew
- The relative rotational inertia of the prime movers is small compared to the electrical load
- The ships distribution system consists of AC and DC voltage at different magnitudes and frequencies
- The ships grid has cables of short length compared to land based systems

12

- A significant portion of the total ships load draws non-linear current

These differences make the accurate representation of harmonic generating devices within the IPS imperative for the design and analysis of this system.

1.3 Scope

This research will be accomplished in three steps. The fist step will involve developing accurate models of non-linear power system components for an IPS. In the second step, a notional distribution system with loads representative of a future surface combatant will be developed. The final step will be to analyze this notional IPS for voltage and current distortion over the wide range of operating conditions experienced by Navy ships at sea.

This page intentionally left blank.

Chapter 2 Measures of Distortion

The simple full bridge rectifier shown in Figure 2-1 and its associated voltage and current waveforms, Figure 2-2 and Figure 2-3 , will be used to illustrate some characteristics of power system harmonics.

Figure 2-1 Full Bridge Rectifier
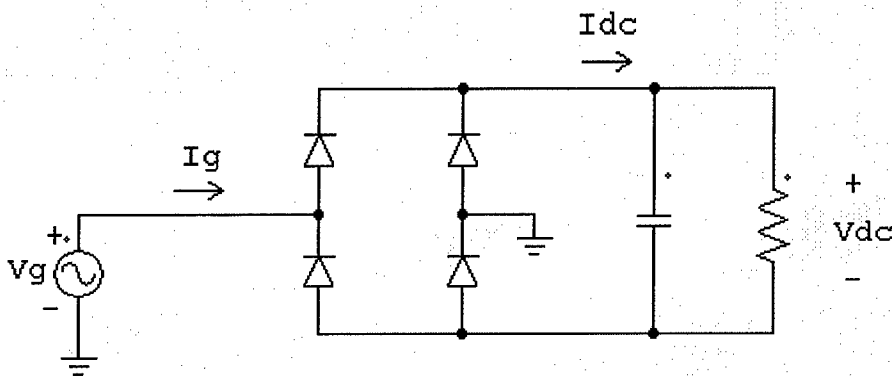
Figure 2-2 Full Bridge Voltage and Current
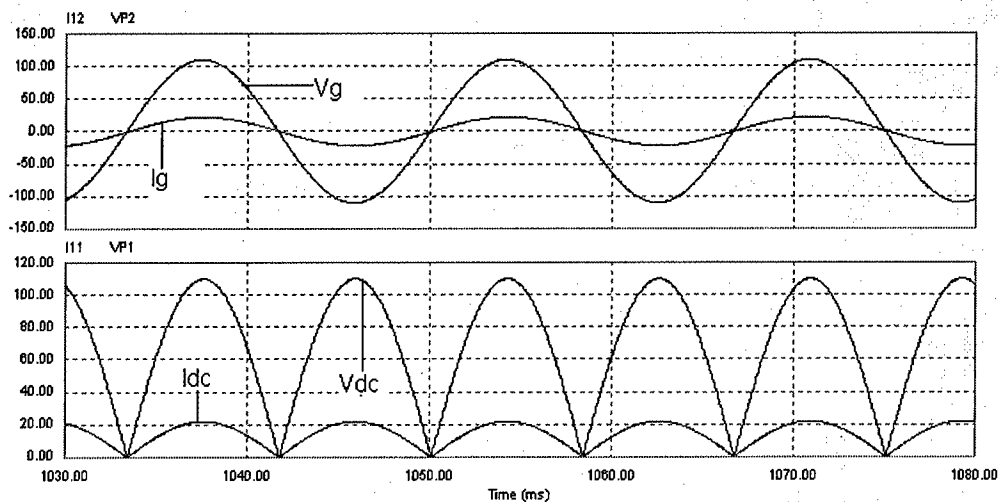
Figure 2-3 Bridge Rectifier with Output Filter
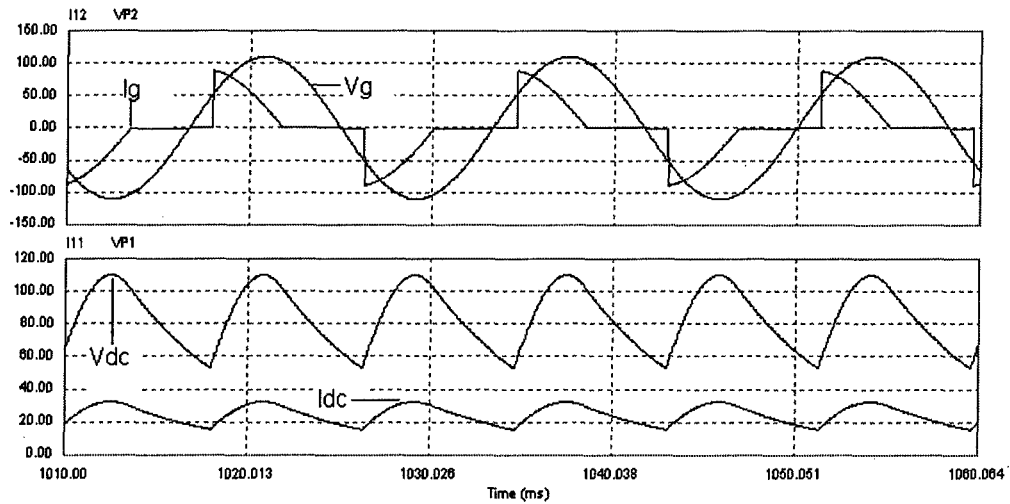
Figure 2-2 shows the voltage and current waveforms of the bridge rectifier with the output capacitor set at 0, and assuming ideal diodes. The source current is transferred between the diodes the moment the source voltage changes polarity. In a real bridge rectifier, the source will have some amount of inductance and typically an output capacitor will be installed to reduce the ripple of the output voltage. Figure 2-3 shows the same bridge rectifier waveforms but now with an output capacitor. The output capacitor prevents the diodes from turning on until the polarity of the source voltage is greater than the voltage on the output capacitor. This results in regularly appearing distortion of the source current at a multiple of the source frequency as evidenced by the source current waveform of Figure 2-3. This distortion is referred to as harmonic distortion.

In order to measure harmonic distortion Fourier analysis is used. Fourier analysis allows us to represent any periodic wave form as a Fourier series. [9][10][16] Consider a periodic function $f(t)$. This function can be represented as:

$$f(t) = C_0 + \sum_{n=1}^{\infty} C_n \cos(n\omega t + \theta_n)$$

Equation 2-1

16

$$C_n = \sqrt{A_n^2 + B_n^2} \qquad\qquad \theta_n = \tan^{-1}(-B_n / A_n)$$

With T=$2\pi/\omega$ the coefficients A_n, B_n, and C_0 are defined as: (note: T must be a multiple of a period)

$$A_n = \frac{2}{T}\int_0^T f(t)\cos(n\omega t)dt \quad B_n = \frac{2}{T}\int_0^T f(t)\sin(n\omega t)dt \quad C_0 = \frac{1}{T}\int_0^T f(t)dt$$

Equation 2-2

Using Equation 2-1 and Equation 2-2 we will determine a measure of the distortion of the line current in Figure 2-2. Assume that the voltage input is purely sinusoidal and is given by:

$$v_s = \sqrt{2}V_s \sin\omega_1 t$$

Equation 2-3

The input current into the bridge rectifier can be written as a sum of its Fourier components.

$$i_s(t) = i_{s1}(t) + \sum_{h\neq1} i_{sh}(t)$$

$$i_{s1} = \sqrt{2}I_{s1}\sin(\omega_1 t - \phi_1) \text{ and } i_{sh} = \sqrt{2}I_{sh}\sin(\omega_h t - \phi_h)$$

Equation 2-4

The rms value of $i_s(t)$ is:

$$I_s = \sqrt{\frac{1}{T}\int_0^T i_s^2(t)dt}$$

Equation 2-5

Substituting Equation 2-4 gives:

$$I_s = \sqrt{I_{s1}^2 + \sum_{h\neq1} I_{sh}^2}$$

Equation 2-6

17

Define the distortion current, ($i_{dis}(t)$), as that component of the current not at the fundamental frequency then this current (rms) is given by:

$$I_{dis} = \sqrt{I_S^2 - I_{S1}^2} = \sqrt{\sum_{h \neq 1} I_{sh}^2}$$

<div align="right">**Equation 2-7**</div>

%THD can now be defined as:

$$\%THD = 100 * \frac{I_{dis}}{I_{S1}} = 100 * \frac{\sqrt{I_S^2 - I_{S1}^2}}{I_{S1}} = 100 * \sqrt{\sum_{h \neq 1} \left(\frac{I_{sh}}{I_{s1}} \right)^2}$$

<div align="right">**Equation 2-8**</div>

Another useful measure of distortion is power factor (PF). [9][10] Consider the voltage and current waveforms shown in Figure 2-4. The voltage is purely sinusoidal while the current is a distorted waveform containing the first and fifth harmonic.

Figure 2-4 Current Distortion
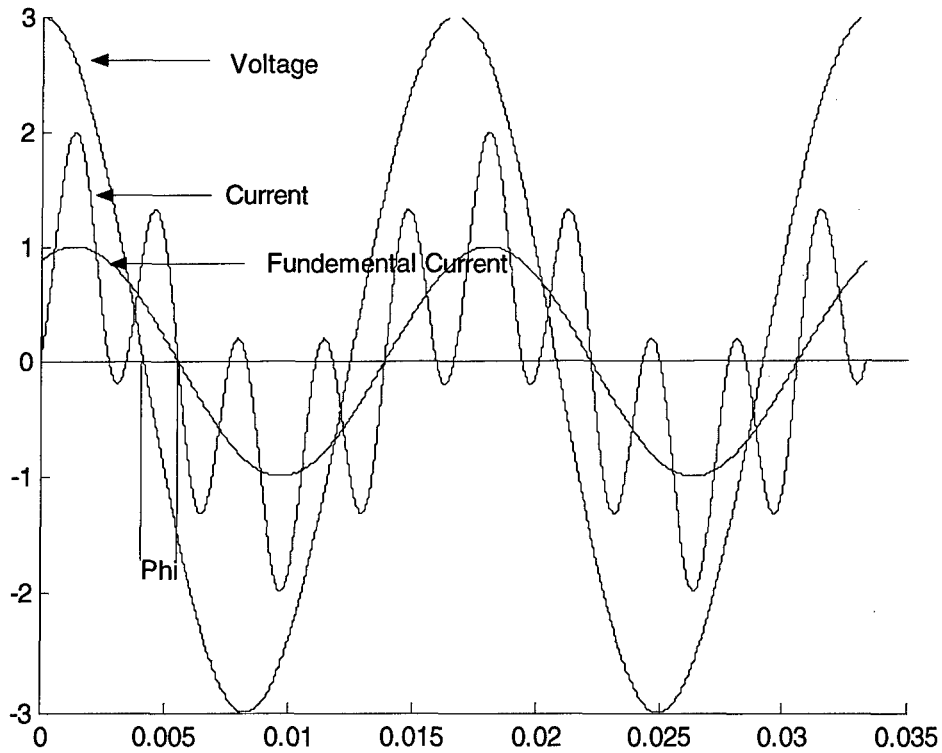
The average power can be calculated by:

$$P = \frac{1}{T}\int_0^T p(t)dt = \frac{1}{T}\int_0^T v_s(t)i_s(t)dt$$

<div align="right">**Equation 2-9**</div>

Substituting Equation 2-3 and Equation 2-4:

$$P = \frac{1}{T}\int_0^T \sqrt{2}V_s \sin \omega_1 t * \sqrt{2}I_{s1} \sin(\omega_1 t - \phi_1)dt = V_s I_{s1} \cos \phi_1$$

<div align="right">**Equation 2-10**</div>

Note that the only component of the current that contributes to the average power drawn from the source is the fundamental current. For sinusoidal quantities the apparent power (S) and the power factor (PF) are defined as:

$$S = V_s I_s$$

Equation 2-11

$$PF = \frac{P}{S}$$

Equation 2-12

Using Equation 2-10 and Equation 2-11:

$$PF = \frac{V_s I_{s1} \cos\phi_1}{V_s I_s} = \frac{I_{s1}}{I_s} \cos\phi_1$$

Equation 2-13

Equation 2-13 shows that when dealing with distorted waveforms there are two components that effect PF, the displacement factor, $k_\theta = \cos\phi_1$, and the distortion factor, $k_d = \frac{I_{s1}}{I_s} k_d$. k_θ is the familiar power factor angle and represents the phase difference between the voltage and current. k_d is a measure of the amount of distortion in the line current of a load. When both the current and voltage are sinusoidal $k_d = 1$. It is sometimes useful to represent PF using THD.

$$PF = k_d k_\theta = \frac{I_{s1}}{I_s} k_\theta = \sqrt{\frac{1}{1+THD^2}} k_\theta$$

Equation 2-14

Chapter 3   Harmonic Analysis

Harmonic analysis of power systems can be conducted in both the frequency domain and the time domain. An overview of the various techniques will be presented.

3.1   Frequency Domain

Frequency domain analysis requires development of the admittance matrix of the system. This method is based on multi-port network theory. The positive sequence admittance matrix is developed from component level two port admittance parameters. A detailed discussion of this method can be found in [6] and [16]. The admittance matrix must be determined for each frequency of interest. Various frequency domain algorithms are used in conjunction with the admittance matrix in order to conduct the analysis.

3.1.1   Frequency Scan

The most common and also the simplest method of analysis is called a frequency scan. This method involves the solution of Equation 3-1:

$$\left[\underset{=}{Y_n} \right] \left[\underset{-}{V_n} \right] = \left[\underset{-}{I_n} \right]$$

Equation 3-1

Where $\left[\underset{=}{Y_n} \right]$ is the admittance matrix, $\left[\underset{-}{I_n} \right]$ is the known current vector, and $\left[\underset{-}{V_n} \right]$ is the nodal voltage. The subscript n denotes the integer multiple of the base frequency. The system response as a function of frequency is determined through solution of Equation 3-1 at integer multiples of the base frequency. If a one per unit sinusoidal current is injected into the system at a specific point, the corresponding node voltages will represent the driving point impedance of the system as seen from this point. The frequency is varied from the base frequency to the highest harmonic frequency of interest and then the impedance over this range can be plotted. The peaks of this plot correspond to parallel resonance conditions (high impedance to current flow), and the valleys of the plot correspond to series resonance conditions (low impedance to current flow). This method provides an excellent visual indication of resonance conditions and

is especially useful when trying to assess the impact of the addition of a new piece of equipment which draws non-linear current. [6][16]

3.1.2 Current Source Injection

This method requires information about the magnitude of the current drawn by a non-linear load in addition to the admittance matrix of the network the load is connected to. Many harmonic sources can by characterized by a typical spectrum. These spectrums can be found in references such as [6],[9], and [20]. Equation 3-1 is solved at specific harmonic frequencies and the voltage at that frequency is obtained. The magnitude of the voltages at each harmonic frequency can be used in Equation 2-8 to determine THD.

There are some limitations when using this method for calculation of system distortion. When more than one non-linear load is present this method loses accuracy because it does not accurately reflect the phase angle of each harmonic. Studies have shown that when more than one non-linear load is present a significant amount of cancellation, due to difference in phase angle, takes place. [7][15] This method is also limited in that many non-linear loads present vary different harmonic spectra depending on load level or control strategies. Figure 3-1 and Figure 3-2 show the input current to a six pulse rectifier operating at two different thyristor firing angles. Clearly the harmonic content of these two signals is different.

Figure 3-1 Six Pulse Rectifier alpha = 0 degrees
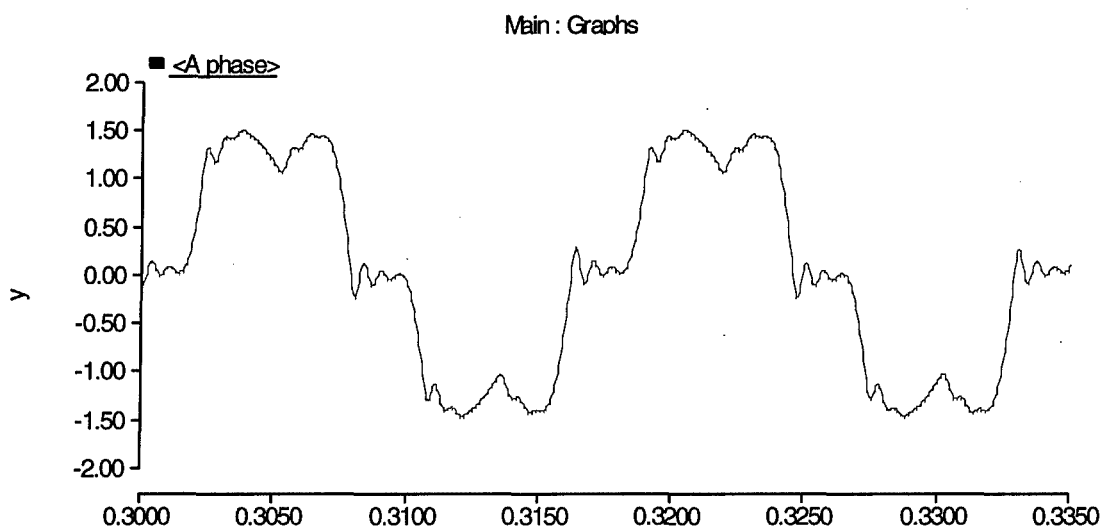
Figure 3-2 Six Pulse Rectifier alpha = 45 degrees

Main : Graphs
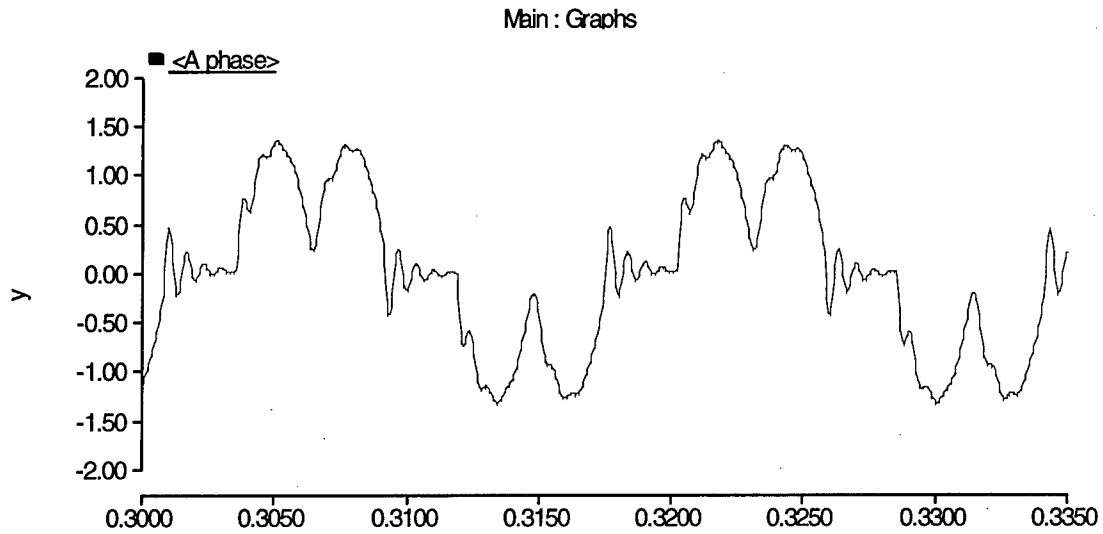
3.1.3   Harmonic Load Flow

This method requires that non-linear load current be represented as a function of harmonic voltages existing at the device terminals and control variables applicable to the load (ie thyristor firing angle in a rectifier). In this method variations as depicted in Figure 3-1 and Figure 3-2 can be accommodated. Each load is represented as follows:

Where C_a, C_b,... represent control variables for load parameters

V_1, V_2, ... V_n represent harmonic voltages at the device terminals

$$I_n = F(V_1, V_2,...V_n, C_a, C_b......)$$

Equation 3-2

This representation is used in conjunction with Equation 3-1 to form a complete mathematical model of the system. These equations are then solved iteratively using Newton or Gaussian algorithms. The limitation of this technique is that in many cases a representation of the non-linear loads in the form of Equation 3-2 is not possible. When this is the case, techniques that represent non-linear loads by their time domain differential equations have been developed.[6][16][20]

3.2 Time Domain

Harmonic studies involving widely varied load patterns are often best suited to simulating a complete time domain model using electromagnetic transient programs such as EMTP or EMTDC. These programs are based on the principles outlined in [11]. EMTDC (Electromagnetic Transients including DC) was originally developed as a simulation tool for the Nelson River HVDC Power System in Manitoba, Canada. EMTDC represents and solves differential equations in the time domain given a fixed time step. This allows the response of the system to be solved at all frequencies, limited only by the user selected time step.[12] The method primarily used in this research will be using EMTDC with the graphical interface of PSCAD.

The network impedance can be represented by models of the components primarily responsible for the impedance properties of the system. For example, in rotating machines the magnetic field created by stator time harmonics rotates at speeds significantly higher than the mechanical speed of the rotor. Therefore, the inductance of a synchronous machine can be modeled as the negative sequence impedance or the average of the direct and quadrature subtransient impedances. An induction machine can be approximated as the locked rotor impedance. Linear passive loads can be modeled as an aggregate load if reasonable estimates of real power and reactive power are available. [6][20]

In large networks it may be necessary to represent a portion of the network by its dynamic equivalent. This strategy represents the driving point and transfer impedances between busses by a lumped RLC branches. An overview of this technique is outlined in [6].

Harmonic sources can be represented as rigid harmonic sources, as a switching function, or with detailed models. Rigid harmonic sources are described by Equation 3-3.

$$i(t) = I_1 \cos(wt + \theta_1) + I_n \sum_2^n \cos(nwt + \theta_n)$$

$$\theta_n = n\theta_1 + (n+1)\frac{\pi}{2}$$

Equation 3-3

The magnitude of the current can be obtained from typical spectrum or from measurements and the phase angle can be determined from the load power factor.

The switching function can be used to determine a state space model for a converter. Consider the Up/Down converter shown in Figure 3-3:

Figure 3-3 Up/Down Converter
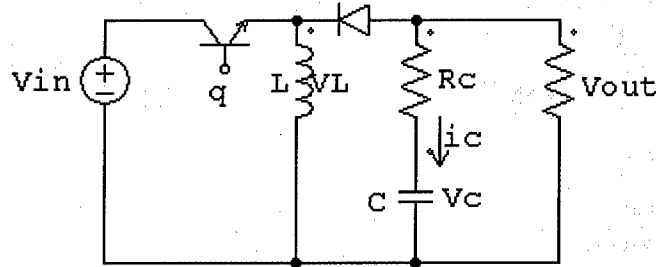
Let the switching function q(t) = 1 when the transistor is on and q(t) = 0 when the transistor is off and let q'(t) = 1-q(t). The following equations define the circuit when the q(t)=1.

$$v_L(t) = L\frac{di_L}{dt} = v_{in}(t)$$

$$i_c(t) = C\frac{dv_c}{dt} = \frac{-1}{R+R_c}v_c(t)$$

Equation 3-4

When q(t)=0,

$$v_L(t) = L\frac{di_L}{dt} = \frac{R}{R+R_c}\left[-R_c i_L(t) + v_c(t)\right]$$

$$i_c(t) = C\frac{dv_c}{dt} = \frac{-1}{R+R_c}\left[Ri_L(t) + v_c(t)\right]$$

Equation 3-5

Combining Equation 3-4 and Equation 3-5 and introducing q(t) results in the state space model of the Up/Down converter.[9]

$$\frac{di_L}{dt} = \frac{R}{L(R+R_c)}\left[-R_c q'(t)i_L(t) + q'(t)v_c(t)\right] + \frac{1}{L}q(t)v_{in}(t)$$

25

$$\frac{dv_c}{dt} = \frac{-1}{C(R+R_c)}[Rq'(t)i_L(t) + v_c(t)]$$

<div align="right">**Equation 3-6**</div>

The final method is through a detailed representation of the non-linear load and its associate control mechanisms. Weak systems, such as an IPS, require this method in order to accurately represent harmonic distortion. The simulation consists of a transient phase followed by the steady state phase. The transient phase is due to the network natural frequencies and the interaction between network voltage and frequencies and converter controls. The transient phase can last as long as ten fundamental cycles. At the end of the transient phase, steady state conditions should be verified. For example, the average DC current of a converter could be checked. At steady state this current should be constant. Once the steady state is reached, programs such as EMTP and PSCAD/EMTDC contain tools to extract the frequency components of the desired voltages and currents.

Chapter 4 Model Validation

This chapter will focus on the steps taken to validate the PSCAD/EMTDC model of an IPS. The validation consists of three steps. The first step (section 4.1), is a simple comparison of results generated on a test system simulated in ACSL and SABRE. Measured data was not available from the ACSL and SABRE simulations so the comparison was based on the magnitude and shape of the waveforms. The second step (section 4.2), was accomplished by comparing the PSCAD/EMTCD simulation results to test results measured at the IPS Land Based Test Site (LBES) during the Full Scale Advanced Development (FSAD) system testing conducted on June 28 and July 1 of 1999. The final step (section 4.3), was to compare PSCAD/EMTDC simulation results to the current source injection method outlined in 3.1.2. A simple plant consisting of a motor drive, transformer, and resistive load was constructed for the purpose of the comparison.

4.1 Test System Comparison

The test system used in this comparison is shown in Figure 4-1 and characterized in Table 4-1. S.D. Sudhoff, S.F. Glover, B.T. Kuhn simulated the test system as part of their work in validating models for LBES. The system was obtained from [17]. This was meant as a preliminary comparison. The only data available for comparison were the reproductions of the waveforms. The following figures compare the simulation results for the a-phase current into the rectifier. The PSCAD plot has a very strong correlation to the plots from the SABRE and ACSL simulations. The magnitude of the current as well as the frequency of oscillations is similar. Due to the lack of the underlying data for the ACSL and SABRE simulations a more detailed comparison can't be made. However, the similarities in shape, magnitude, and oscillation frequency of the output waveforms suggest that the PSCAD has accurately modeled the test system. Figure 4-3 and

Figure 4-4 were reproduced from [17].

Figure 4-1 Test System
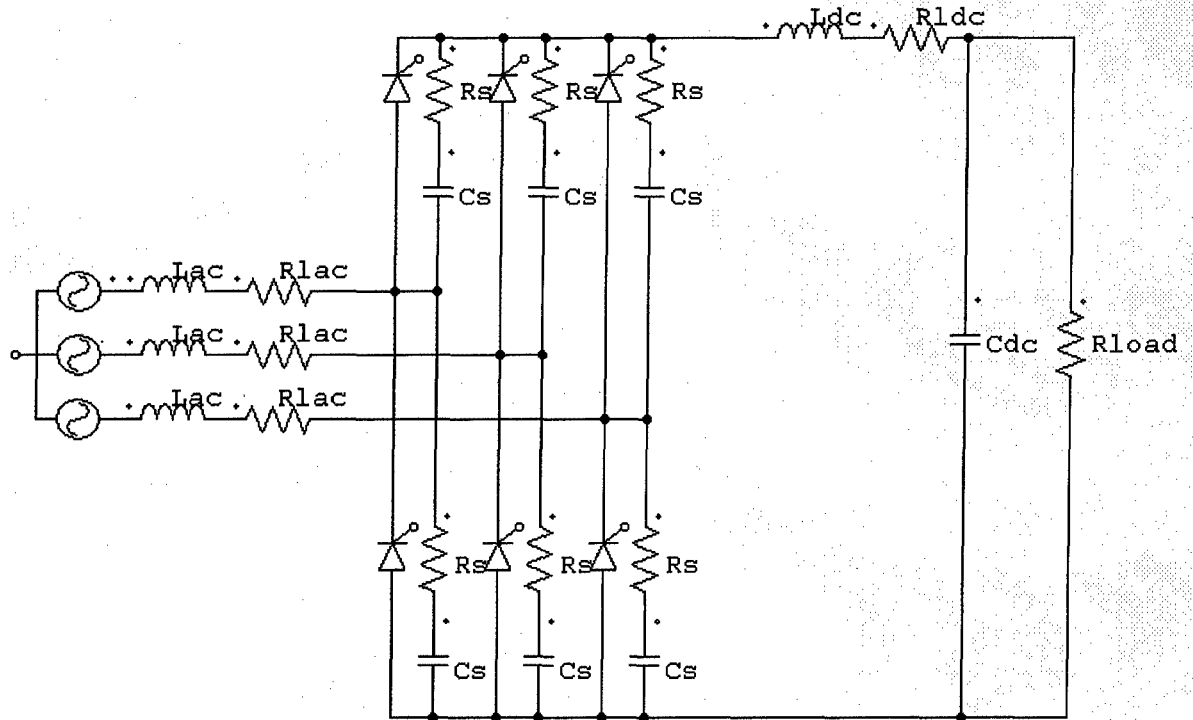
Table 4-1 Parameter Values for Test System

Parameter	Symbol	Value
Source frequency	F	60 Hz
Line to neutral peak voltage	Vpeak	3396.6 V
AC line inductance	Lac	391.7 μH
AC line resistance	Rlac	1.272 mΩ
Thyristor on state voltage drop	Vscr	1 V
Thyristor on state resistance	Rscr	130 μΩ
Snubber capacitance	Cs	9 μF
Snubber resistance	Rs	3.33 Ω
DC link inductance	Ldc	666.67 μH
DC filter capacitance	Cdc	30 mF
DC link resistance	Rldc	3.3 mΩ
Load Resistance	Rload	4.13 Ω

Figure 4-2 PSCAD/EMTDC Simulation
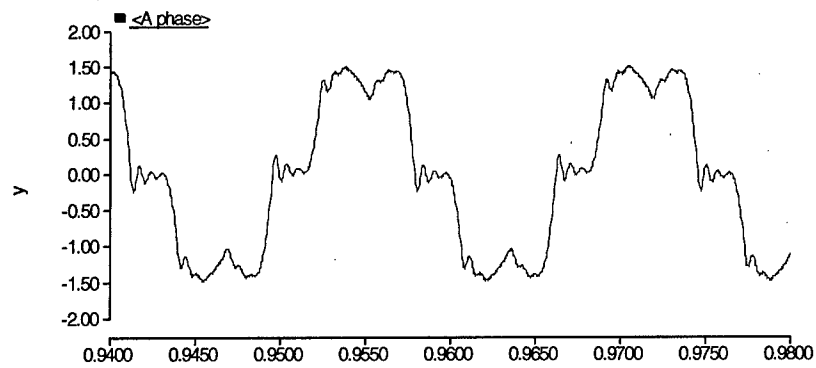
Figure 4-3 ACSL Simulation
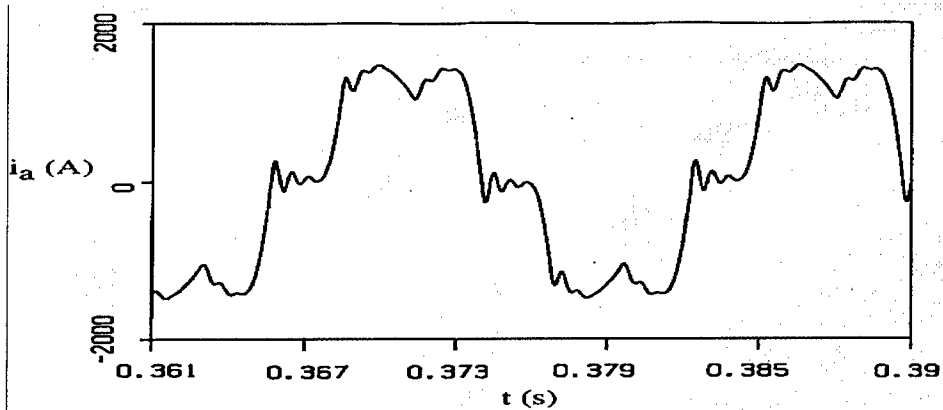
Figure 4-4 SABRE Simulation
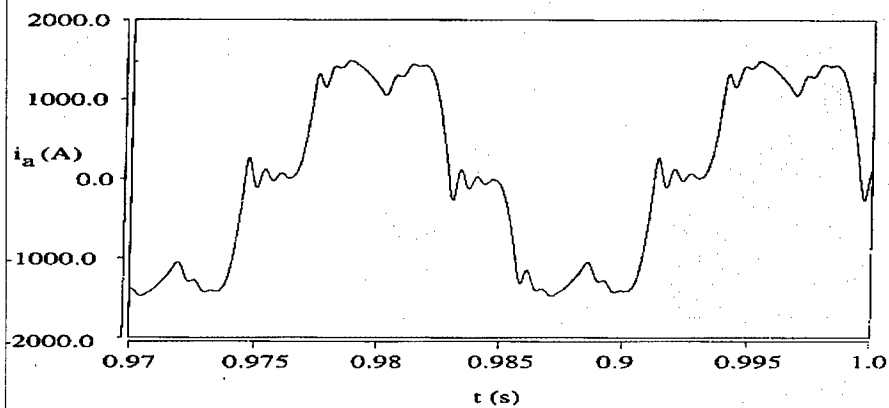
4.2 LBES System Comparison

LBES is a full scale prototype of a 4160-volt IPS. The components online during the study were the 21 MW 4160 V generator, a 19 MW 15 phase induction motor, and a three phase filter tuned to the 5th harmonic. The components are shown in Figure 4-5.

Figure 4-5 LBES Components
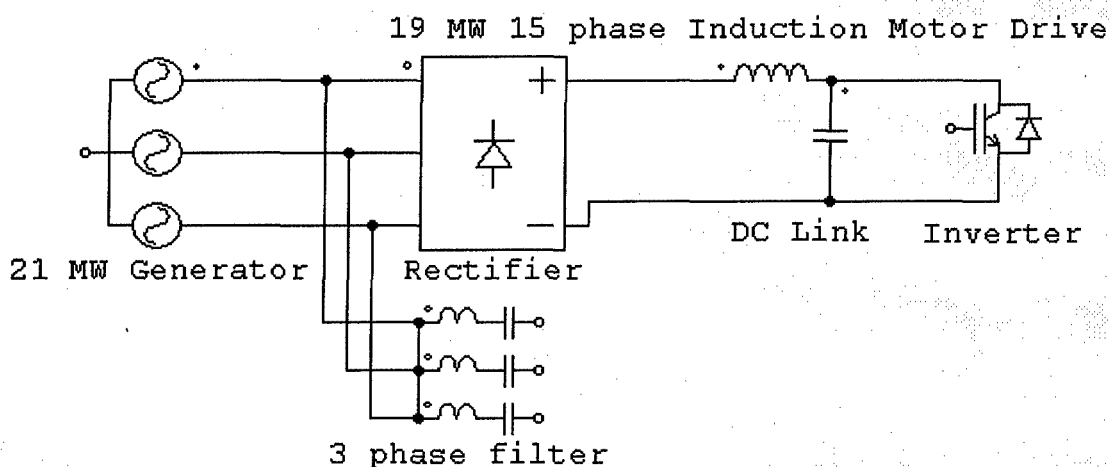
4.2.1 Generator

The Generator was modeled in PSCAD/EMTDC as a modified version of the general synchronous-machine steady state equivalent circuit. Normally the machine is modeled as an ideal voltage source behind a synchronous reactance. The synchronous reactance is the effective reactance seen by a phase of the machine under normal machine operations. In this case, the synchronous reactance was replaced with the subtransient reactance as that value is the impedance of interest in harmonic distortion studies. The generator was initially modeled using the component library synchronous machine model in PSCAD/EMTDC. This model is programmed in state variable form using generalized machine theory and can take as input either equivalent circuit data for the machine or the machines time constants. A simulation was performed with the synchronous machine model with the parameters in Table 4-2. A second simulation was also conducted with an ideal voltage source behind an inductance equivalent to a 20% subtransient reactance for a 25 MVA machine. Figure 4-6 and Figure 4-7 show the generator current and motor current for the detailed model and the steady state model. It can be seen that the simplified steady state method produced identical steady state results as the detailed

30

model. The voltage distortion of both simulations was also recorded. The detailed model produced 18.52% voltage distortion while the steady state model produced 18.47% voltage distortion. The detailed model slowed the simulation down considerably without providing improved results, so the ideal voltage source behind a subtransient reactance method was implemented.

Figure 4-6 Simplified Model Motor and Generator Current
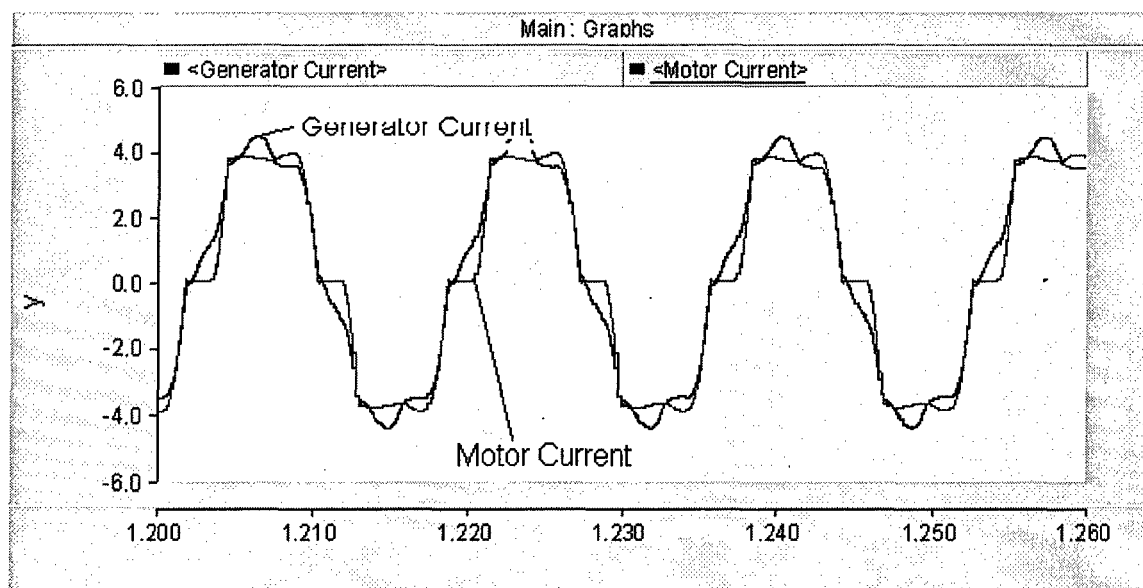
Figure 4-7 Detailed Model Steady State Generator and Motor Current
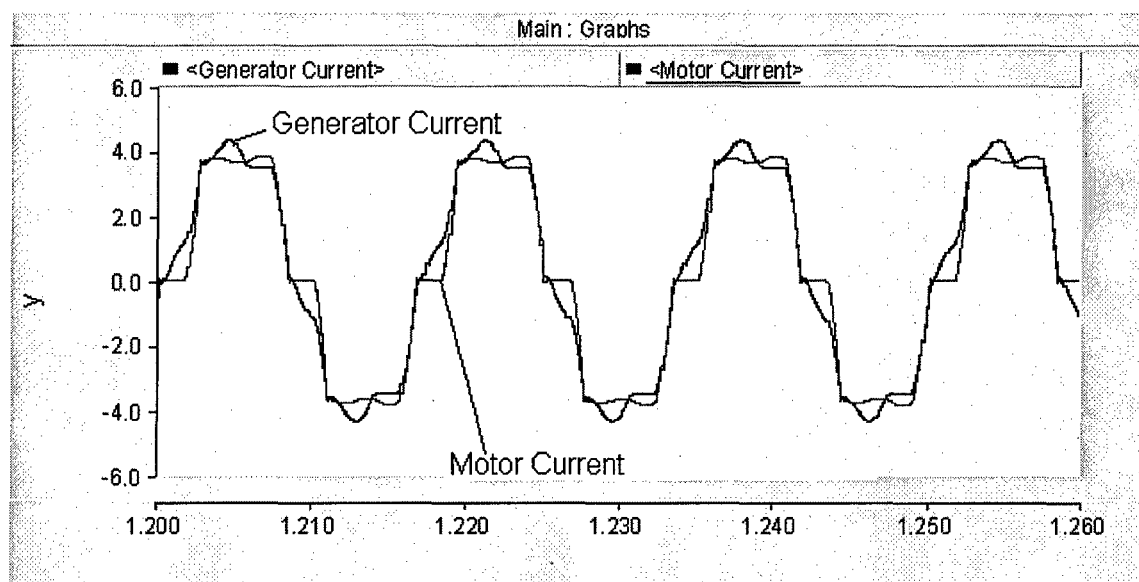
Table 4-2 Generator Parameters

Parameter	Value
Nominal Voltage (LL RMS)	4160 V
Rated MVA	25 MVA
Fundamental Current Limit	3469 A
5th Harmonic Current Limit	312 A
7th Harmonic Current Limit	277 A
Synchronous Inductance	0.36 mH
D axis Unsaturated Reactance Xd	2.0 per unit
D axis Unsaturated Transient Reactance Xd'	.25 per unit
D axis Unsaturated Subtransient Reactance Xd"	.2 per unit
Q axis Unsaturated Reactance Xq	1.85 per unit
Q axis Unsaturated Subtranient Reactance	.2 per unit
Series Line Resistance	2.27 mΩ
Line to Earth Capacitance	0.145 μF

4.2.2 Harmonic Filter

The harmonic filter is used to filter fifth harmonic currents drawn by the propulsion motor in order to protect the generator from heating. The filter parameters were obtained from [18] and are shown in Table 4-3 .

Table 4-3 Harmonic Filter Parameters

Parameter	Value
Filter Inductance	1.19 mH
Series Resistance	12 mΩ
Filter Capacitance	282 μF
Capacitor Voltage Limit	2900 V
Reactor Current Limit	656 A

In [17], the impedance characteristics of the harmonic filter were calculated from the measured current and voltage wave forms. It was found that the calculated component values of the capacitance and inductance were 0.58% and 10.03% higher than the values listed in Table 4-3. This resulted in the magnitude of the impedance at the 5th harmonic increasing from 0.2432 Ω to 0.4532 Ω. The values calculated in [17] provided the most accurate results in the simulation and were implemented in the model.

4.2.3   Induction Motor

The propulsion motor installed at LBES is a 19 MW, 15 phase squirrel cage induction motor driven by a 15 phase converter. There are three identical modules within the motor drive consisting of a six pulse rectifier, DC link, and H-bridge inverter. Each module supplies five phases to the induction motor. The Induction motor was simulated as three separate controlled six pulse rectifiers with a DC link feeding a resistive load. The converter is operated in a controlled fashion to resolve DC link stability issues discovered when the hardware was initially operated with the rectifier in an uncontrolled mode. The total power of the motor was distributed evenly to each module. The resistive load and firing angle of the rectifier were controlled to produce different power levels. The motor and its AC drive circuitry were not modeled because they would have no effect on the power system harmonics; the front end rectifier and DC link isolate the main bus from the motor drive inverter. Model parameters were obtained from [17] and are shown in Table 4-4 and Figure 4-8. A single module for the induction motor drive is shown in Figure 4-9.

Table 4-4 Motor Drive Parameters

Parameter	Value
Snubber Resistance	60 Ω
Snubber Capacitance	0.5 μF
DC Link Inductance	2.6 mH
DC Link Capacitance	670 μF

Figure 4-8 Firing Angle vs Speed
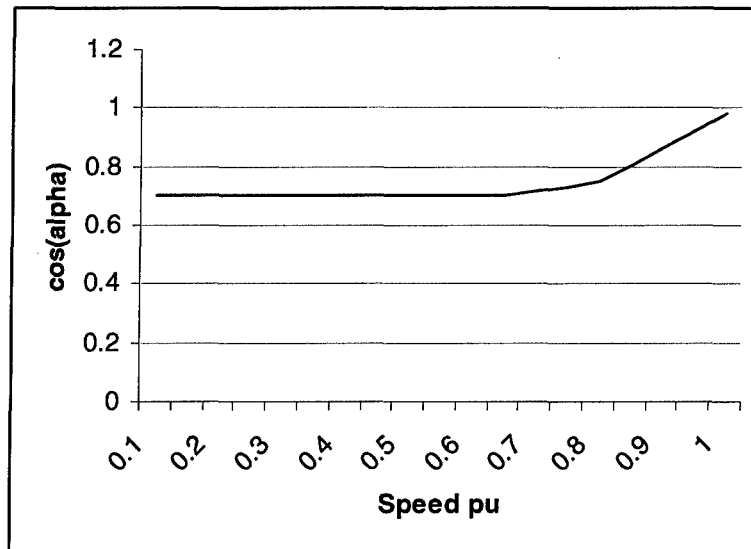
Figure 4-9 Induction Motor Drive Circuit
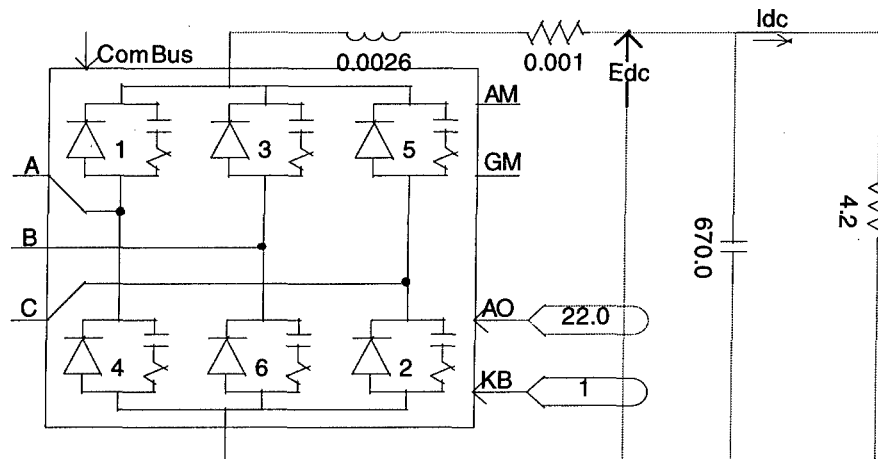
The component library for PSCAD/EMTDC contains a model for a DC converter. The converter consists of a six pulse Graetz converter bridge, an internal phased locked oscillator (PLO), valve firing and blocking controls, and RC snubber circuits. The converters basic operation is as follows. The AO input is the ordered firing angle for the converter. With an input of zero degrees the rectifier operates as a line commutated six pulse rectifier. A detailed description of line commutated converters will not be presented but can be found in [9] and [10]. The DC link voltage can be controlled by varying the firing angle alpha. The resulting average DC link voltage is:

34

$$\langle V_{DC} \rangle = \frac{3V_p}{\pi} \cos\alpha$$

Equation 4-1

4.2.4   Simulation Results

Data for steady state testing at LBES was obtained from [17] and [19]. The data consisted of current measurements for the propulsion motor drive, the harmonic filter, and the generator. Main bus voltage was also measured. The measurements consisted of the magnitude and phase for each harmonic up to the 25th harmonic. In order to compare simulation results to the test results, a MATLAB script was written that reconstructed the time domain signals of the measured data from the phase and Fourier coefficient data. Simulation signals and measured signals were normalized to the fundamental magnitude. The MATLAB script is contained in Appendix A. The primary objective of this simulation was to ensure that an accurate model for the motor drive circuit could be constructed; therefore this section will only present the comparison of the current and harmonic distortion of the motor drive. Plots of the filter current, generator current, and line voltage can be found in Appendix B. Simulation of the motor drive at 10%, 50%, and 90% rated power were conducted. Results are shown in Figure 4-10 through Figure 4-15 and Table 4-5. The simulations are more accurate at the 50% and 90% motor power. The overall distortion error is less than 2% for each of these simulations. At 10% motor power the distortion error is slightly under 5%. The error percent increases with harmonic order due to the smaller magnitude of the higher harmonics relative to the fundamental magnitude. At the high power levels the contribution to the overall distortion of the higher harmonics is so small that the error in simulating these harmonics does not significantly affect the overall results. At the 10 percent power rating, the smaller fundamental current results in an increase in the error of the total distortion. Even with relatively high percent error of harmonics above the 17th, the waveforms are remarkably similar as evidences by Figure 4-11, Figure 4-13, and Figure 4-15 .

Figure 4-10 LBES 90% Harmonic Magnitude Comparison
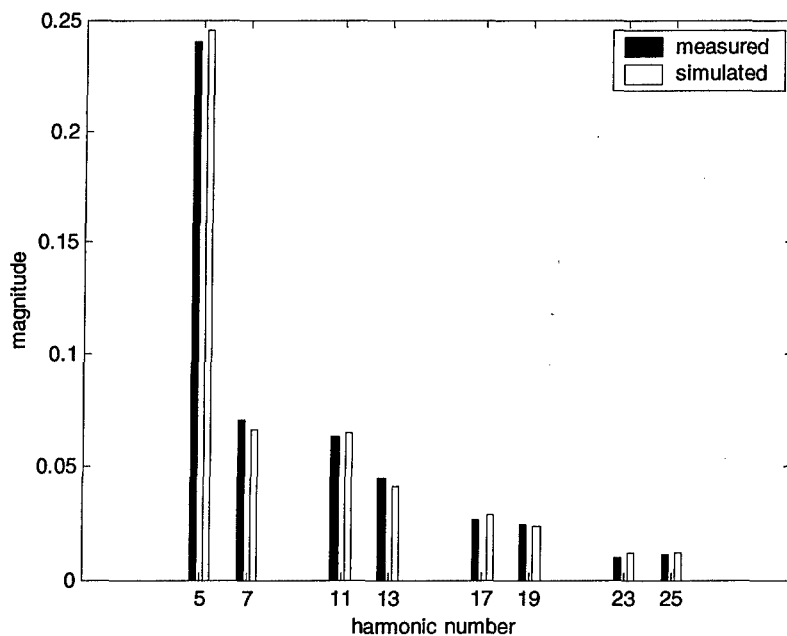
Figure 4-11 LBES 90% Power Motor Current
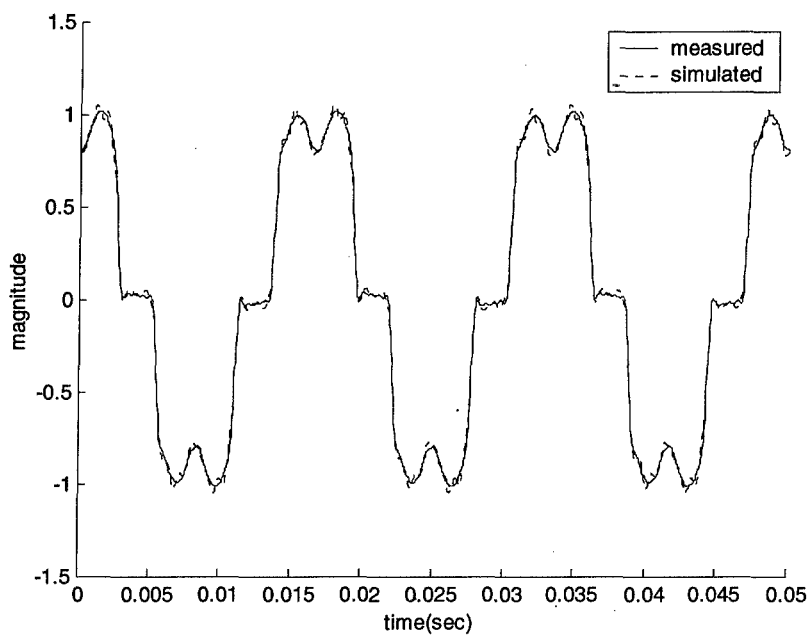
Figure 4-12 LBES 50% Harmonic Magnitude Comparison
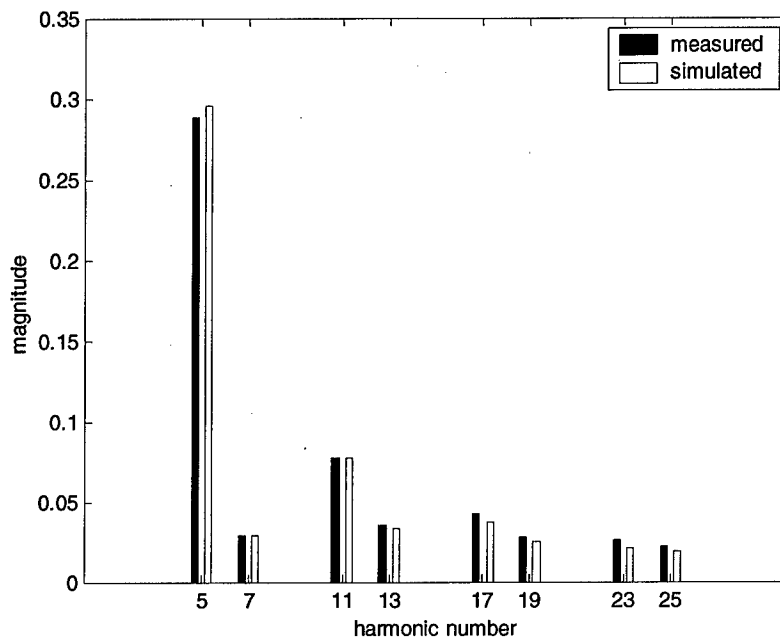
Figure 4-13 LBES 50% Motor Current
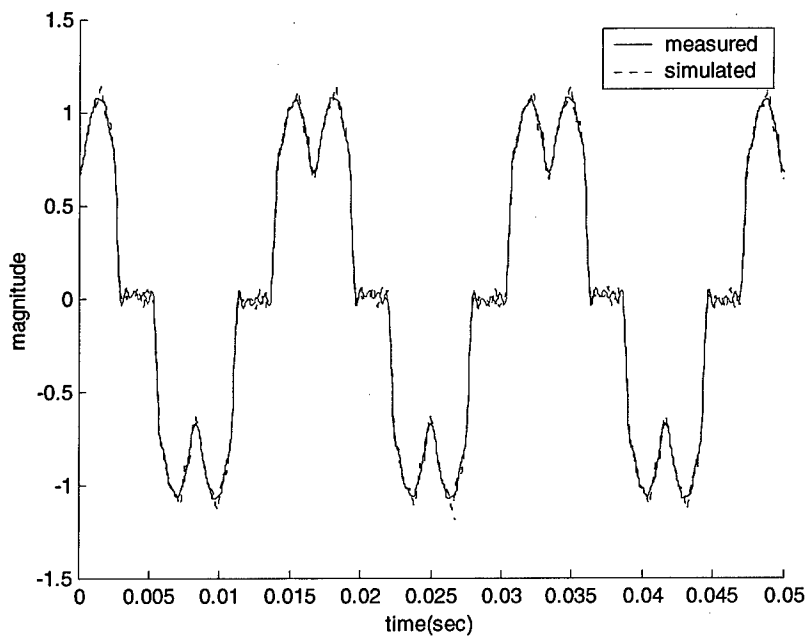
Figure 4-14 LBES 10% Harmonic Magnitude Comparison
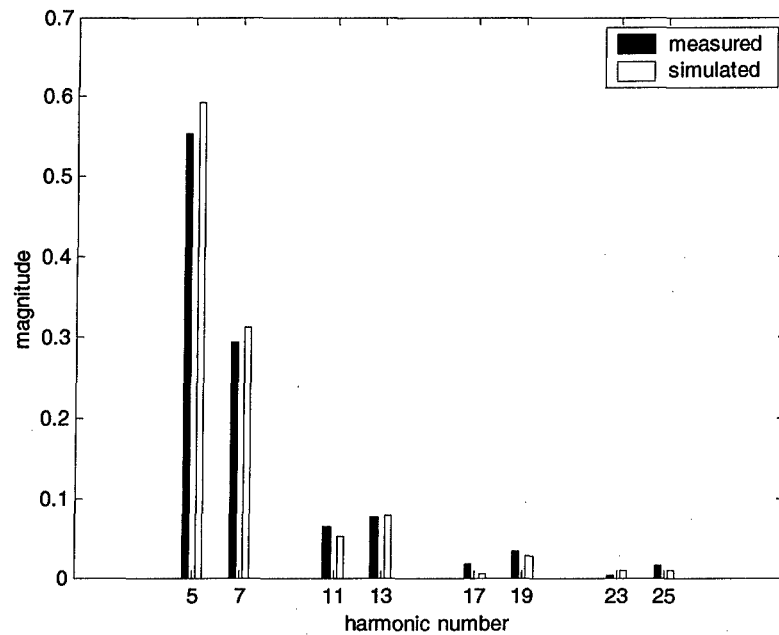
Figure 4-15 LBES 10% Motor Current
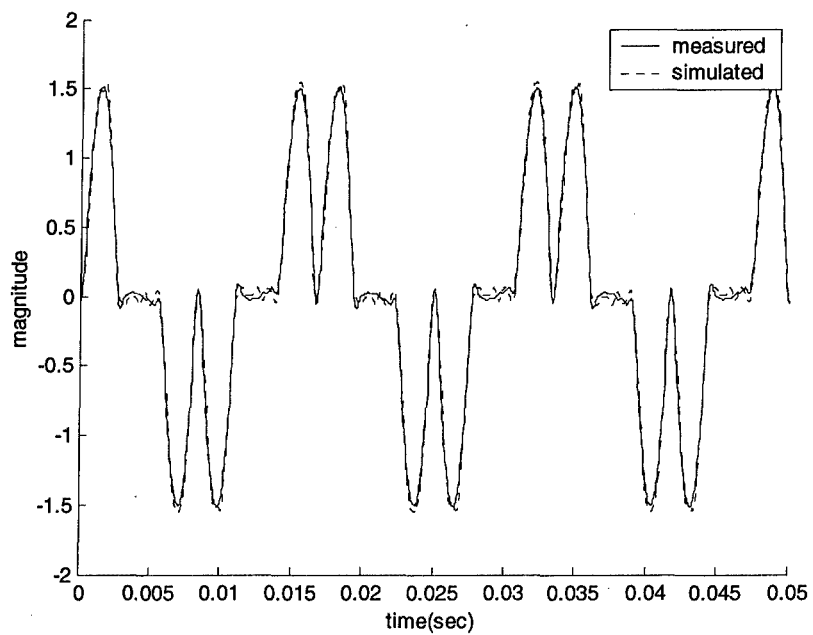
Table 4-5 Tabulated LBES Simulation Results

| | 90% Power | | | 50% Power | | | 10% Power | |
Measured	Simulated	Error %	Measured	Simulated	Error %	Measured	Simulated	Error %
1	1		1	1		1	1	
0.2402	0.2456	2.25	0.2896	0.2965	2.38	0.5544	0.593	6.96
0.0707	0.0691	2.26	0.0293	0.029	1.02	0.2927	0.3116	6.46
0.0634	0.0649	2.37	0.077	0.0768	0.26	0.0648	0.0588	9.26
0.0451	0.0415	7.98	0.0354	0.0336	5.08	0.0777	0.0779	0.26
0.0268	0.0285	6.34	0.0421	0.0381	9.50	0.0181	0.0112	38.12
0.0248	0.0235	5.24	0.0282	0.0254	9.93	0.0337	0.0276	18.10
0.0098	0.0105	7.14	0.0266	0.0214	19.55	0.0026	0.0019	26.92
0.0114	0.0117	2.63	0.0221	0.0188	14.93	0.0155	0.0101	34.84
25.63%	26.02%	1.53	29.55%	29.97%	1.42	53.69%	56.10%	4.49

4.3 Harmonic Source Comparison

The final step of model validation consisted of analyzing a simple system shown in Figure 4-16 using the current source injection method as outlined in Chapter 3. This method is highly accurate when only one harmonic source is present but leads to exaggerated distortion as more non-linear loads are added.[6] The primary reason for this section was that the previous validation sections did not include a distribution transformer or additional loading of the system. The technique outlined in [21] and [6] is well established and establishes a means of comparing results from the PSCAD simulation.

Figure 4-16 Current Source Comparison Circuit
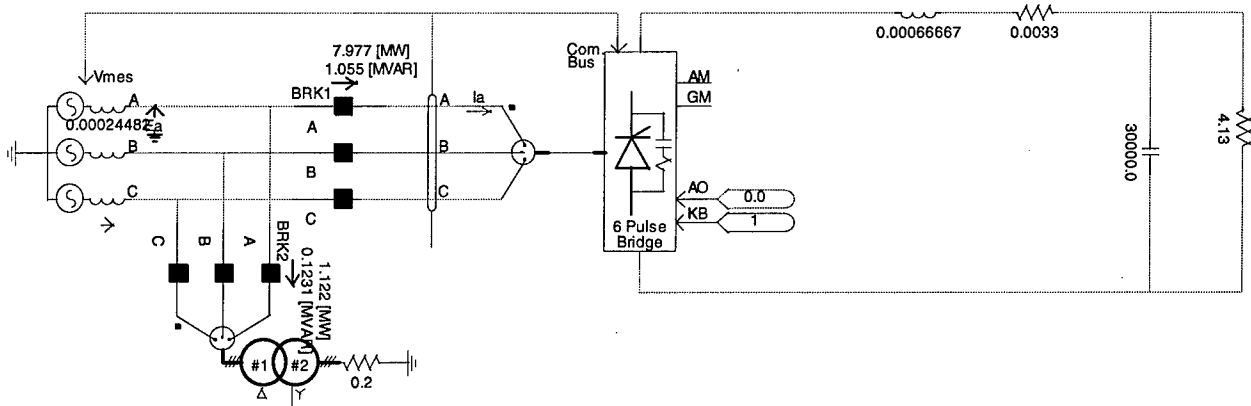
The system impedances of interest in the circuit above are the transformer, load, and generator phase-to-neutral values. The harmonic currents generated by the six-pulse rectifier flow through these impedances creating the voltage distortion on the main bus. Testing has shown a consistent relationship between the negative sequence impedance of rotating machines and the harmonic impedance. The negative sequence impedance is roughly equivalent to the subtransient reactance and therefore is used in determining the equivalent harmonic impedance.[21] In the test system above a subtransient reactance of 20% is used for the generator. The harmonic impedance of the generator is given by:

$$Z_{gen} = jX_{gen} = jnX_d''$$

Equation 4-2

The transformer and load impedance is estimated in the phase-to-neutral equivalent circuit by assuming a transformer impedance of 3%. The harmonic impedance of the transformer and load on the primary side is:

$$Z_{tran} = .2\left(\frac{V_1^2}{V_2^2}\right) + jn(0.03)\left(\frac{V_1^2}{VA}\right)$$

Equation 4-3

where: V1 is the primary voltage
V2 is the secondary voltage
VA is the volt-amp rating of the transformer
n is the harmonic number

The phase to neutral equivalent circuit of the test system is shown in Figure 4-17, the calculations are carried out in the MATLAB script included in Appendix A.

Figure 4-17 Phase-to-Neutral Equivalent Circuit
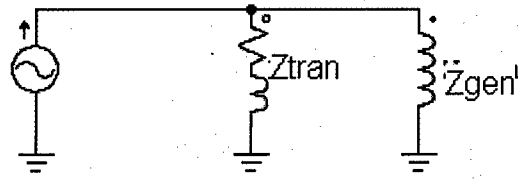
The test system was simulated in PSCAD and the harmonic current and harmonic voltage magnitudes were recorded. The recorded harmonic current magnitudes were then applied to the phase-to-neutral equivalent circuit. The harmonic voltages up to the 25th harmonic are shown in Figure 4-18 for the PSCAD simulation and the phase-to-neutral equivalent circuit. It is clear that the PSCAD simulation has accurately simulated the effects of a transformer and linear load.

Figure 4-18 PSCAD Current Source Comparison
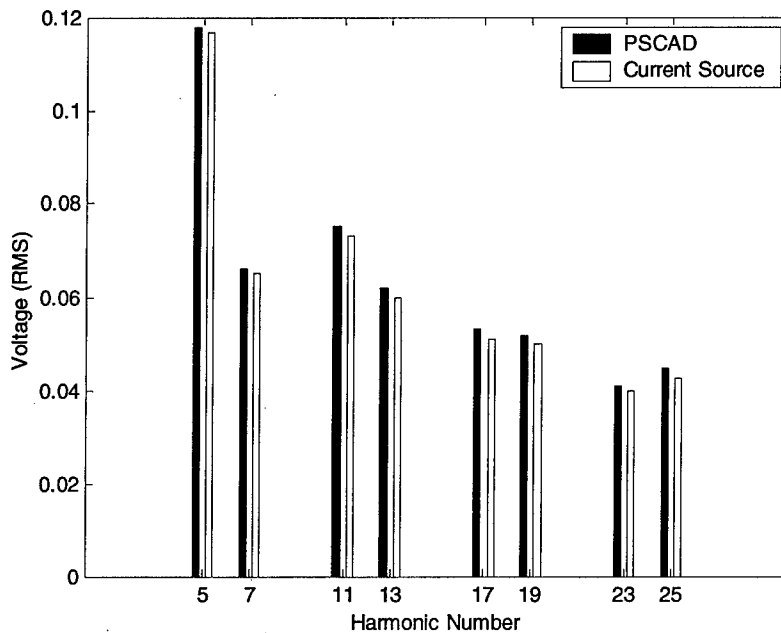
4.4 Model Validation Summary

The preceding sections demonstrate that this modeling technique accurately reflects harmonic current and voltage distortion in power systems such as those found on Navy ships. PSCAD simulations were compared to actual measurements taken on a system equipped with a ship generator and propulsion motor drive (4.2). Simulations were also compared to established

41

harmonic analysis techniques (4.1 and 4.3). In both cases highly accurate results were obtained. In the next chapter a more detailed system will be developed that is more representative of an actual shipboard power system. However, as there is no hardware developed for such a power system, there are no measurements available at this time for validation purposes. All the elements of this proposed power system are common with the previous studies that have been compared to either actual measurements or proven analytical techniques in this chapter. Therefore, we can be relatively confident in the simulation results of the proposed power system, even without hardware validation.

Chapter 5 Integrated Power System Development

The baseline IPS for this research is developed and analyzed in this chapter. This system is one approach to an IPS for a future surface combatant and is not intended to be an optimized solution for any particular ship design. The purpose of the system is to give a realistic picture of harmonic distortion over the wide operating range of Navy ships.

5.1 Approach and Assumptions

The development of an IPS requires assumptions that define the characteristics of the system. Changes in these assumptions may affect the results and conclusions of the study. The entering assumptions for the development of this architecture include:

- 4160 V, three-phase main bus

- Hybrid Distribution System (Some loads powered from a 450 V bus and some loads fed from DC load centers connected to the 450 V bus)

- Generator sets capable of 5-30 MW available for use. Commercially available prime mover ratings are not considered herein.\

- Generator subtransient reactance of 20 %

- Circuit breakers capable of 5000 amps steady state and 63 kA fault current capacity available. (i.e. Siemens 8BK40)

- Induction motor drive capable of 30 MW based on scaling of LBES Motor

- Ship Service Power requirements based on anticipated future surface combatant requirements

- Propulsion Power requirements based on anticipated future surface combatant requirements

5.2 System Description

The system developed for this study is shown in Figure 5-1. Simplification of the overall system was required due to the limitations of the PSCAD Educational version. This version of the PSCAD software is limited to 220 electrical nodes. In order to meet this constraint, all ship service loads were allocated to only two load centers, each with a 4160/450 V transformer. An actual design would have multiple load centers distributed throughout the ship each with its own

transformer. The radar and gun system power requirements were also combined into a single load and to evaluate the worst-case harmonics were assumed to be fed from a six pulse rectifier. Four generators, two 10 MW and two 30 MW, and two main motors (30 MW each) were installed. Finally, loads were split evenly between two halves of the system.

Figure 5-1 Baseline IPS
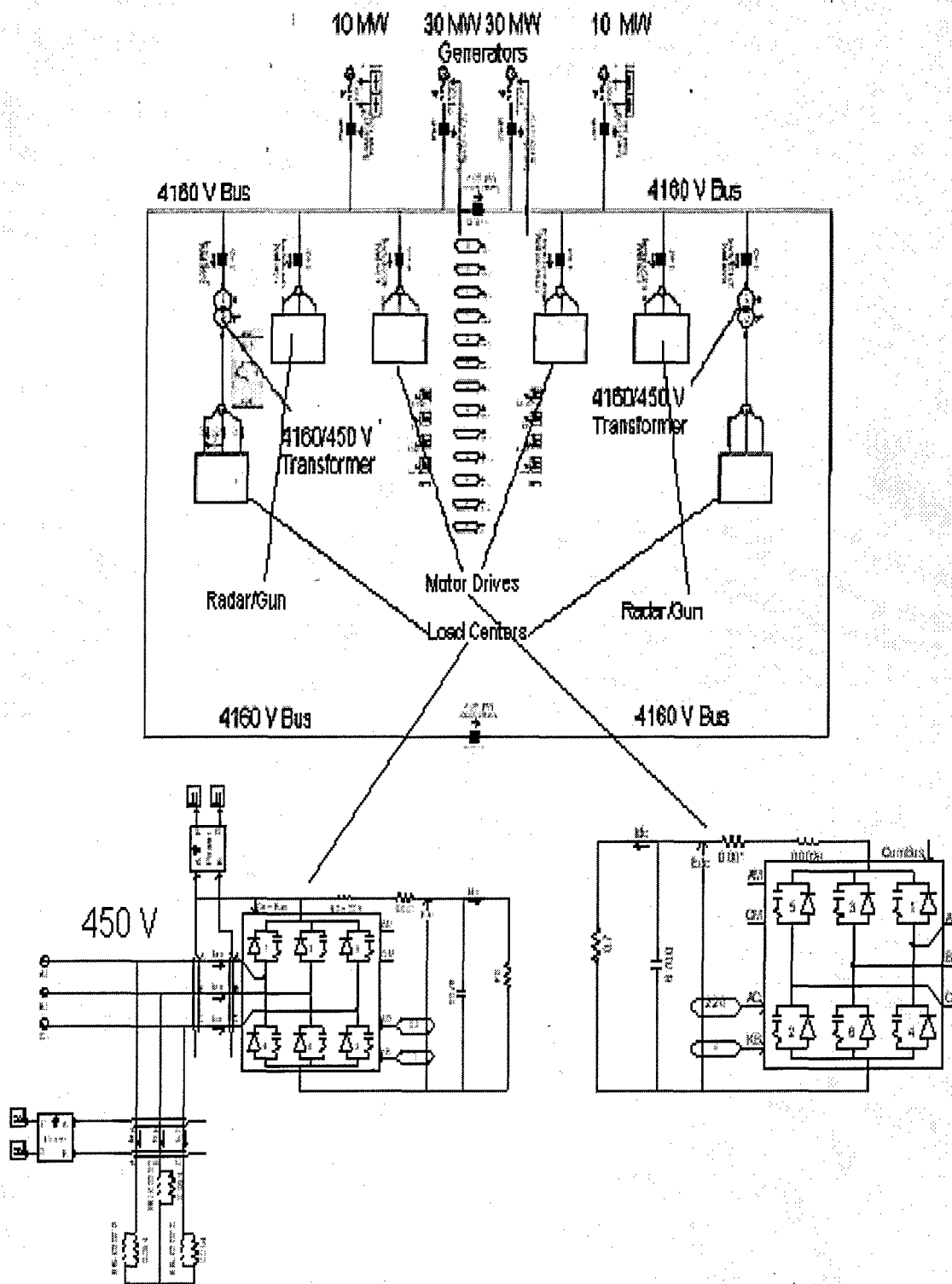
5.2.1 Generator

The system generator is the most important component in determining harmonic distortion characteristics of the system. The generator presents the lowest impedance at harmonic frequencies. This impedance can be determined from the subtransient reactance (Xd'') of the generator. As discussed in Chapter 4, harmonic voltages are developed across the phase to neutral system impedance due to harmonic currents generated by non-linear loads. In general for a given harmonic current content, voltage distortion increases with Xd''. This study assumed Xd'' of 20%. This is a typical value for generators of the size used in this study.[13]

A useful model for a synchronous machine is shown in Figure 5-2. This model represents the effects of rotor currents on the direct and quadrature axis. These are the per unit equivalent circuits for a synchronous machine with a single damper circuit on both the direct and quadrature rotor axis. The model terminals are constrained by voltage, assumes sinusoidal winding distribution, and employs the equal mutuals base system. There are the three phase windings on the stator and the field, direct, and quadrature windings on the rotor. The direct and quadrature windings are representations of current paths in the rotor. This machine model follows the derivation in [25]. In order to analyze this model, the stator variables are shifted to a reference frame attached to the rotor by the Park's transformation.

$$
T = \frac{2}{3}
\begin{bmatrix}
\cos(\theta) & \cos(\theta - \frac{2\pi}{3}) & \cos(\theta + \frac{2\pi}{3}) \\
-\sin(\theta) & -\sin(\theta - \frac{2\pi}{3}) & -\sin(\theta + \frac{2\pi}{3}) \\
1/2 & 1/2 & 1/2
\end{bmatrix}
$$

Equation 5-1

Stator phase quantities are transformed into direct and quadrature quantities as follows:

$$
\begin{bmatrix} v_d \\ v_q \\ v_0 \end{bmatrix} = T *
\begin{bmatrix} v_a \\ v_b \\ v_c \end{bmatrix}
$$

Equation 5-2

Phase variables can be recovered from the direct and quadrature quantities using the inverse transformation.

Currents are used as auxiliary variables as follows:

$$\begin{bmatrix} i_d \\ i_{kd} \\ i_f \end{bmatrix} = \begin{bmatrix} x_d & x_{ad} & x_{ad} \\ x_{ad} & x_{kd} & x_{ad} \\ x_{ad} & x_{ad} & x_f \end{bmatrix}^{-1} \begin{bmatrix} \psi_d \\ \psi_{kd} \\ \psi_f \end{bmatrix}$$

$$\begin{bmatrix} i_q \\ i_{kq} \end{bmatrix} = \begin{bmatrix} x_q & x_{aq} \\ x_{aq} & x_{kq} \end{bmatrix}^{-1}$$

Equation 5-3

And the state equations become:

$$\frac{d\psi_d}{dt} = \omega_0 v_d + \omega \psi_q - \omega_0 r_a i_d$$

Equation 5-4

$$\frac{d\psi_q}{dt} = \omega_0 v_q + \omega \psi_q - \omega_0 r_a i_q$$

Equation 5-5

$$\frac{d\psi_{kd}}{dt} = -\omega_0 r_{kd} i_{kd}$$

Equation 5-6

$$\frac{d\psi_{kq}}{dt} = -\omega_0 r_{kq} i_{kq} + \omega_0 v_f$$

Equation 5-7

$$\frac{d\psi_f}{dt} = -\omega_0 r_f i_f$$

Equation 5-8

$$\frac{d\omega}{dt} = \frac{\omega_0}{2H}(T_e - T_m)$$

Equation 5-9

$$\frac{d\delta}{dt} = \omega - \omega_0$$

Equation 5-10

Figure 5-2 Synchronous Machine Transient Model
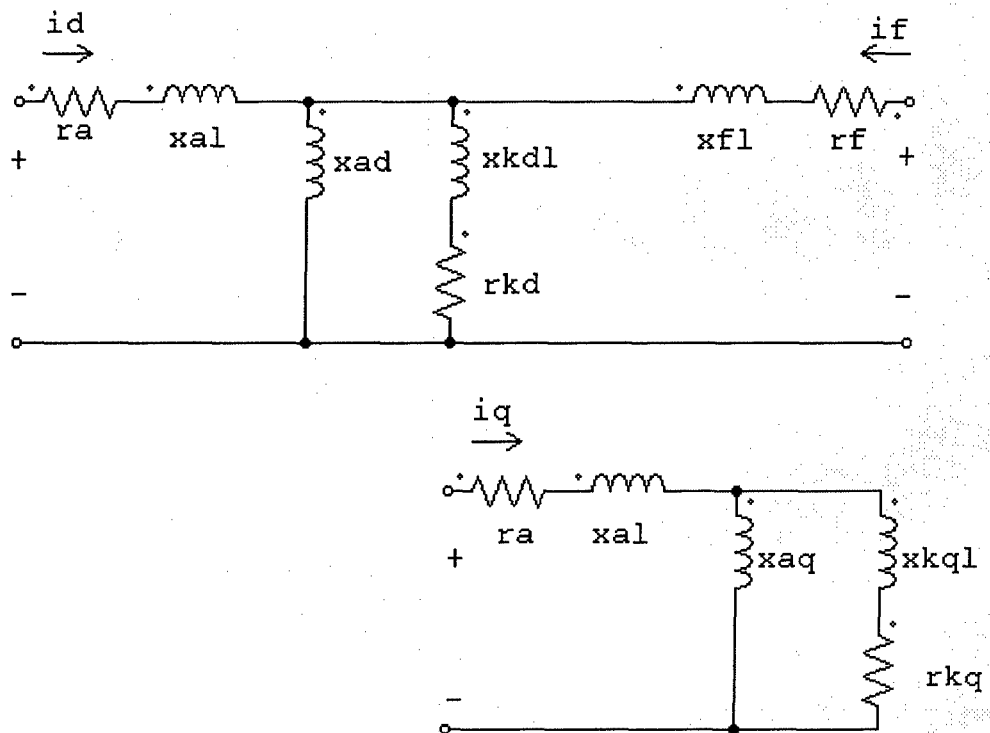
The model described above provides accurate results in a wide variety of situations. However, representations such as this are unnecessarily complicated for harmonic distortion studies and slow simulations considerably.

Harmonic distortion is a steady state phenomenon and therefore does not require the modeling of machine dynamics; however a modification of the typical steady state machine model is required for this study. A synchronous machine steady state equivalent circuit is normally represented as a voltage source behind a synchronous reactance where the synchronous reactance represents the combined effect or the air gap and leakage components.

Figure 5-3 Steady State Synchronous Machine Model
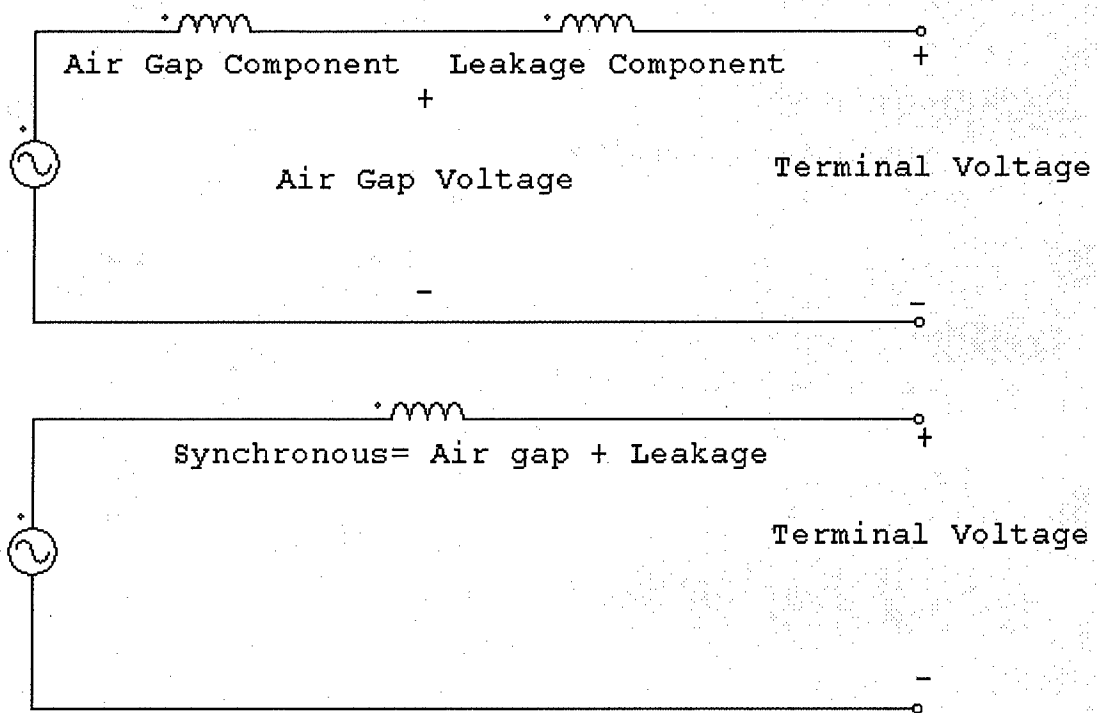
This model would not be adequate for this study in that the synchronous reactance is not the reactance seen by the harmonic currents. Instead, the generator was modeled as a voltage source behind subtransient reactance (X_d'') in order to accurately model harmonic distortion. The voltage source allowed for control of voltage, phase angle, and frequency. In situations where two generators were operating in parallel, one machine was set to automatically maintain bus voltage while the voltage and phase angle of the other machine were adjusted to ensure proper distribution of real and reactive power between the two machines.

The sizes of the generators were based on operational cost considerations. The prime mover for the generator on a surface combatant is a gas turbine engine. Gas turbines operate inefficiently when lightly loaded. For this reason generator sizing was chosen so that the system could be operated as much as possible with the generators loaded at 50% power or above. The power requirements for the future surface combatant are shown in Figure 5-4. A surface combatant spends the vast majority of its time at sea under cruise loading at speeds of less than

15 knots. The power requirements show a consumption of 10 MW with no propulsion power. This increases to roughly 20 MW at 15 knots. The power requirements dictated installation of two 10MW generators and two 30 MW generators operated in the following manner. For ship speeds up to 15 knots the two 10 MW generators would be online in a ring bus configuration. These generators would both be at 50% loading with no propulsion power required and increased to full loading at 15 knots. For ship speeds from 15 knots to 25 knots one 30 MW generator would be added to the ring bus. Finally, for speeds up to 30 knots the final 30 MW generator would be brought online and the bus would be split. It should be noted that marinized gas turbines in these power ranges at 4160 V are not in use by the US Navy. While this configuration allows the online gas turbines to be operated in the most fuel efficient manner, the costs associated with certifying gas turbine in these power ranges could negate these savings.

Splitting the electric bus for ship speeds above 25 knots is necessary due to circuit breaker fault current limitations. In addition to determining the harmonic distortion Xd'' also determines the maximum fault current in the case of a short circuit as follows:[14]

$$I_{sc} = \frac{VA_{rated}}{\sqrt{3}V_{line}x_d''}$$

Equation 5-11

In a 4160 V distribution system with Xd'' of 20%, the breaker limitation of 63 kA requires generating capacity on a single bus to be less than 73 MW.

Figure 5-4 Future Surface Combatant Power Requirements
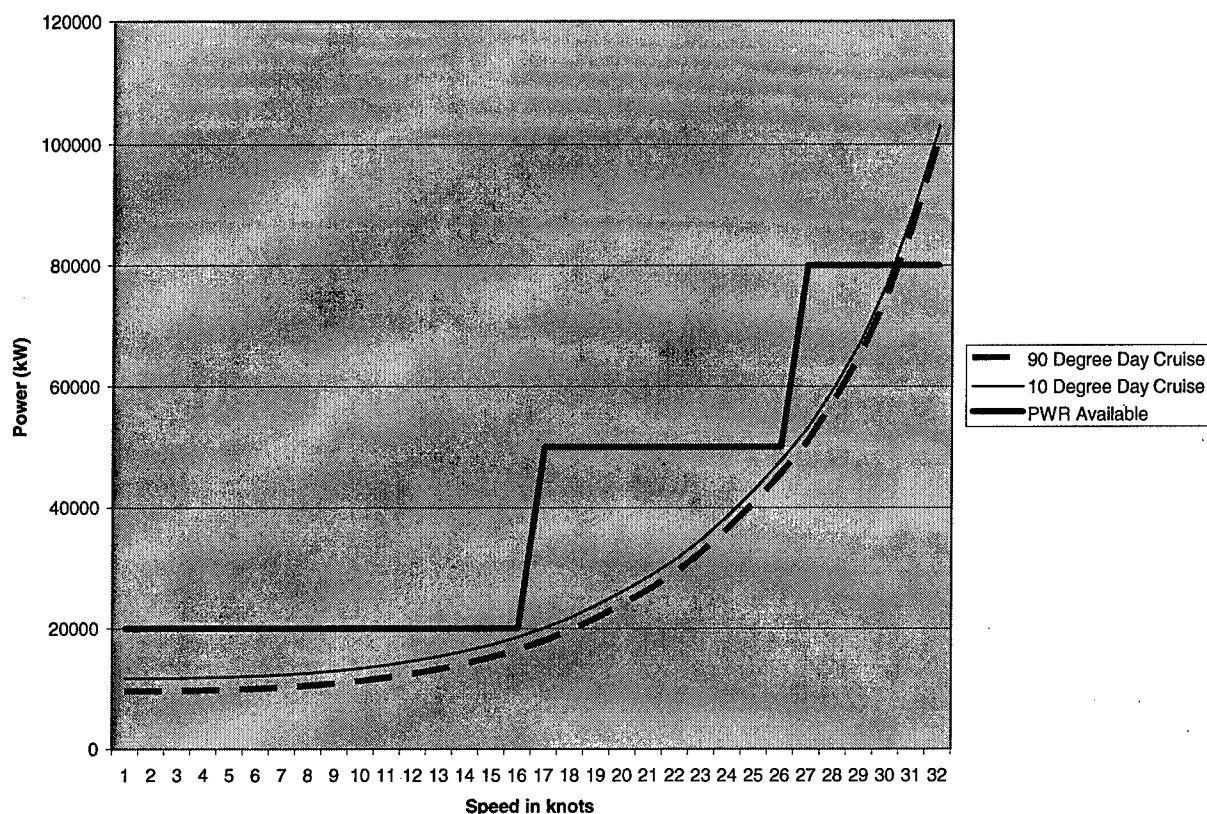
5.2.2   450 V Distribution and CAPS/AGS

The 450 V distribution block was developed to model the 3 phase 450 V equipment such as pumps, heaters, and other linear loads in addition to the DC load centers supplying sensitive equipment such as communication gear, computers, and unique DC power requirements. This architecture requires a transformer to reduce the main bus voltage to 450 V necessary to drive the legacy loads. Table 5-1 shows the ship service power requirements for the future surface combatant for various operating conditions. The total 450 V load was split evenly between the two busses of the distribution system. The linear load was modeled as a parallel R, L three phase load with a .8 power factor according to the following equations:

$$R = \frac{V^2}{P} \text{ and } L = \frac{V^2}{2\pi f_0 Q}$$

Equation 5-12

51

To account for worst case conditions, the non-linear load contribution was modeled as a six pulse rectifier and DC link driving a resistive load. The DC link for this component was designed for maximum power factor and minimum line current harmonics according to [22]. The script used for calculations of the DC link is included in Appendix A.

The combined array power system (CAPS) and the advanced guns system (AGS) power requirements were combined. The total power draw was split evenly between the two busses and was again simulated as a six pulse rectifier with a DC link designed for maximum power factor and minimum line current harmonics.

Table 5-1 Future Surface Combatant Ship Service Power Requirements

	Battle		Cruise		Anchor	
	90 degree	10 Degree	90 Degree	10 Degree	90 Degree	10 Degree
CAPS/AGS (KW)	3500	4500	2800	3700	800	1300
450 V Linear (KW)	5300	7700	5100	6300	2300	3400
450 V Non Linear (KW)	1800	1800	1600	1600	700	700
Total (KW)	10600	14000	9500	11600	3800	5400

5.2.3 Six Pulse Induction Motor Drive

The induction motor drive was modeled using the same parameters contained in 4.2.3.

Chapter 6 Baseline Simulations and Mitigation Techniques

This system described in Chapter 5 was simulated for ship speeds of 0, 15, 25, and 30 knots under each of the loading conditions listed in Table 5-1. The following parameters were measured:

- 450 V bus
    o Magnitude and phase of individual voltage harmonics
    o THD
- Generators
    o Magnitude and phase of individual current harmonics
    o THD

The results were compared to the requirements of MIL-STD-1399, IEEE STD 45-1998 Recommended Practices for Installation of Electric Installations on Shipboard, and IEEE STD 519- 1992, Recommended Practices and Requirements for Harmonic Control in Electrical Power Systems. MIL-STD-1399 and IEEE STD 45-1998 require THD for voltage not to exceed 5% with individual harmonic distortion less than 3%. These requirements are the same as those recommended in IEEE STD 519-1992 for general systems. Recommendations for dedicated systems in IEEE STD 519-1992 allows for up to 10% voltage THD. The more stringent requirements of MIL-STD 1399 and IEEE STD 45-1998 are based on protecting sensitive equipment such as communications and weapons systems. In an IPS system, this sensitive equipment is isolated form the distortion on the main bus by a rectifier and inverter. As long as the front end rectifier is designed to operate off of a bus with higher distortion levels the sensitive equipment should not be effected. In that motors and generators are normally rated with a consideration of 10% harmonic content (NEMA MG-1), the higher distortion limits of IEEE Std 519-1992 for dedicated systems should be adequate for the 450 V bus.

Setting a limit for current harmonics is more complicated than for the voltage harmonics. MIL-STD-1399 places the responsibility on the user equipment and its effect on the system bus. 60 Hz equipment of 1 kVA or more "shall not cause single harmonic line currents to be generated that are more than 3% of the unit's full rated load fundamental current". This requirement will be difficult to meet without extensive filtering or unnecessarily increasing the size and complexity of all electronic interfaces. Table 6-1 shows the IEEE STD 519 harmonic current profile for a six pulse converter. Every harmonic up to the 19th violates the requirements

of MIL-STD-1399. MIL-STD-1399 was written with segregated power systems in mind where the relatively small generators (2.5 MW on a typical surface combatant) are more easily affected by ship service loads. On an IPS ship, the only load that draws enough harmonic current to significantly affect the bus voltage profile is the propulsion motor drive.

Table 6-1 IEEE STD 519 Harmonic Current Profile

Harmonic	p.u. of Fundamental
1	1
5	0.192
7	0.132
11	0.073
13	0.057
17	0.035
19	0.027
23	0.02
25	0.016

The philosophy of IEEE STD 519-1992 is to limit harmonic injection from individual consumers in order to prevent voltage distortion that violates the previously stated limits. It is not realistic to apply the limits of IEEE STD 519-1992 to an IPS due to the differences in system characteristics between the terrestrial grid and an IPS. The limits imposed by IEEE STD 519-1992 are meant to control a wide number of customers all connected to the same power source. In an IPS, the Navy directly controls all pieces of equipment attached to the main bus and can more accurately predict the effect of each component on overall system performance. As long as the overall voltage distortion remains in specification the system will function properly.

Another complication in trying to set current distortion limits in the same way as the voltage distortion limits were set is that high current distortion does not necessarily result in high voltage distortion. The motor drive (LBES 19 MW) with a six pulse rectifier front end will be used to illustrate this point. Figure 6-1 and Figure 6-2 show the voltage and current on the AC side of the pulse width modulated (PWM) motor drive (the voltage in Figure 6-1 has been scaled to allow plotting on the same graph). At 10% power the current distortion is 67% and the voltage distortion is 4.8%. At 90% power the current distortion is 26% and the voltage distortion is 16.8%. The higher current distortion at 10% power does not lead to high voltage distortion because the magnitude of the harmonic current is small due to the lower power demand. The high current distortion at low powers is a characteristic of PWM motor drives. This

characteristic is due to a large capacitor in the DC link. Current only flows when the output of the rectifier is higher than that of the capacitor. At light loads, the ac side current is discontinuous and only becomes continuous as load on the DC link increases.

For the reasons listed above it makes sense to establish current distortion limits based on the ratings of the generators. The fifth and seventh harmonic current limits for the generator installed at LBES are 9% and 8% of the fundamental limit. [23] NEMA MG-1 allows for 10% voltage distortion in the ratings of machines suggesting that higher current distortion levels are acceptable. For the purpose of this study the LBES generator limits will be used as a benchmark for acceptable levels of current distortion. Table 6-2 shows the current limits for the generators used in this study.

Table 6-2 Generator Current Ratings

	10 MW Generator	30 MW Generator
Fundamental Current Limit	1734 A	5204 A
5th Harmonic Current Limit	156 A	468 A
7th Harmonic Current Limit	138 A	416 A

Figure 6-1 Voltage and Current 10% Power
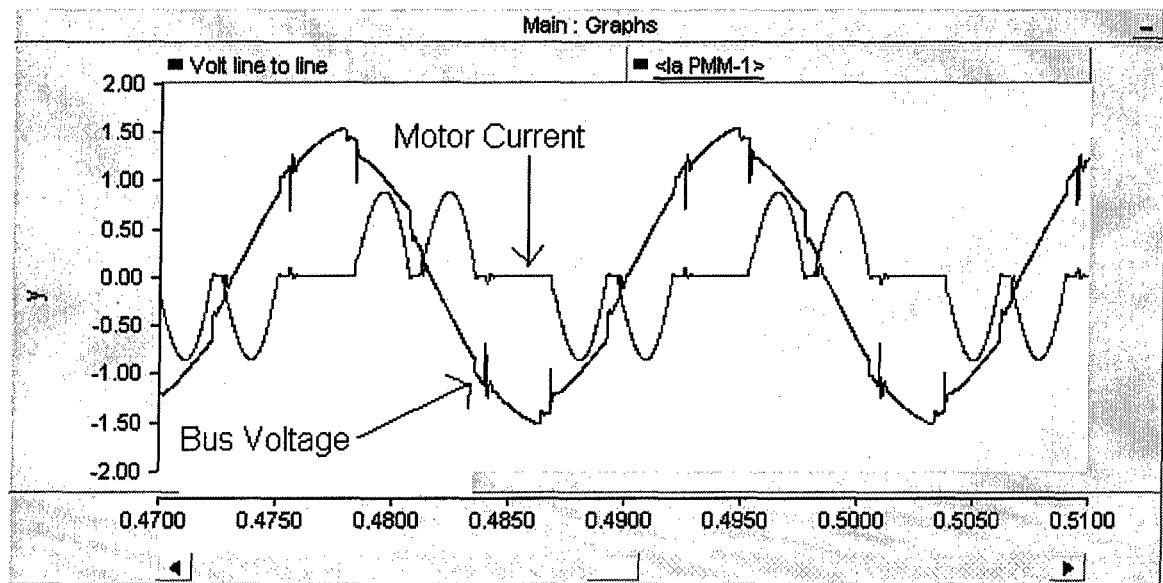
Figure 6-2 Voltage and Current 90% Power
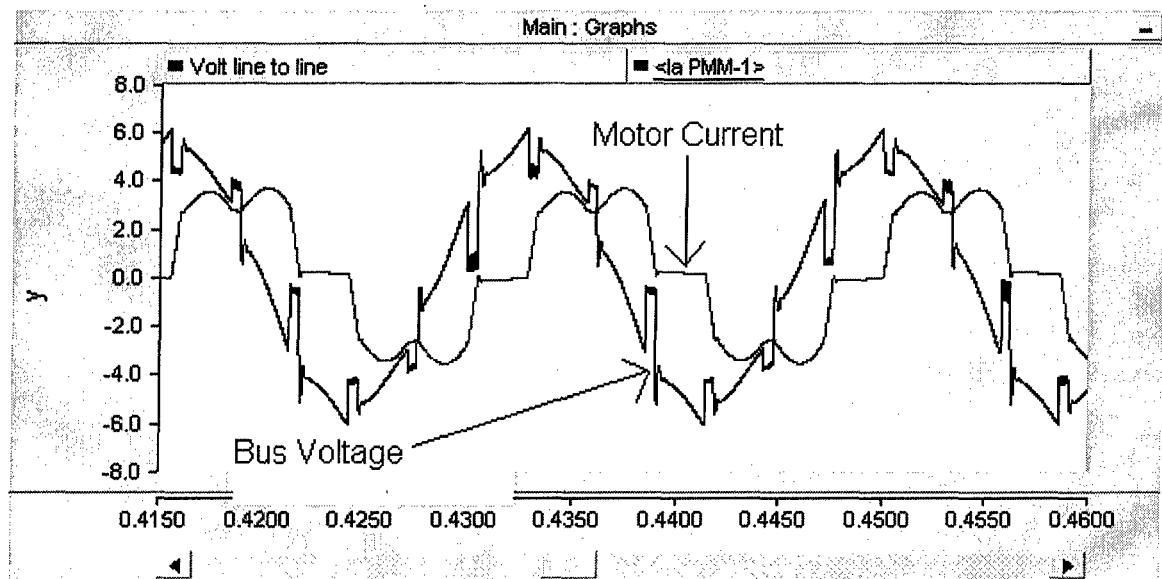
6.1.1 THD on the 450 V bus

The most important simulation results concern the voltage distortion on the 450 V bus.
Figure 6-3 shows THD on the 450 V bus for each of the simulation cases. The baseline six pulse
system violates MIL-STD 1399 and the guidelines of IEEE 519-1992 for dedicated systems for
all loading conditions and ship speeds simulated when the propulsion motors are operating. The

voltage distortion meets both criteria without the propulsion engines operating (the 0 knot series of Figure 6-3). Typically, you would expect that as propulsion power increases so would voltage distortion due to the increased magnitude of the harmonic currents. In these simulations this is the case but only within the discrete generator operating configurations. For example, at 15 knots both 10 MW generators are operating at full power. If an 18 knot ship speed is desired, the 30 MW generator must be brought onto the bus in order to supply this additional power. The addition of the 30 MW generator reduces the phase to neutral system harmonic impedance and possibly reduces the overall system voltage distortion despite the additional harmonic current from the power increase

In the baseline IPS simulation the highest distortion occurs at 25 knots. However, the distortion level is only slightly higher than the 15 and 30 knot conditions. The 15, 25, and 30 knot speeds correspond to the maximum propulsion power for a given generator configuration and therefore the highest voltage distortion in each configuration. Even though propulsion power (and harmonic current magnitude) more than doubles between the 15 and 25 knot conditions, and again between the 25 and 30 knot conditions, THD(voltage) remains relatively constant due to the decrease in system harmonic impedance from the additional power generation capability brought online to meet the propulsion demand.

Figure 6-3 also illustrates that the distortion level of the power system is not significantly influenced by changes in loads other than the propulsion motor. The cruise loading condition on a 90 degree day is the condition with the least amount of non propulsion load and results in the worst case distortion for the system but only by a marginal amount. This is particularly true at the highest propulsion motor powers. Table 5-1 shows that there is almost a 5 MW difference in ship service loading between the 90 degree cruise condition and the 10 degree battle condition. At full propulsion power this additional load reduces total distortion by only 0.3 %. At 15 knots, where the total propulsion power (6 MW) is less than ship service loads, the reduction in distortion is 2%.

Figure 6-3 THD 450 V Baseline System
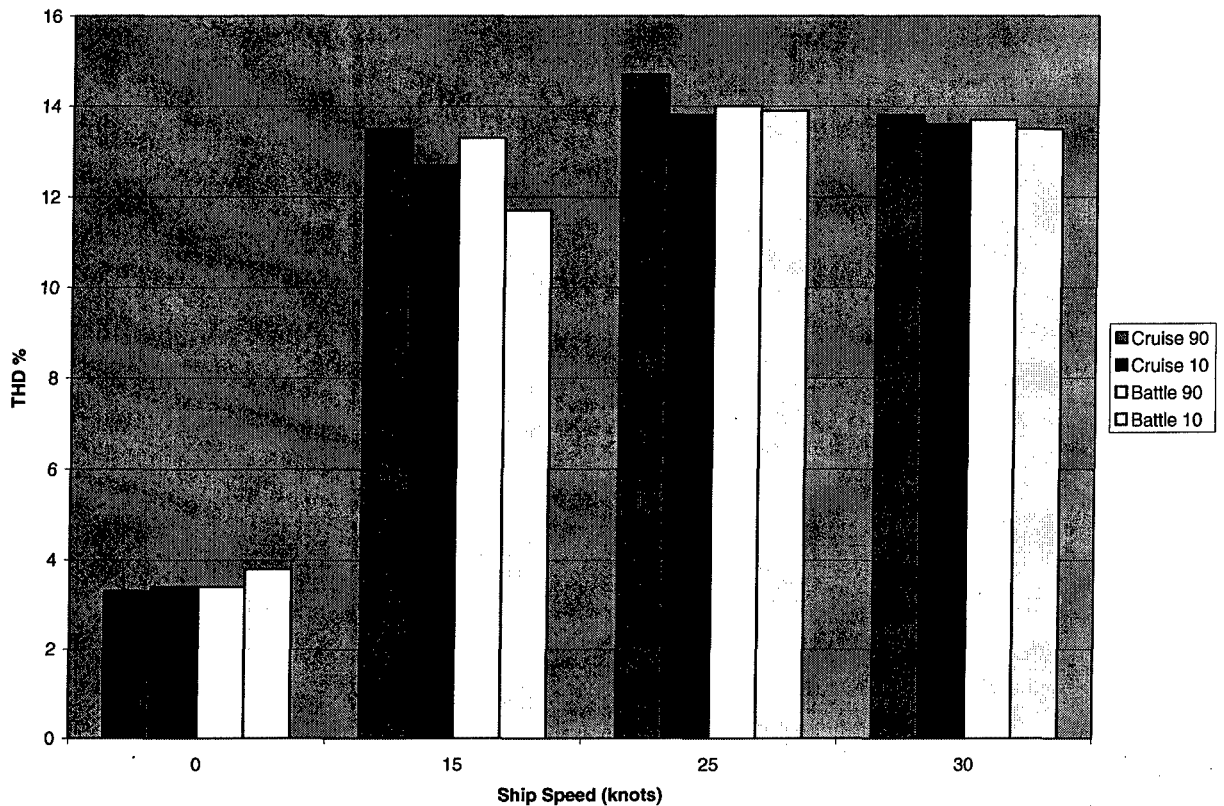
The 90 degree, cruise loading condition was chosen to conduct a more detailed look at THD over the entire propulsion motor loading range. As mentioned in the preceding paragraph, this was the loading condition that resulted in the highest distortion levels. It can be assumed that the other loading conditions would exhibit a similar response over the operating range but at slightly lower distortion levels. Figure 6-4 shows the voltage distortion from 0 knots to 30 knots. The three curves represent the discrete electric plant configurations. The three configurations are:

- Two 10 MW generators in parallel on a ring bus (0-15 knots)
- Two 10 MW and one 30 MW generators in parallel on a ring bus (15-25 knots)
- Split plant with a 10 MW and 30 MW generator on each side (25-30 knots)

The drop in distortion levels at the transitions between the configurations is evident. The lower generator impedance results in lower distortion levels. The figure also shows that the voltage

58

distortion levels meet IEEE Std 519-1992 at speeds less than 13 knots. This is significant in that navy ships spend 90% of their time at sea at speeds less than 13 knots.

Figure 6-4 THD vs Speed, Cruise Loading, 90 degree day
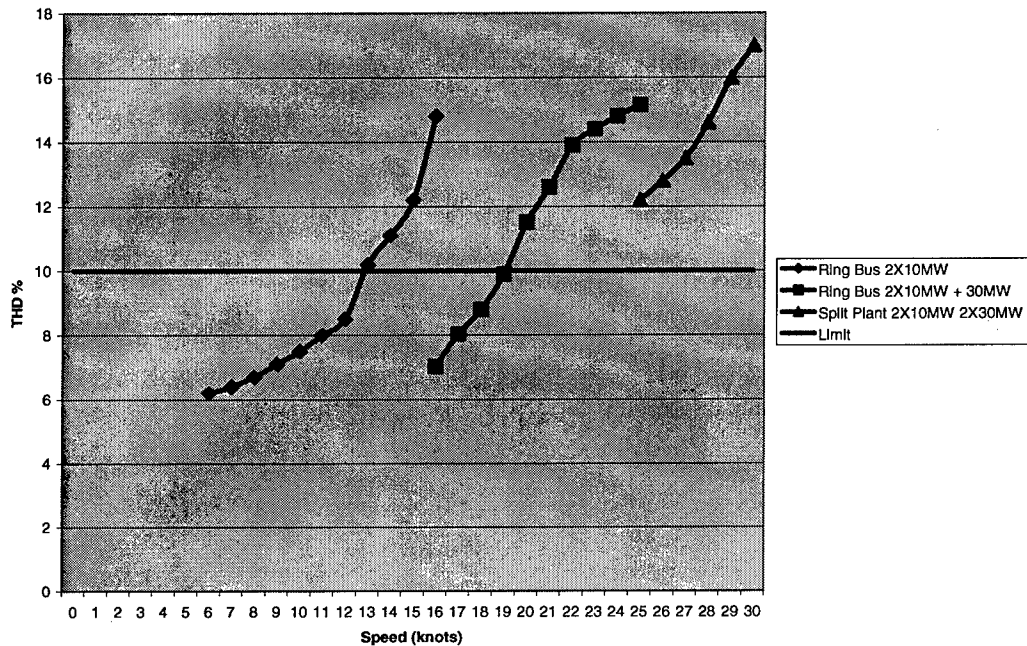
The individual harmonic components for each speed and loading case are shown in Figure 6-5 through Figure 6-8. The figures show that the fifth and seventh harmonics are the major contributors to the voltage distortion. These harmonics violate MIL-STD- 1399 in every simulation except for the 0 knot simulation. Tabulated results of the baseline simulations are included in Appendix C.

Figure 6-5 Individual Harmonic Voltages, Cruise Loading, 90 degrees
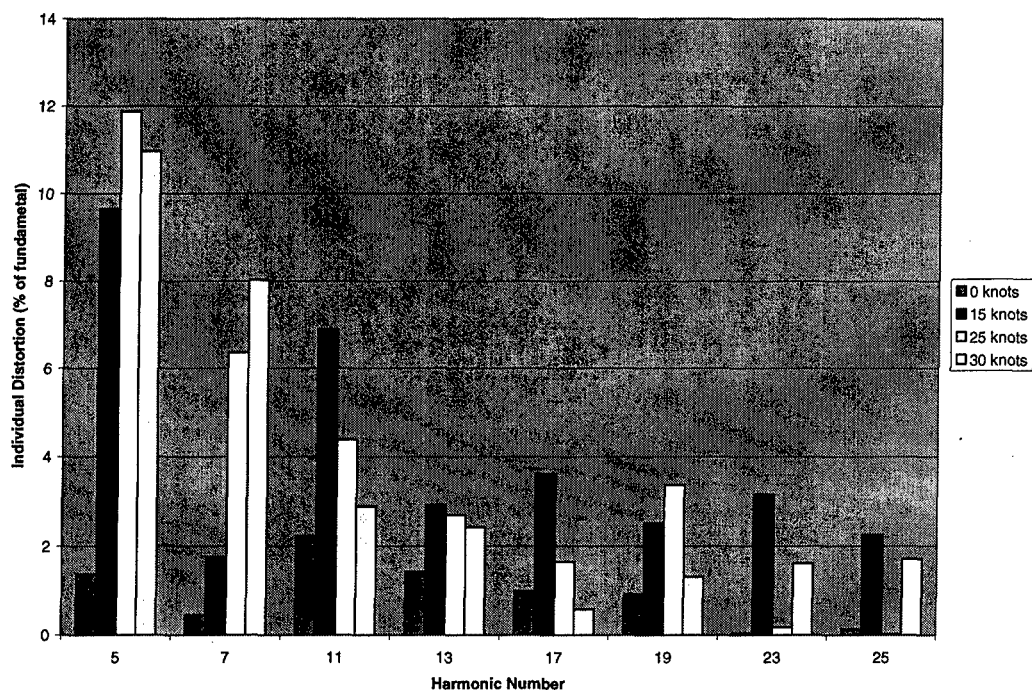
Figure 6-6 Individual Harmonic Voltages, Cruise Loading, 10 Degrees
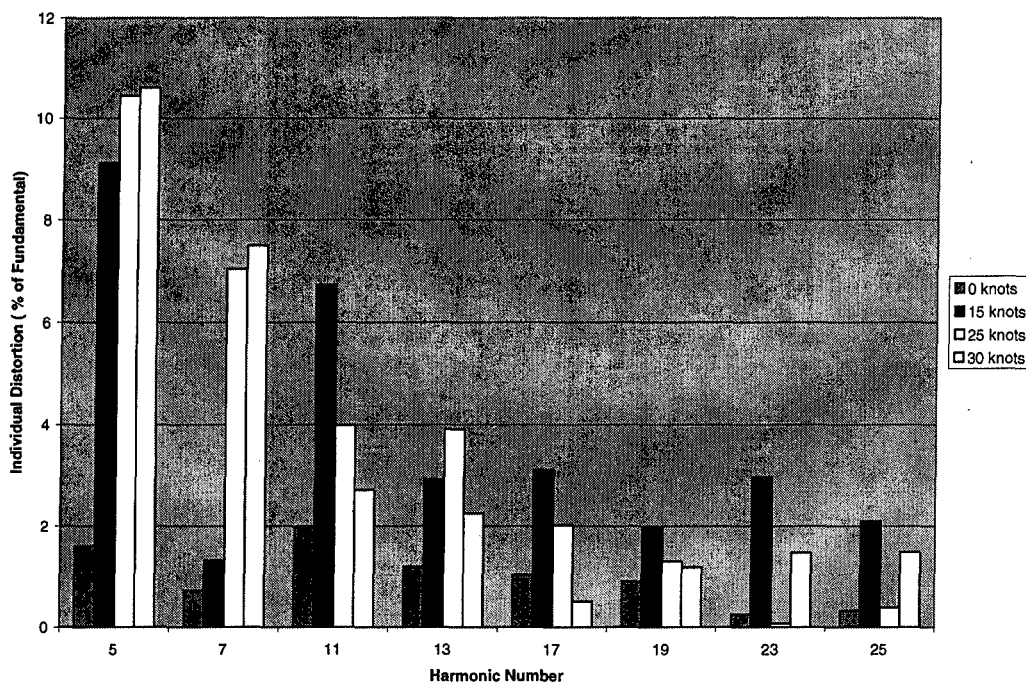
Figure 6-7 Individual Harmonic Voltages, Battle Loading, 10 degrees
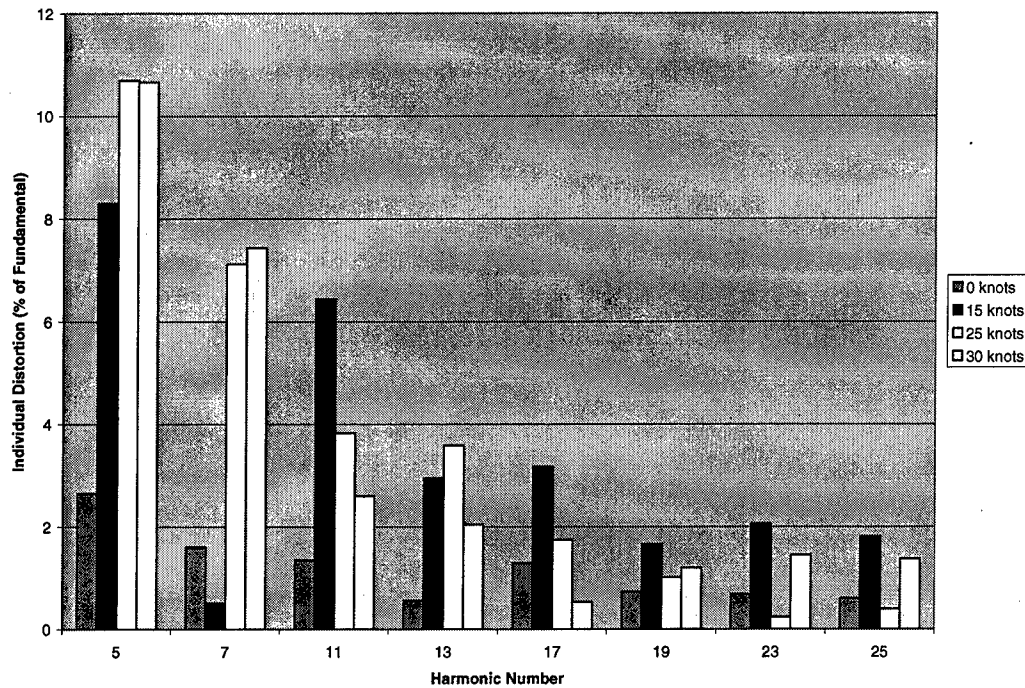
Figure 6-8 Individual Harmonic Voltages, Battle Loading, 10 degrees
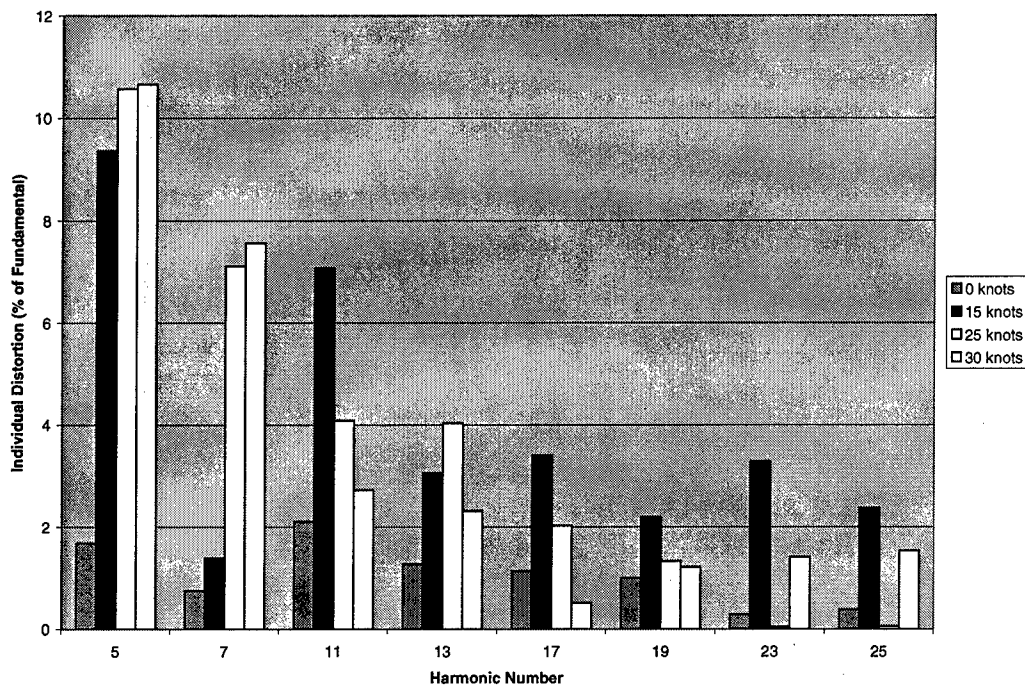
6.1.2   Generator Current Distortion

The individual harmonic current magnitudes for the 90 degree day cruise loading

conditions are shown for each generator in Figure 6-9 and Figure 6-10. As with the voltage

distortion, the ship service loading had little effect on the overall results for current distortion.

The results for the other loading conditions were similar. Tabulated results of all baseline

simulations are included in Appendix C. The fifth harmonic current limit for the 10 MW

generator and the 30 MW generator is 156 A and 468 A respectively. The seventh harmonic

current limits are 138 A and 416 A. The baseline system violates the fifth harmonic limit for

both the 10 MW generator and the 30 MW generator at the 25 and 30 knot speeds. The seventh

harmonic is within the limit for all cases.

Figure 6-9 Harmonic Current Magnitude (RMS) 10 MW Generator
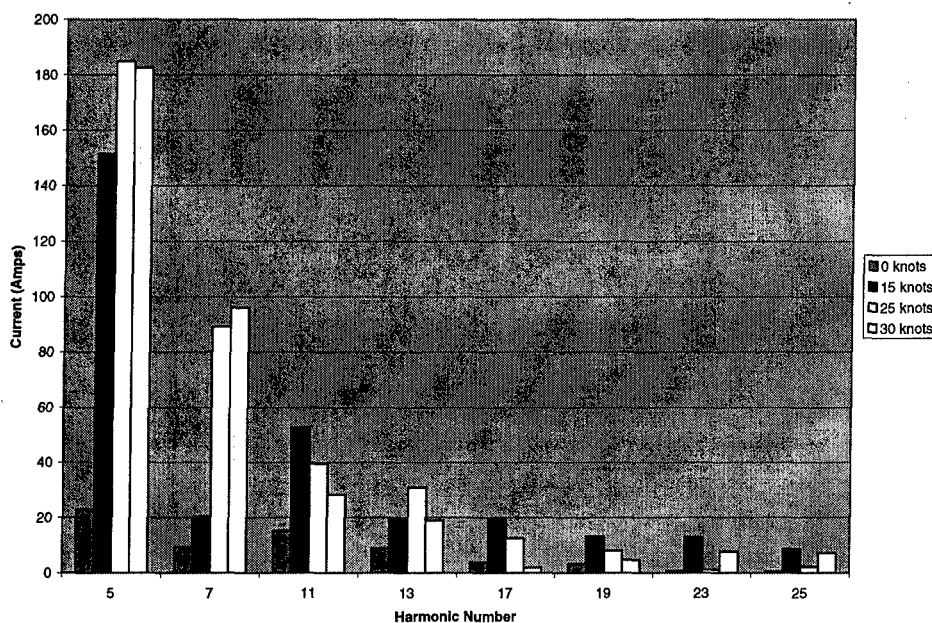
Figure 6-10 Harmonic Current Magnitude (RMS) 30 MW Generator
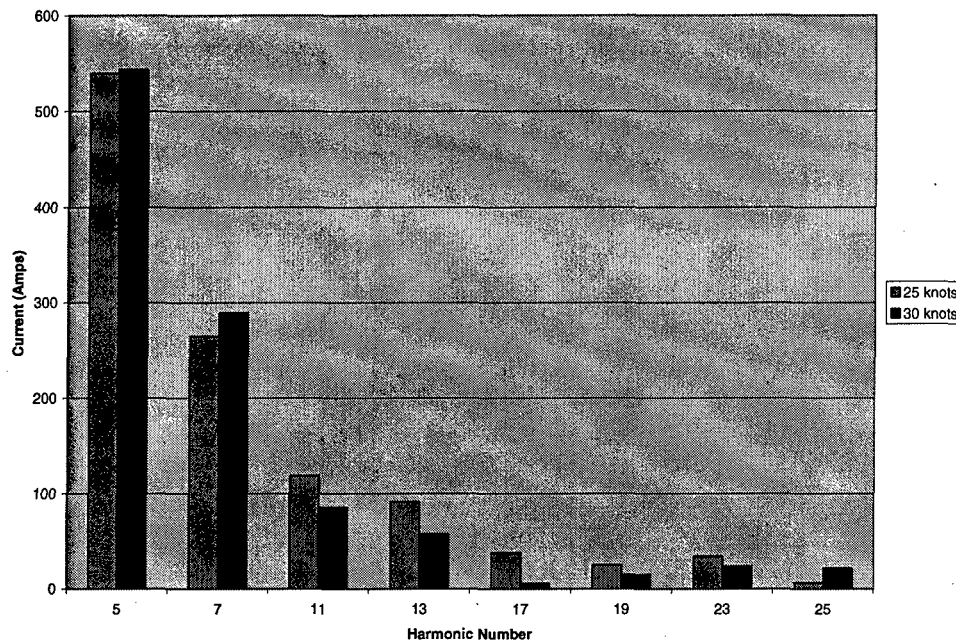
6.1.3 Baseline Simulation Conclusions

The baseline IPS with a six pulse motor drive results in unacceptable voltage distortion and current distortion levels which could cause overheating of rotating machinery such as the main generators and various shipboard loads. While the voltage distortion levels are high for speeds above 13 knots, the system operates within the guidelines of IEEE Std 519-1992 for speeds less than 13 knots. The generator current data suggests that the majority of the distortion is caused by the fifth and seventh harmonic. Figure 6-11 shows the 30 MW generator current for the 10 degree day loading condition and the ship at 25 knots. This waveform was generated in a MATLAB script (Appendix A) from the magnitude and phases of the individual harmonic components. In Figure 6-12 the generator current waveform was generated with the fifth and seventh harmonic removed. The improvement in THD suggests that if the fifth and seventh harmonics were attenuated a design which meets the established criteria for voltage and current could be achieved. In the following section methods of removing these harmonics will be investigated.

Figure 6-11 Generator Current, 10 deg day, 25 knots

THD =25.1951%
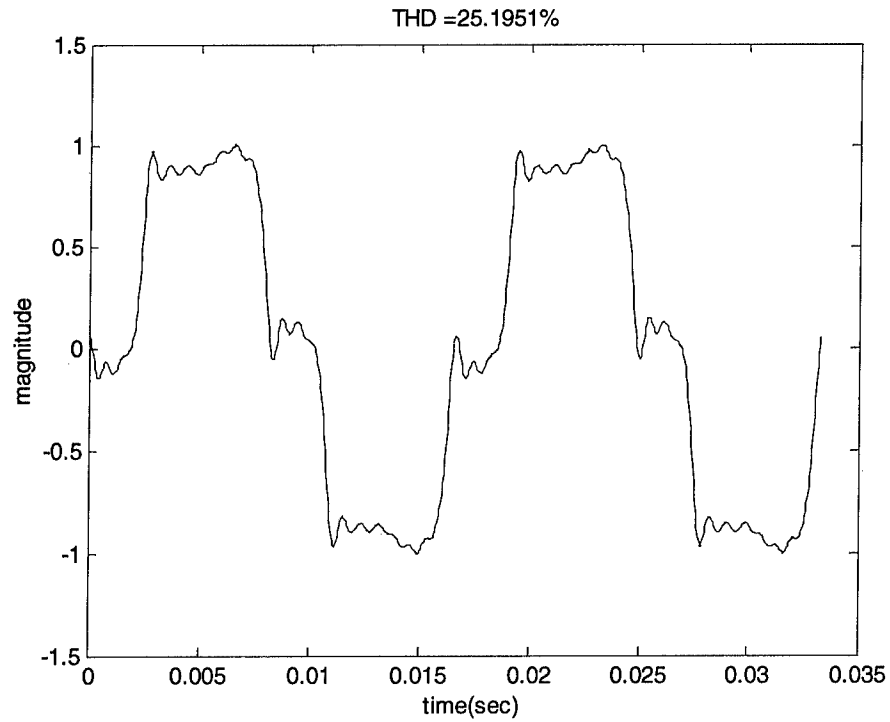
Figure 6-12 Generator Current, 10 deg day, 25 knots, 5th and 7th Harmonics Removed

THD =10.4033%
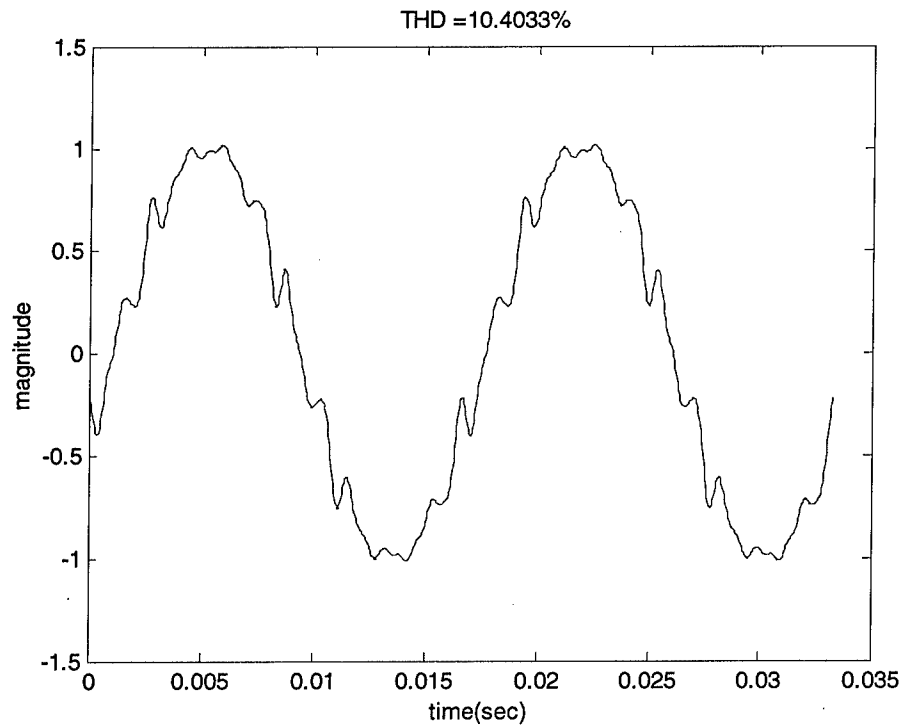
6.2 Harmonic Distortion Mitigation Techniques

The results of Chapter 6 clearly indicate that in order to implement an IPS with this configuration the harmonic current magnitudes at the fifth and seventh harmonics must be reduced. There are three methods employed in industrial and commercial power systems to reduce the flow of harmonic currents. These are: [24]

- Use of shunt filters
- Use of multipulse power converters
- Harmonic current injection

In this section the first two methods of attenuation listed above will be simulated in order to obtain system results. In addition to these two methods a modification to the operation of the propulsion motor drive will also be simulated.

6.2.1 Line Commutated Rectifier Motor Drive

Section 4.2.3 describes the operation of the propulsion motor drive used in the simulation. As mentioned earlier, this is a phase controlled converter whose firing angle is controlled as shown in Figure 6-13. The firing angle of the converter is controlled to maintain stability on the DC link between the rectifier stage and inverter stage of the motor drive circuit. One consequence of controlling DC link voltage in this manner is that it degrades the power factor of the motor drive. The relationship between power factor and THD is established in Equation 2-11 through Equation 2-14. In general, the power factor of the converter decreases with increasing alpha. [9]

Figure 6-13 Propulsion Motor Firing Angle
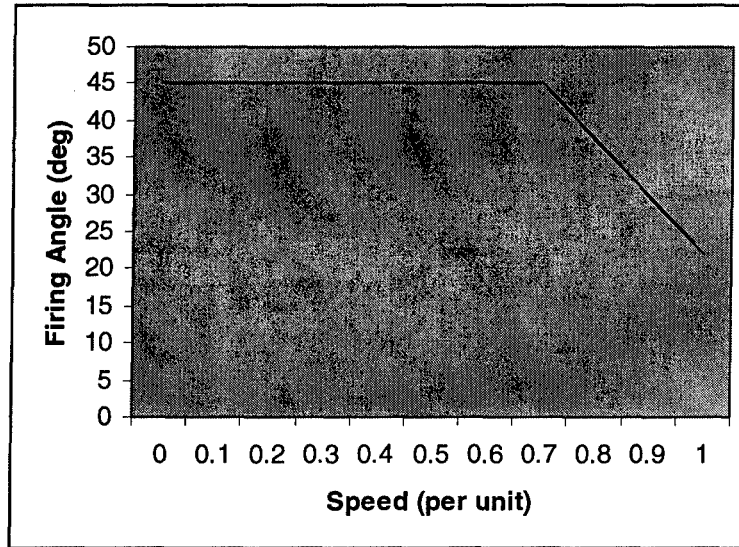
The system was simulated with the motor drive rectifier operating as a line commutated rectifier by setting the firing angle of the bridge thyristors to zero degrees. Operating the rectifier in this manner will result in lower harmonic distortion. The 90 degree day cruise loading condition was used in the model and propulsion loads up to 30 knots were simulated. The results are shown in Figure 6-14. As expected, operating the front end rectifier as a line commutated converter significantly reduces the voltage distortion of the system. The limits of IEEE Std 519-1992 are only exceeded at the highest propulsion loads for the last two electric plant configurations. Figure 6-15 shows the individual harmonic contribution for the line commutated and the phase controlled propulsion motor drive of the baseline system simulated with 90 degree day cruise loading at 30 knots. A marked reduction in the fifth and seventh harmonic is noticed.

Figure 6-14 Six Pulse Line Commutated Propulsion Converter
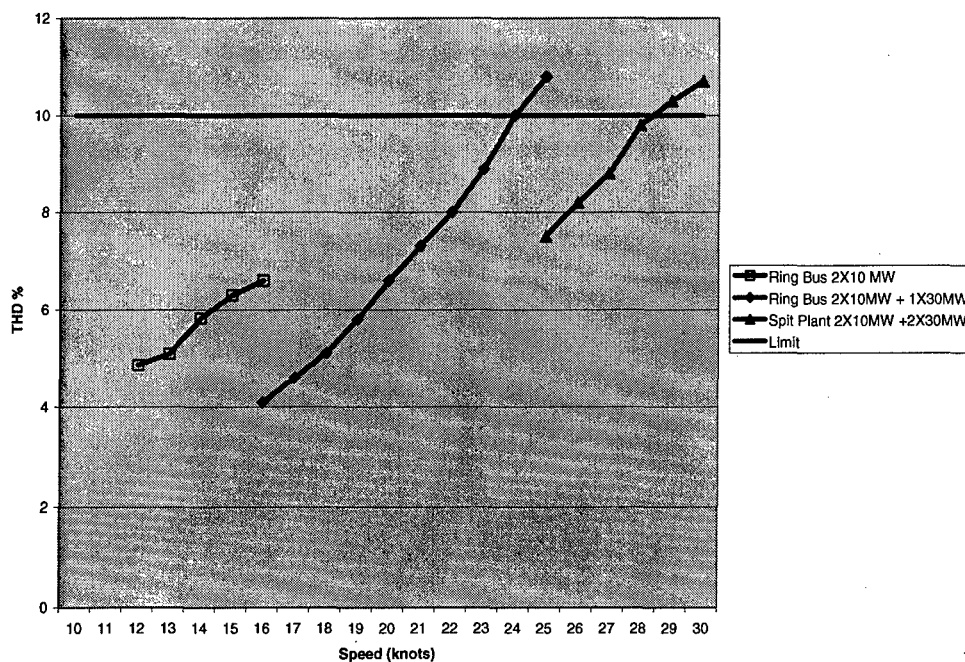
Figure 6-15 THD Comparison, Line Commutated vs Phase Controlled Motor Drive
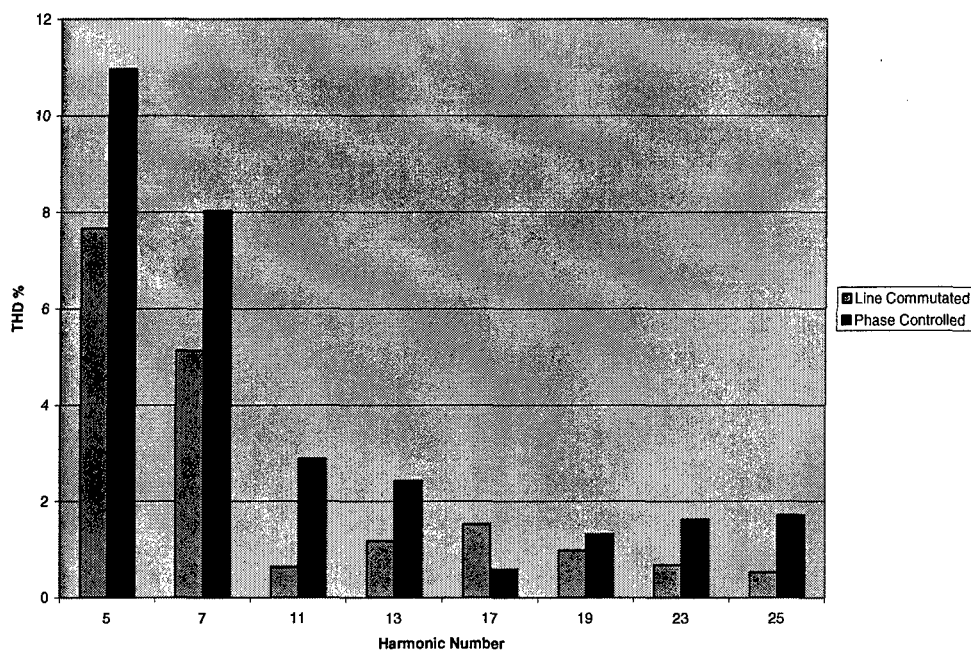
The fifth harmonic current for the baseline system was above the limit for both the 10MW and the 30MW generator in the baseline system at 25 and 30 knots. Figure shows the individual

67

harmonic current magnitudes at 25 and 30 knots for the baseline and the line commutated system. The fifth harmonic is now less than the limit for both generators. (156 A -10MW, 468 A -30 MW) Tabulated results of the simulations are contained in Appendix C Table 8-7.

Figure 6-16 Individual Harmonic Current (10 MW Generator)
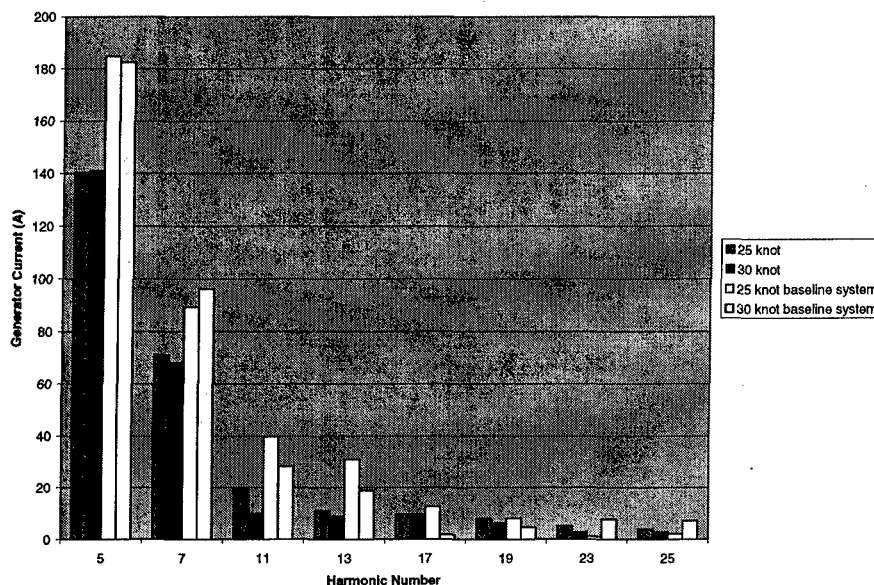
Figure 6-17 Individual Harmonic Current (30 MW Generator)
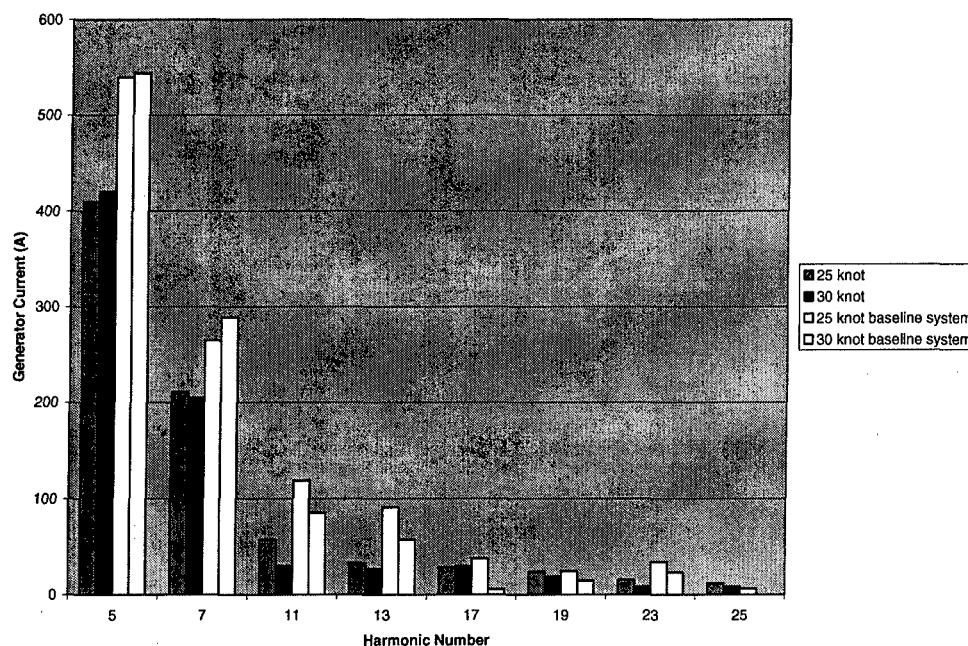
6.2.2 Multipulse Motor Drive and Harmonic Filter Systems

The two methods most commonly used to reduce harmonics on power systems are the addition of shunt harmonic filters and/or the use of a multipulse converter. The baseline system described in 5.2 was modified to incorporate these two methods of harmonic mitigation. Each method was implemented separately.

The fifth harmonic filter described in 4.2.2 was used as the basis of the filter designed for this simulation. The resonant frequency of the filter is given by:

$$f_0 = \frac{1}{2\pi\sqrt{LC}}$$

Equation 6-1

Where f_0 is the resonant frequency
      L   is the inductance of the filter
      C   is the capacitance of the filter

IEEE Std 141-1993 recommends the following steps in the design of a filter for harmonic mitigation.

- Selection of a capacitor value based on power factor improvement

- Design an inductor to series tune the capacitor to the desired harmonic

- Calculate peak voltage and current in order to select components

This method is not suitable for an IPS due to the wide range of reactive load experienced by the power system. The capacitor selection step presumes that the amount of MVar is known and relatively steady. In the baseline system of 5.2 the system MVar increases for 7 to 38 when propulsion power increases from 0 to 100%. Designing a filter for the 38 MVar at full power would be far too large for normal operations and would be larger than needed to reduce distortion within limits. Due to space consideration on ships, the ideal filter is the smallest filter that reduces distortion limits to within specifications.

The capacitor in the filter injects reactive power according to the following equation:

$$M\,\mathrm{var}_c = \frac{kV^2}{X_c}$$

Equation 6-2

The LBES uses a 282uF capacitor rated at 2900V for the fifth harmonic filter. Equation 6-2 tells us that this filter will inject 1.83 MVar. The inductor necessary to tune the filter to the fifth

harmonic is 1mH according to equation 5-3. This filter was added to the input to the propulsion motor drive of the baseline system in order to reduce the fifth harmonic.

The 12 pulse motor drive was derived from the LBES motor drive of 4.2.3. Two six pulse rectifiers can be combined to produce twelve pulse operation if the ac input signal to one rectifier is phase shifted by 30^0. The phase shift is accomplished by use of transformer connections and shown Figure 6-18. One transformer is connected wye-wye while the other is connected delta-wye. The delta-wye connection produces the necessary phase shift and the combination of the two transformers produce six phases necessary for 12 pulse operation. The currents of interest are shown in Figure 6-19. The current Iwye is the normal six pulse input current. The current Idelta contains no triple-n harmonics due to the delta connection of the transformer. The line current Iline is the sum of Iwye and Idelta and results in a waveform where the fifth and seventh harmonics are cancelled. The first non-zero harmonic present in the line current is the 11th.

Figure 6-18 12 Pulse Converter
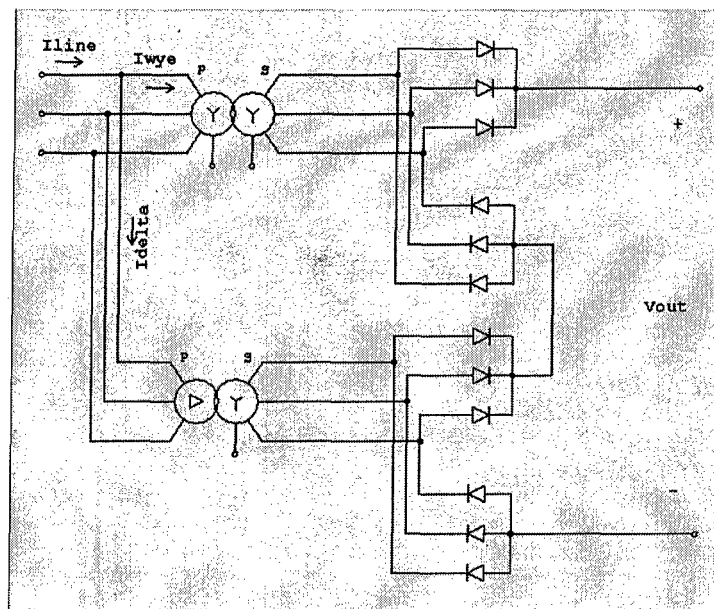
Figure 6-19 12 Pulse Line Current
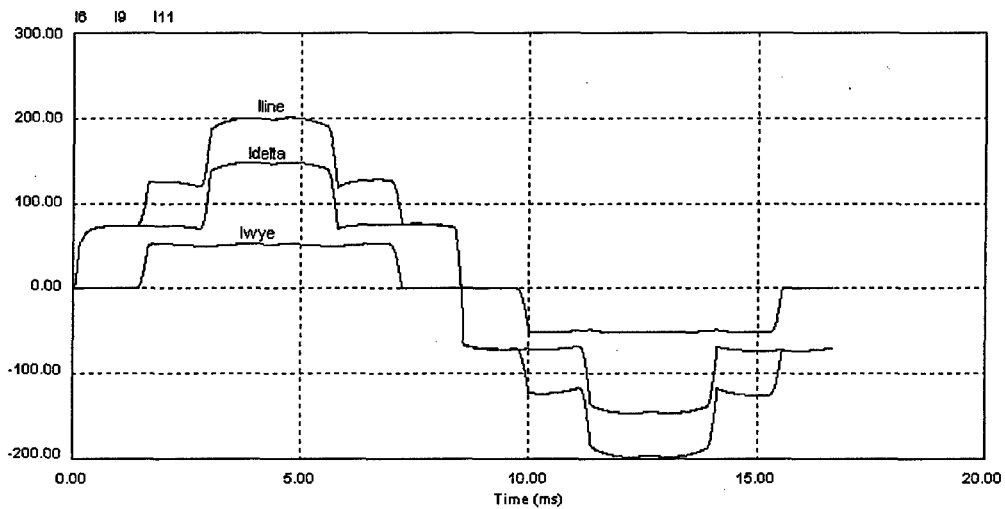
Simulations for the 15, 25, and 30 knot speeds with the 90 degree day cruise loading condition were performed for the baseline system with the harmonic filter addition and the baseline system with a 12 pulse motor drive. Both of the alterations reduced voltage distortion levels to within the limits of IEEE Std 519-1992. Figure 6-20 shows a comparison of the distortion levels for the baseline system compared to the filter system and the 12 pulse motor drive system. Figure 6-21 and Figure 6-22 show the THD for the filter system and 12 pulse system over the operating range of the ship. Tabulated results are contained in Appendix C, Table 8-8 and Table 8-9.

Figure 6-20 THD Comparison
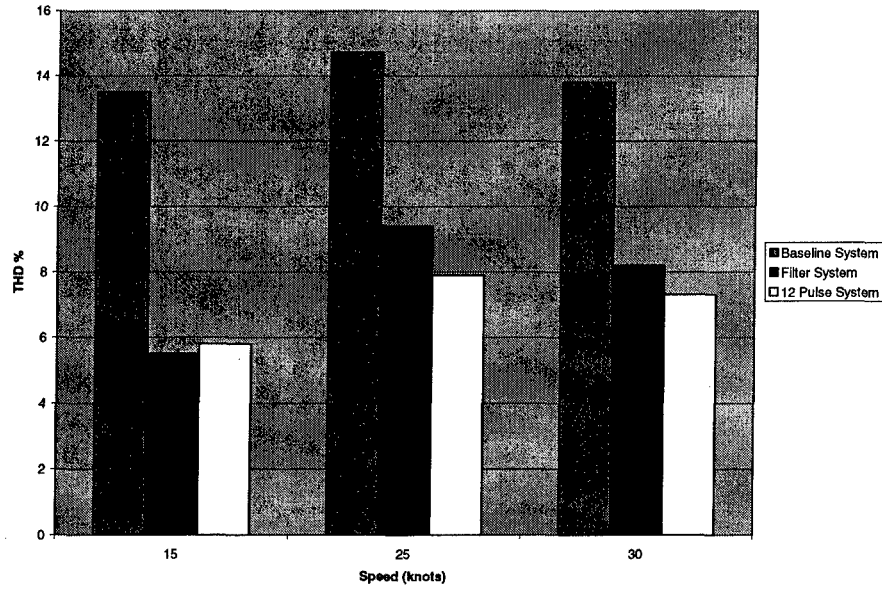
Figure 6-21 Filter System THD
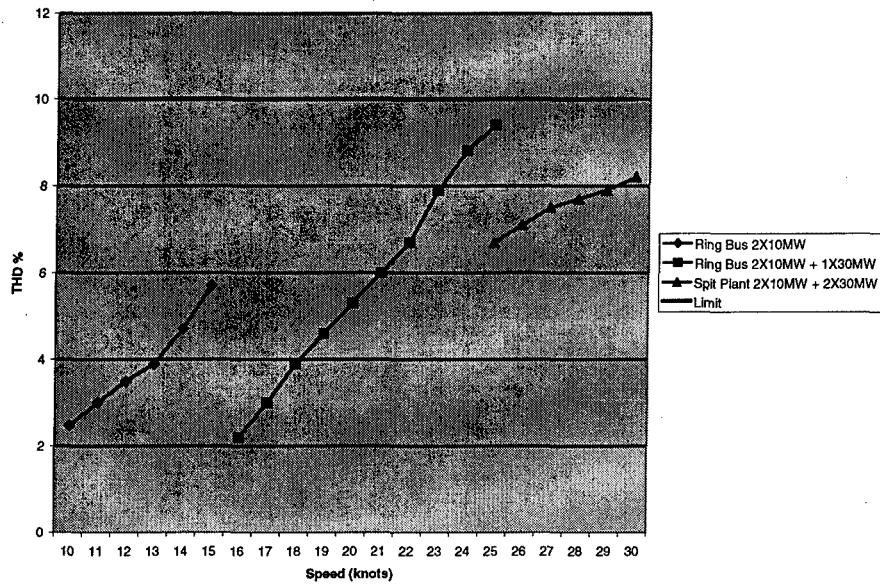
Figure 6-22 THD 12 Pulse System
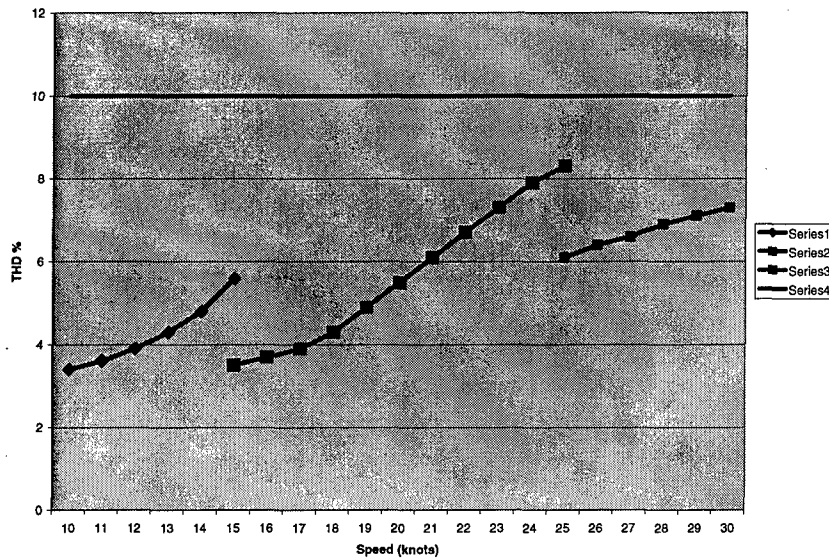
The individual harmonic voltages are plotted as a percent of the fundamental in Figure 6-23 and Figure 6-24 the 12 pulse and the filter system respectively. The fifth and seventh harmonics have almost been eliminated in the 12 pulse system as expected. They are still present due to the fact that the DC load centers and AGS/CAPS system still draw fifth and seventh harmonic. In the filter system, the fifth harmonic is the only harmonic which has been significantly reduced due to the design of filter. However, as mentioned above this attenuation is enough to bring the system to within the limits of IEEE Std 519-1992 for dedicated systems.

Figure 6-23 Individual Distortion 12 Pulse System
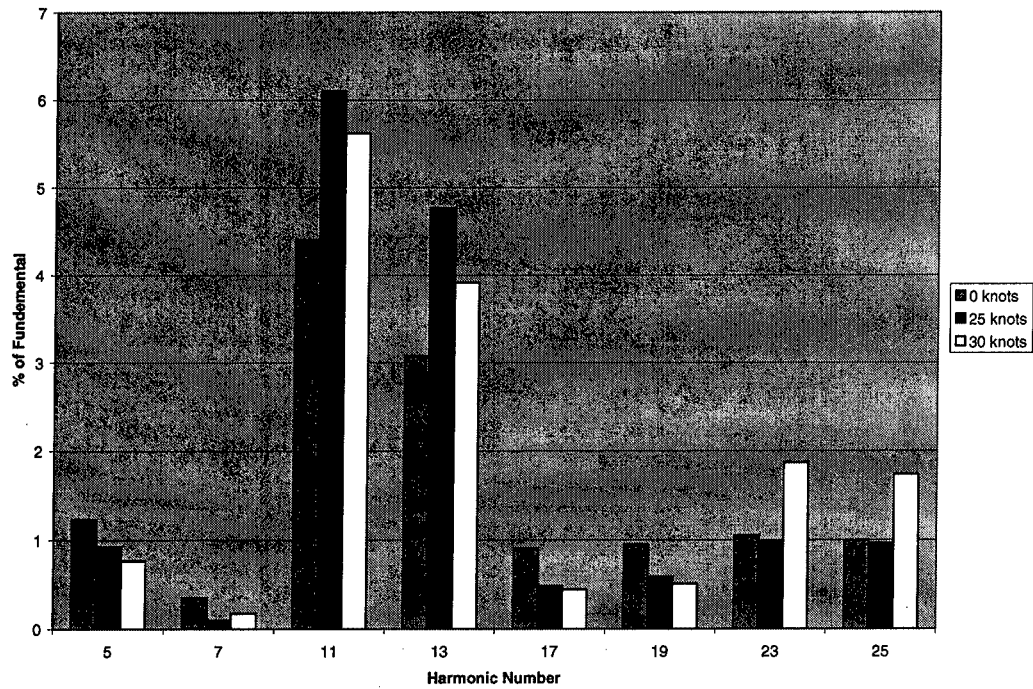
Figure 6-24 Individual Distortion, Filter System
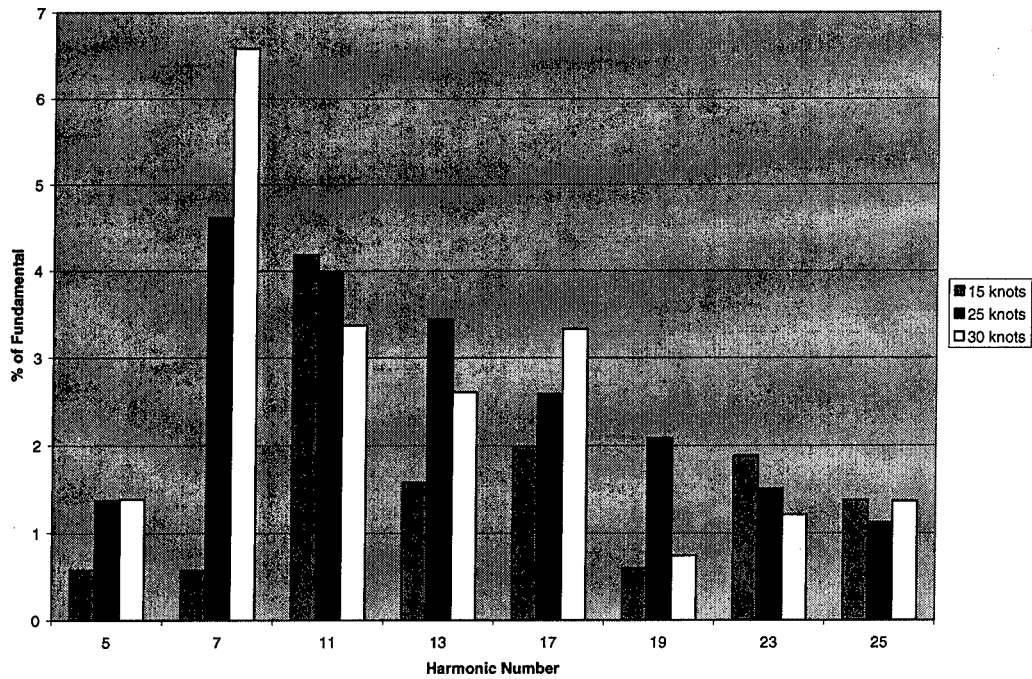
6.3 Overall Conclusions

The baseline system simulations showed that the distortion levels on an IPS system are most affected by the propulsion motors. Simulations over all loading cases were conducted and included large variations in ship service loads (Table 5-1). These variations produced very small changes in voltage distortion, especially at high powers (Figure 6-3). The baseline simulations also showed that distortion in excess of IEEE Std 519-1992 is present on this system. A six pulse propulsion motor drive similar to the motor tested at the LBES requires some form of harmonic mitigation to reduce distortion levels.

Three harmonic mitigation techniques were employed. The first method was to change the motor drive rectifier from a phase controlled rectifier to a line commutated rectifier. The second method was though the addition of a fifth harmonic filter, and the third method was changing the motor drive rectifier to a 12 pulse rectifier. Figure 6-25 summarizes the distortion results of all three methods.

Figure 6-25 Summary of Distortion Results

75
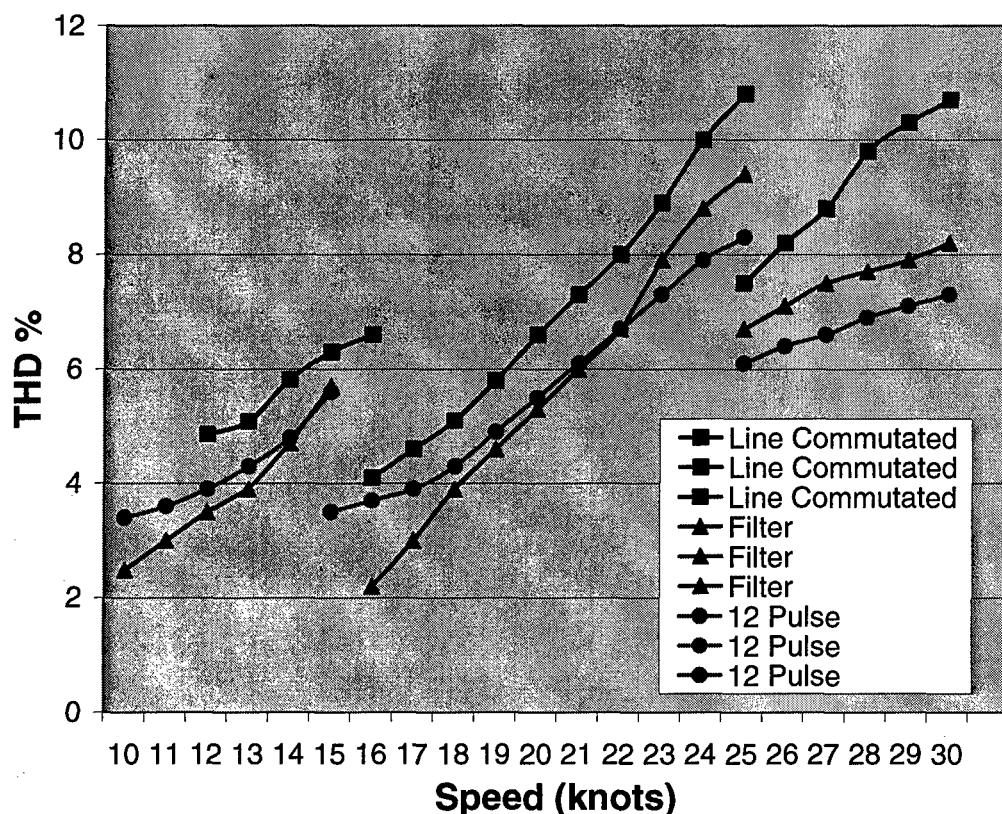
All three methods significantly reduce distortion. The line commutated rectifier simulations show that while IEEE Std 519-1992 is exceeded between 24 and 25 knots and again between 29-30 knots the margin is so small that this system should still be considered for implementation. Operational procedures could address the distortion levels between 24 and 25 knots. For instance, procedures could dictate shifting to split plant earlier in order to reduce system impedance and also distortion. The distortion at top speed may not even be an issue due to the limited amount of time a ship spends at flank speed. Component failure due to high distortion levels is not an immediate event, degradation takes place over time. Terrestrial distortion limits already allow for short periods of distortion in excess of the limits. This system would have the least impact on the ship as it does not require installation of a filter or a transformer. Additionally, the motor drive would be less complicated due to the fact that thryristor firing angle control would no longer be necessary. For these reasons the line commutated rectifier systems should be further investigated. The filter system and the 12 pulse system both reduced distortion levels to less than IEEE 519-1992 and also reduced the fifth and seventh harmonics to less than the generator limits. Either of these systems could be implemented, however, the 12 pulse system includes a significant size and weight penalty. The two systems differ only in that the 12 pulse system would require two phase shifting transformers for each of the motor drive while the filter system would require installation of a single three phase filter at the input to each motor drive. The total component weights are shown in Table 4-1. These weights were determined based on transformer power densities obtained from [14], and the size and weight of the fifth harmonic filter at LBES. Based on the size and weight of the two systems the filter system would be preferable to the 12 pulse system.

Table 6-3 Size and Weight of Harmonic Filter and Propulsion Transformers

	Harmonic Filters	Propulsion Transformers
Area (m^2)	19.3	94.9
Volume (m^3)	41.3	213.8
Weight (mton)	8.3	172.4

Chapter 7 Subtransient Reactance

To this point in this research a subtransient reactance of 20% has been assumed. This a typical value for generators of this size but variations do exist. ABB Marine and Turbo charging quotes generator subtransient reactance as low as 10% in their project guide for Azipod propulsion units. As discussed earlier, the subtransient reactance of the generator is the dominant impedance seen by harmonic currents in the system. Higher subtransient reactance will lead to higher voltage distortion for a given harmonic current environment. Subtransient reactance also determines the maximum initial generator current when the generator is subjected to a three phase fault. Increasing subtransient reactance lowers initial fault current levels but also increases voltage distortion. Understanding the nature of this tradeoff as it pertains to the IPS described so far is the purpose of this chapter.

7.1 Fault Current

The current sourced by a generator subjected to a sudden three phase short circuit can be described over three time periods; subtransient, transient, and steady state. The magnitude of the current sourced by the generator is a damped sinusoidal whose initial amplitude is limited by the subtransient reactance during the first few cycles after the short circuit. During the transient and steady state time periods the amplitude is limited by the transient reactance and synchronous reactance of the machine. The transient reactance of the generator is associated with the field winding on the rotor and the subtransient reactance is associated with additional current paths on the rotor of the machine. The damping of the response is associated with the resistance of these current paths. For a given generator this current can be predicted by solving Equation 7-1. Figure 8 shows the response of a generator with 25% and 15% subtransient reactance to a sudden three phase fault. The lower subtransient reactance results in significantly higher initial current.

$$i_a = \frac{1}{x_d''}e^{\frac{-t}{T_a}} - \left\{ \frac{1}{x_d} + \left(\frac{1}{x_d'} - \frac{1}{x_d} \right)e^{\frac{-t}{T_d'}} + \left(\frac{1}{x_d''} - \frac{1}{x_d'} \right)e^{\frac{-t}{T_d''}} \right\}\cos(\omega t)$$

Equation 7-1

Where:

T_a = armature time constant

77

T_d' = transient time constant
T_d'' = subtransient time constant
x_d = synchronous d axis reactance
x_d' = transient d axis reactance
x_d'' = subtransient d axis reactance

Figure 7-1 Generator Fault Current
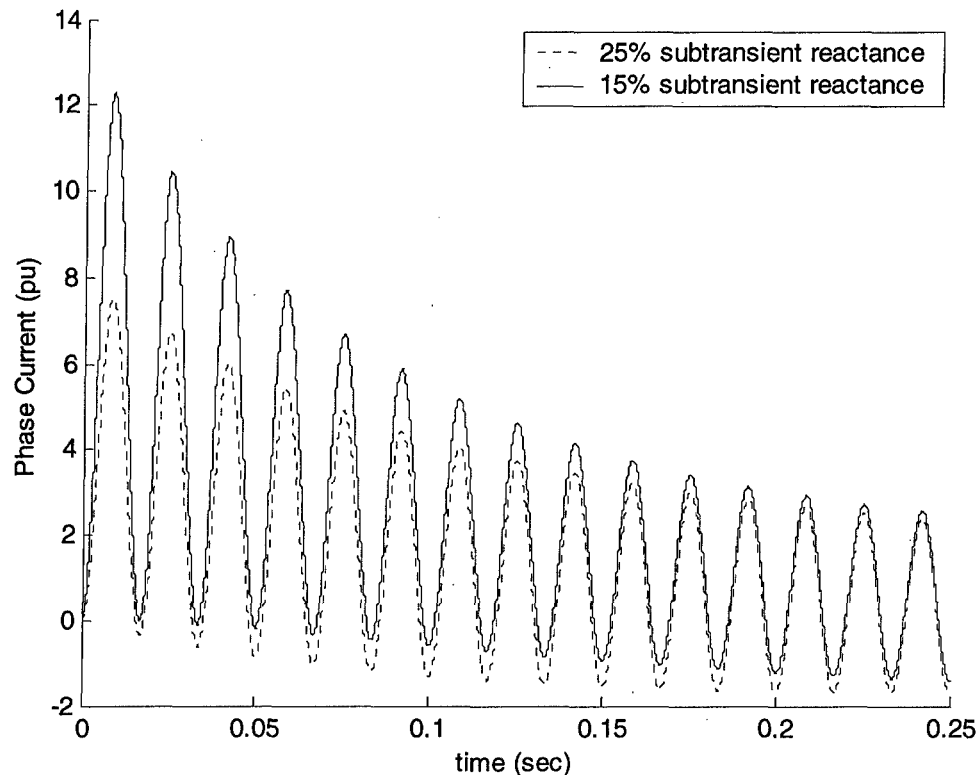
When choosing a low or medium voltage system for a ship IPS, the current handling capabilities of available circuit breakers can easily be exceeded. Without going through a product development for a specialized breaker or employing fault current limiters, the ratings of the circuit breaker with the highest current handling capabilities are 5000 amps steady state and 63kA fault. These ratings limit the power handling capability of the electrical bus as follows. Equation 5-11, repeated below, determines the fault current for a given bus voltage, generator subtransient reactance, and power capability. Figure 7-2 shows the fault current expected for subtransient reactances of 15%, 20%, and 25%. At 15%, the 63kA breaker rating is exceeded at approximately 55 MW, limiting the power handling capability of the electrical bus.

78

$$I_{sc} = \frac{VA_{rated}}{\sqrt{3}V_{line}x_d^{"}}$$

Figure 7-2 Generator Fault Current vs. Installed Power
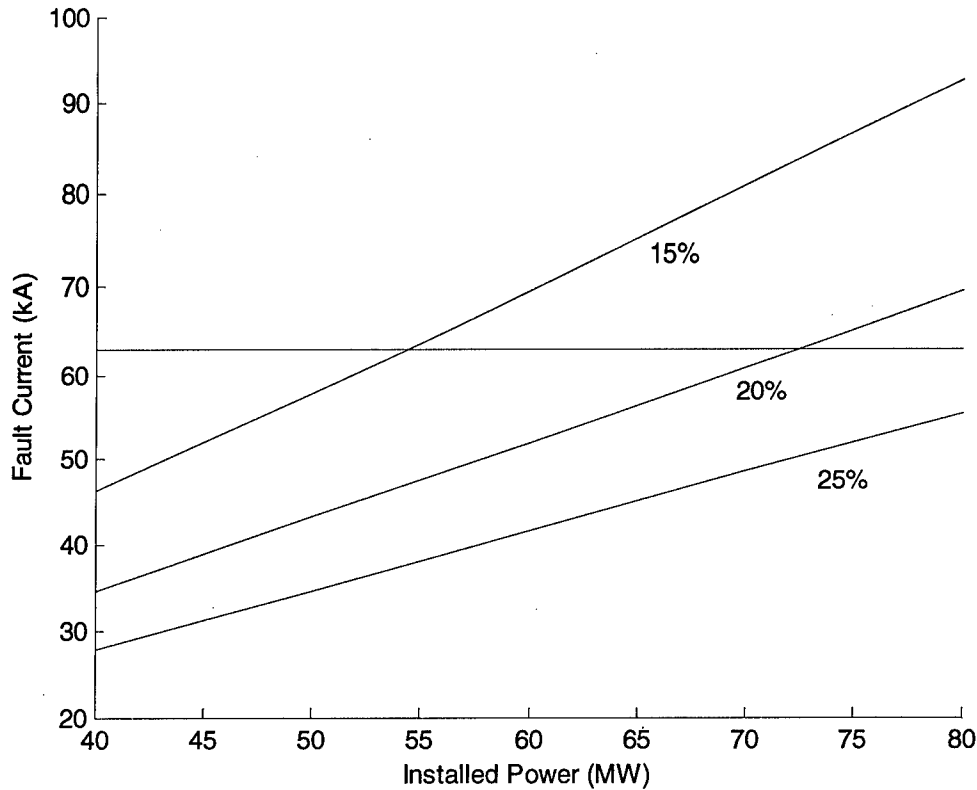
7.2 Voltage Distortion

A higher value of subtransient reactance is desirable to support higher power demands on an electrical bus but this leads to increased voltage distortion. In order to gain an understanding of the effect of subtransient reactance on voltage distortion the circuit in Figure 7-3 was constructed. The circuit consists of a single 20MW generator supplying the propulsion motor drive of section 4.2.3. Generator subtransient reactance was varied from 15%-25% and the propulsion motor drive was simulated at powers from 2MW to 20MW. Voltage and current distortion were measured and results are plotted in Figure 7-4, Figure 7-5, and Figure 7-6. The data shows that voltage distortion is significantly effected by the subtransient reactance value. Figure 7-6 shows that at low motor power, where the harmonic current magnitudes are small, the difference in the resulting voltage distortion is relatively small. However, as the drive power

increases, the effect of the subtransient reactance on voltage distortion is clearly evident, resulting in increases of distortion levels on the order of 15%. The effect of the DC link voltage control is also clearly evident in this simulation. We see the voltage distortion decrease significantly as the thyristor firing angle is decreased at the higher power levels.

Figure 7-3 Subtransient Reactance Simulation Circuit

Figure 7-4 Voltage Distortion

Figure 7-4 Voltage Distortion
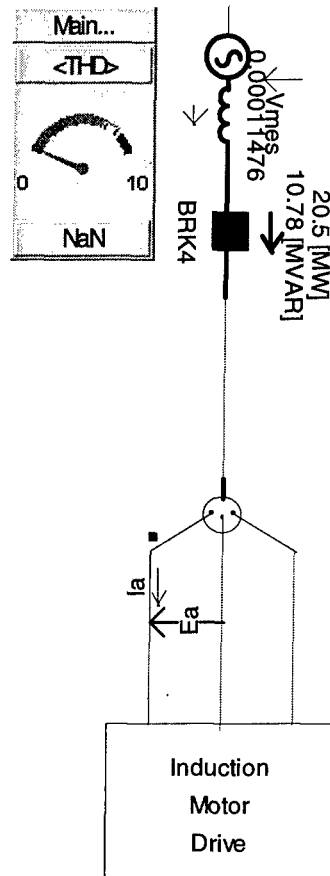
Figure 7-5 Current Distortion
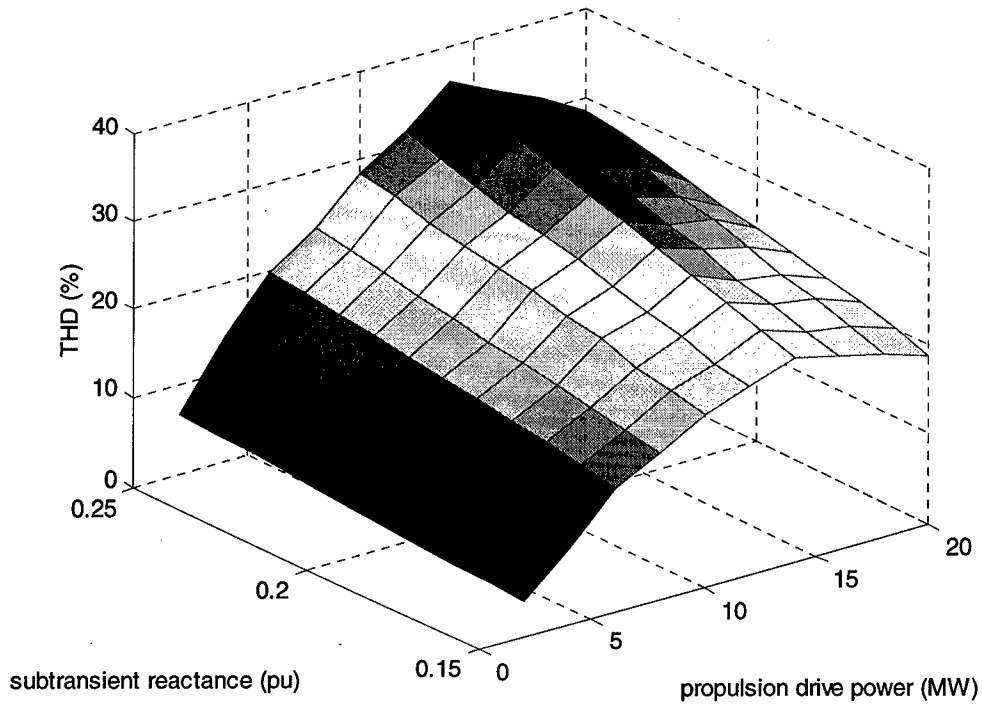
Figure 7-5 Current Distortion
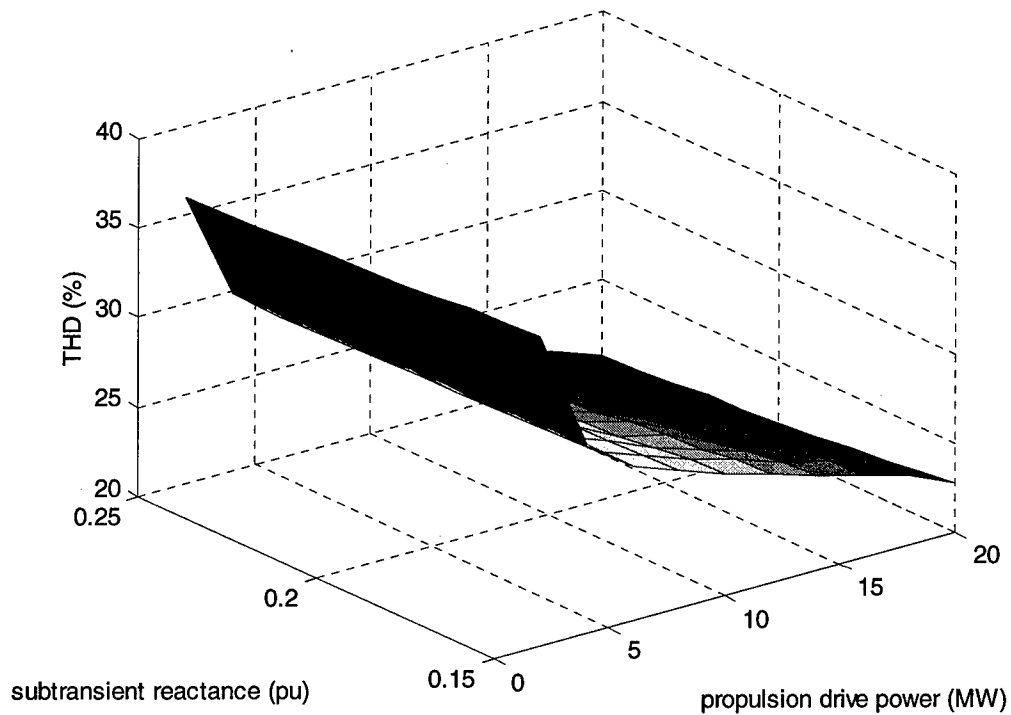
Figure 7-6 Voltage Distortion vs Motor Drive Power
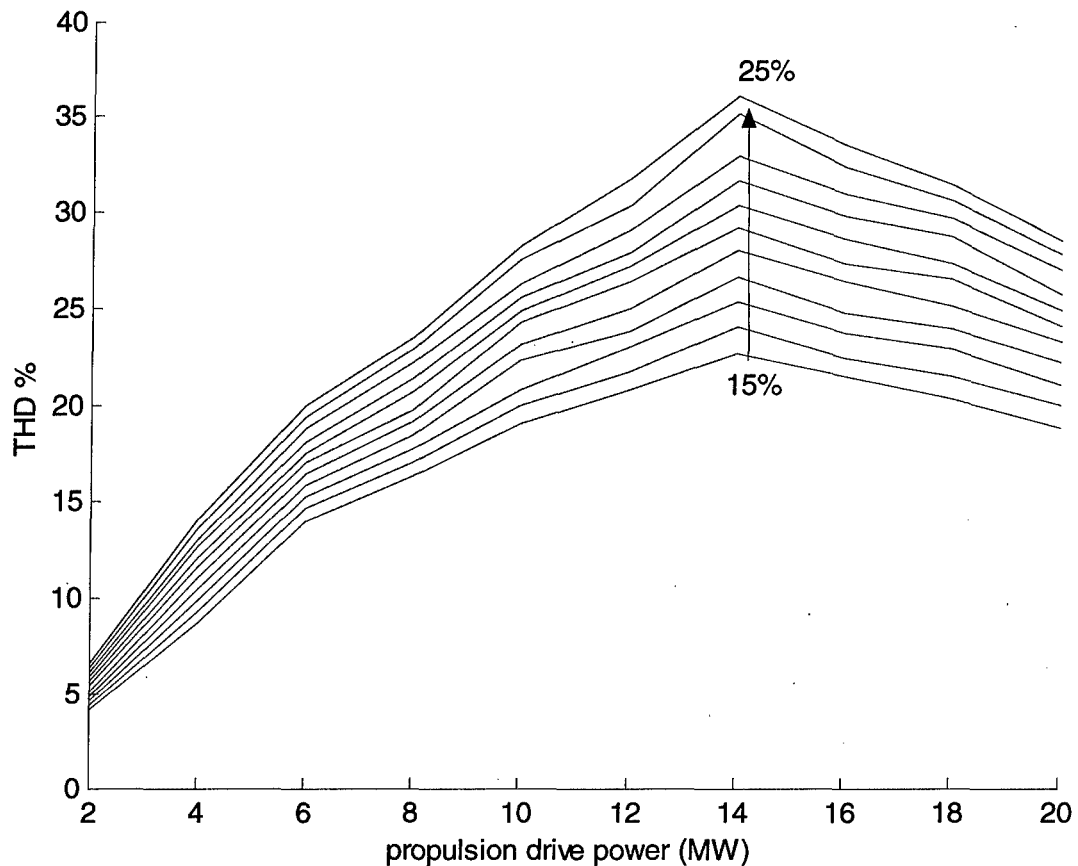
7.3 Impact on the Baseline System

When the baseline system was developed a subtransient reactance of 20% was chosen because this was a typical value for marine generators. This selection resulted in the requirement of splitting the main bus in order to supply the full 80MW of power. A more practical approach when designing an IPS would be to set a minimum subtransient reactance for the generators based on the power of each bus. In the case of the baseline system if we limited subtransient reactance to no less than 22% we would be able to provide the entire 80MW of power from a single bus. The 12 pulse system simulations for the 90 degree cruise loading were repeated with the 22% subtransient reactance and plotted over the results from the earlier simulations. The increase in subtransient reactance results in an increase in THD on the order of 1-2 %. The slight increase in distortion is more than offset by the operational flexibility gained with the higher subtransient reactance. Figure 7-7 shows the results. Conversely, you could limit the power on

each bus in order to accommodate a lower subtransient reactance. Limiting power to 40 MW on each bus and operating with a subtransient reactance of 15% could allow operation without a harmonic filter or a 12 pulse system. The worst case distortion for the baseline system (six pulse motor drive without harmonic filter) drops to 10% if subtransient reactance is lowered to 15%.

Figure 7-7 THD% with 22% Subtransient Reactance
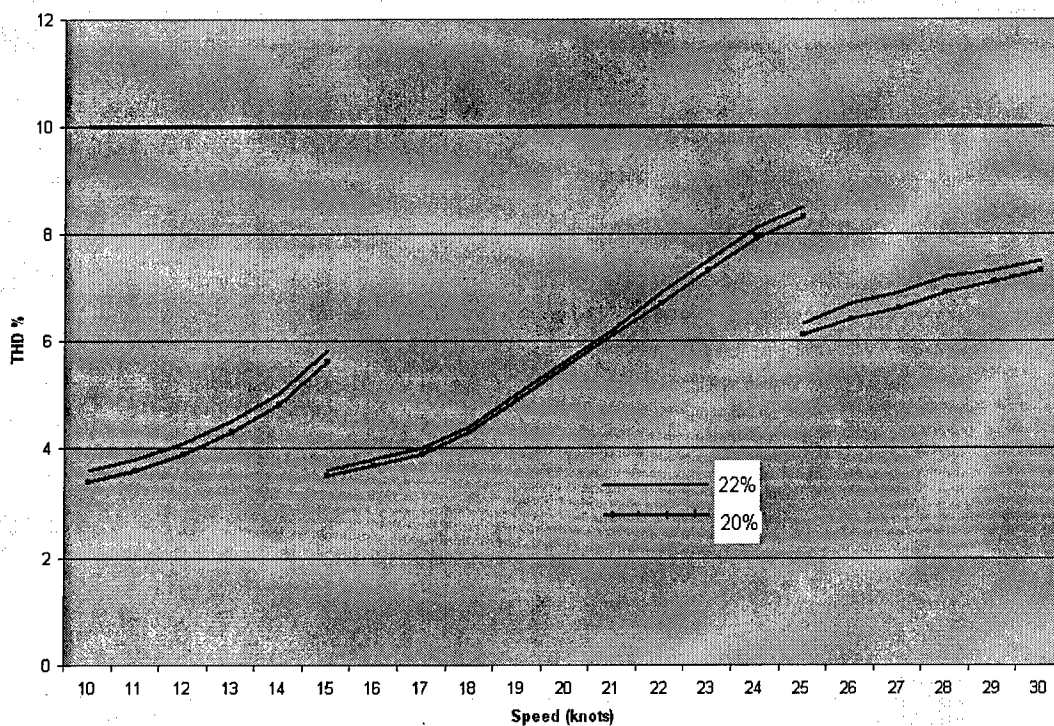
This page intentionally left blank.

Chapter 8 Conclusions

Commitment to powering future Navy ships with IPS requires an understanding of the effect on system power quality of the components of the system. In this research an attempt was made to quantify the distortion characteristics of an IPS that might be used on naval surface combatants. The power requirements of the future surface combatant were simulated in order to present a realistic picture of propulsion and ship service demand and components tested at LBES were simulated in order to validate the modeling techniques used in this research. The results of the analysis illustrate some of the tradeoffs necessary in formulating an IPS for a navy ship. Additionally, these results also show some of the system characteristics necessary to provide adequate power quality in an IPS.

The first conclusion of this research is based on the premise that power requirements for the navy ships of the future will continue to grow. With this premise in mind, system voltage of 4160 is too low to service the power needs of future navy ships using electric propulsion. The primary benefit of the 4160 V system is that step-down transformers are not required at the interface of the rectifier and system bus. While this presents a significant savings in size and weight, future high energy weapons will demand power beyond the capabilities of a 4160 V system. Chapter 7 showed the relationship between subtransient reactance and fault current. It would be necessary to increase the subtransient reactance of installed generators in order to provide additional power but this increase would also have a negative impact on the system power quality. Chapter 6 showed that THD was within the limits of IEEE Std 519-1992 for the 80 MW system, however, increasing the power capability of the system would also increase the harmonic current level. The increase in harmonic currents coupled with the higher subtransient reactance would raise THD above the 10% limit. At 80 MW, a 4160 V system is already at the limits of its power handling capabilities. Selecting this voltage level would limit the prospects for incorporation of the high energy weapons expected in the future.

The first advantage of an IPS arrangement, listed in Chapter 1, was "increased fuel economy due to the efficient operation of the prime mover". This true in that with an IPS the ship is no longer using a large gas turbine (operating at a fraction of its rating when the ship is at less than flank speed) for propulsion and additional gas turbines to supply ship service power

requirements. In theory, with an IPS, fuel efficiency savings will garnered by using the same prime mover to supply propulsion as well as electrical power requirement. In the baseline system of Chapter 6 the generator sizes of 10 MW and 30 MW were selected in order to efficiently operate the prime movers. The selection was based on the following:

- A minimum of two generator sets will be operating in order to have a redundancy
- Gas turbines operate inefficiently a light loads, below 50%

These statements resulted in the generator selection above and an operational philosophy where the two 10 MW generators would be normally operated and ship speeds below 15 knots. When higher speeds were necessary the 30 MW generators would be brought online. Since navy ships spend the majority of their time at speeds below 15 knots, the system would normally operate with its smaller prime movers online and each loaded at 50% rated power or above. However, if we examine the available turbine/generator sets we find that much of this efficiency is lost due to a lack of sets in the desired power range. Table 8-1 shows the turbine/generator sets are available for use in an IPS. The limited selection would result in an 80 MW system with either four LM2500 propulsion generators or three LM 2500+ generators and a single DDA 501-K34G. Both cases result in excess generation capacity at speeds less than 15 knots, which would affect the efficiency of operation over the lifetime of the ship. At a system voltage of 13.8 kV the loss of efficiency is even greater. An 80 MW IPS would require the installation of two RR MT-30 and two GE LM500. The two smaller generators are unable to supply even the non-propulsion loads, so in order to supply redundancy, both of the large generators would be required to be operating at all times. The small generators would only be placed online in order to reach flank speed. This configuration is the opposite of what is desired for efficient operation of the prime movers. A turbine/generator set with a power rating on the order of 10 MW is required to fully capture the efficiency inherent in an IPS.

Table 8-1 Turbine/Generator Sets

Engine	Voltage(kV)	Power(MW)
GE LM2500	4.16	21
GE LM2500 +	4.16	26
DDA 501-K34G	4.16	3
RR MT-30	13.8	36.25
GE LM500	13.8	3.8

The last conclusion of this research is that harmonic mitigation techniques exist that would allow the supply of non-sensitive AC loads from transformers connected directly to the main bus of an IPS with electric propulsion. It was shown that if a motor drive power supply could be constructed that did not rely on thyristor firing angle control to maintain DC-link stability, the IPS may well be operated without installation of a harmonic filter. Even with the extra distortion associated with controlling the thyristor firing angle it was shown that the distortion levels were reduced sufficiently with either the installation of a harmonic filter or using a 12 pulse motor drive.

If the first and last conclusions are taken together it is found that an IPS for a future navy ship would have a 13.8 kV bus with a 12 pulse motor drive. The higher bus voltage would allow for power growth beyond 80 MW. This bus voltage would also necessitate step-down transformers for each of the motor drives. As the transformers were needed for the interface there would be no reason not to select a 12 pulse drive to limit harmonic currents.

8.1   Future Work

Numerous opportunities exist to expand the current IPS model presented in this research. This model was developed specifically to measure harmonic distortion on the 450 V bus of the baseline IPS. Due to the 200 node limitation of the software used to conduct the simulations and the specific nature of the research, simplifications were made.

A simple model was used for the generators and prime movers to speed up the simulations and limit the node numbers. Detailed models of the generators could be developed based on the actual characteristics of the governor, regulator, prime mover, and generator in order expand capabilities of the model to include transient behavior and fault analysis while still retaining the capabilities for analyzing power quality. While the capability to conduct this analysis already exists, a library of these power sources and their associated control systems would allow for rapid reconfiguration of many IPS architectures to include a variety of power sources.

Future weapons systems such as the rail gun will have peak energy demands over very short intervals of time. These future loads are classified as pulsed loads and could have a significant impact on an IPS. The nature of these loads requires an auxiliary power source, such as a capacitor bank, to inject the necessary energy in a short amount of time. A model of these

power sources coupled with a simple pulsed load model could be developed to determine the impact on the system.

This research assumed that the sensitive loads were supplied by an inverter. It was assumed that the power quality on this section of the bus would adequate for these sensitive loads. However, the nature of these sensitive loads negatively impacts power quality. The majority of these loads are electronic loads with a front end rectifier. Research has been conducted into the effect of large numbers of electronic loads supplied from a single source. [14][15][26] This research has focused on the cumulative harmonic currents of these loads and their interaction due to a shared source impedance. Future naval ships will have an increasing number of these loads due to programs such as the Total Ship Computing Environment on DDX and the impact of their cumulative harmonic currents. An analysis into the operation and stability of an inverter supplying loads that generate significant harmonic currents could be conducted.

List of References

[1]   Timothy J. McCoy, Makhlouf Benatmane, "The All Electric Warship: An Overview of the U.S. Navy's Integrated Power System Development Programme", Int'l Conference on Electric Ship, Istanbul, September 1, 1998

[2]   M.L. Cecere III, "Integrated Electric Power for the US Navy", Paper 16, The Institute of Marine Engineers, 1995

[3]   LCDR Norbert Doerry, Henry Robey, LCDR John Amy, Chester Petry,"Powering the Future with the Integrated Power System", Naval Engineers Journal, May 1996

[4]   LCDR Timothy J. McCoy, Mathew Stauffer, Thomas Dalton, Edward Harvey, "Full Scale Testing of the US Navy's Integrated Power System" Presented at INEC-2000, 14-16 March 2000, Hamburg Germany

[5]   Makhlouf Benatmane, LCDR Timothy McCoy, Tracey Cooper, "Electric Propulsion Full Scale Development on U.S. Navy Surface Ships

[6]   "Modeling and Simulation of the Propagation of Harmonics in Electric Power Networks, Part I: Concepts, Models, and Simulation Techniques," Task Force on Harmonics Modeling and Simulation, *IEEE Transactions on Power Delivery*, Vol. 11, January 1996.

[7]   Y.G. Hegazy, M.M.A. Salama, "Calculations of Diversified Harmonic currents in Electric Distribution Systems," *IEE Proceedings- Generation, Transmission, Distribution*, Vol. 150 No. 6 November 2003.

[8]   J. M. Prousalidis, I K Hatzilau, S Perros, "Harmonic Electric Power Quality Concepts for the Electrified Ships", Proceedings of All Electric Ship (AES 2003), pp. 279-290, Edinburg (2003)

[9]   J. G. Kassakian, M. F. Schlecht, G.C. Verghese, Principles of Power Electronics, Addison-Wesley Publishing Company, Reading, MA, 1991

[10]   N. Mohan, T. M. Undeland, W. P. Robbins, Power Electronics: Converters, Applictions, and Design, John Wiley and Sons, New York, 1989.

[11]   H. W. Dommel, "Digital Computer Solution of Electromagnetic Transients in Single and Multiphase Networks," *IEEE Transactions on Power Apparatus and Systems*, PAS-88, #4, pp 388-399, April 1969

[12]   Manitoba HVDC Research Centre, EMTDC The Electromagnetic Transients and Controls Simulation Engine. Users Guide.

[13]   A.E. Fitzgerald, C. Kingsley Jr., S.D. Umans, Electric Machinery, McGraw Hill Inc., New York, 1990.

[14]   R.C. Smith, L. T. Dunnington, G.F.Grater, "Future Shipboard Power System Architecture Analysis Interim Report, Shipboard Electrical Distribution Characteristics," Anteon Corporation, MSD-50-TR-2001/13 December 2001.

[15]   P. J. Moore, I.E. Portugues, "The Influence of Personal Computer Processing Modes on Line Current Harmonics," *IEEE Transactions on Power Delivery*, Vol 18, No. 4, October 2003.

[16]   Arsoy, S.M. Halpin, Y. Liu, P.F. Ribeiro, Modeling and Simulation of Power System Harmonics CDROM, Task Force on Harmonic Modeling and Simulation, Harmonic Working Group, Transmission and Distribution Working Group, IEEE Power Engineering Society, 1999

[17]   S.D. Sudhoff, S.F. Glover, B.T. Kuhn, IPS FSAD Model Verification, Final Technical Progress Report. Energy Systems Analysis Consortium, October 1999.

[18]   C. Newton, "IPS Motor Reduction System Study" ALSTOM Electrical Machines, December 7, 1999.

[19]   Integrated Power System Land Based Engineering Site Test Report for Phase 1,Lockheed Martin Corporation, Ocean, Radar and Sensor Systems. November 1999.

[20]   "IEEE Recommended Practices and Requirements for Harmonic Control in Electric Power Systems," IEEE Std. 519-1993, IEEE, New York, 1993.

[21]   Handbook for the Calculation of Current and Voltage Harmonics on Three-Phase Shipboard Power Distribution Systems due to Controlled Static Power Supplies, MPR Associates, MPR-250, August 1970.

[22]   Arthur Kelley, William F. Yadusky, "Rectifier Design for Minimum Line Current Harmonics and Maximum Power Factor". IEEE Transactions on Power Electronics, Vol 7, No 2, 1992.

[23]   C. Newton, IPS Motor Voltage Reduction System Study Report, Alstom Electric Machines, 12/7/1999

[24]   "IEEE Harmonics in Power Systems", IEEE Std 141-1993, IEEE, New York, 1993

[25]   James L. Kirtley Jr, "Class Notes 9: Synchronous Machine Simulation Models", Course 6.685 Electric Machinery, Massachusetts Institute of Technology, Department of Electrical Engineering and Computer Science, August 25, 2003

[26]   A. Mansoor, W. M. Grady, A. H. Chowdhury, M. J. Samotyj, "An Investigation of Harmonics Attenuation and Diversity Among Distributed Single-Phase Power Electronic Loads" *IEEE Transactions on Power Delivery*, Vol 10, No. 1, January 1995

[27]   J. S. Mayer, O. Wasynczuk, "An Efficient Method of Simulating Connected Power Systems with Stator and Network Transients Included" *IEEE Transactions on Power Systems* Vol. 6, No. 3, August 1991.

This page intentionally left blank.

Appendix A.   Matlab Scripts

```
% Edward West
% Thesis
% Signal Construction From Fourier Coefficients
% 10/04/2005

% This script is used to compare measured data and simulated data.
% The fourier coefficients of the two signals are entered in Imag,
% Iphase,Imag1, and Iphase 1 in addition to the number of coefficients in
% n and n1. The two signals are shifted so that their fundemental components
% begin at zero degrees.

clear

f=60;
om=2*pi*f;
t=0:5e-5:5e-2;

% harmonics of interest from data
n=[1 5 7 11 13 17 19 23 25];
% harmonics of interest from simulation
n1=[1 5 7 11 13 17 19 23 25 29 31];

%set up the fourier coefficients and phases
Imag=[2460 591 174 156 111 66 61 24 28 ]/2460;
Iphase=[-25 59 -152 -78 56 137 -89 -13 120].*(pi/180);
Imag1=[2557 628 169 166 106 73 60 30 30 10.7 10.8]/2557;
Iphase1=[-2.27 -1.8 -2.89 -2.6 2.4 2.8 .06 .03 .03 .51 -.60];

% shift the signal so that fundemental is at zero degrees
for k=1:length(n)
    Iphasecor(k)=Iphase(k)-Iphase(1)*n(k);
end

% compute time domain signal
for i=1:length(n)
    I(i,:)=Imag(i).*cos(n(i).*om.*t+Iphasecor(i));

end

%repeat Process for simulated signal

Iplot=sum(I);
```

```
for k=1:length(n1)
    Iphasecor1(k)=Iphase1(k)-Iphase1(1)*n1(k);
end

for i=1:length(n1)
    I1(i,:)=Imag1(i).*cos(n1(i).*om.*t+Iphasecor1(i));

end

THDs=sqrt(sum(Imag1(2:length(n1)).^2)/Imag1(1)^2)*100
THDm=sqrt(sum(Imag(2:length(n)).^2)/Imag(1)^2)*100

Iplot1=sum(I1);
figure(1)
hold on
plot(t,Iplot);
plot(t,Iplot1,':');
h=legend('measured','simulated')
title(['THDsimulated = ',num2str(THDs),'%   THDmeasured=',num2str(THDm),'%']);
hold off
figure(2)
Ibar=[Imag;Imag1(1:length(n))];
bar(n,Ibar');
xlabel('harmonic number')
ylabel('magnitude')
h=legend('measured','simulated')


%%%%%%%%%%%%%%%%%%%%%%%%%%%%%%%%%%%%%%%%%%%%%%%%%%
%%%%%%%%%%%%%%%%%%%%%%%%%%%%%%%%%%%%%%%%%%%%%%%%%%
%%%%%%%%%%%%%%%%%%%%%%%%%%%%%%%%%%%%%%%%%%%%%%%%%%
%%%%%%%%%%%%%%%%%%%%%%%%%%%%%%%%%%%%%%%%%%%%%%%%%%
```

```
% Edward West
% Thesis
% Harmonic Current Source Comparison

% This script determines the voltage distortion caused
% by a six pulse rectifier in the test system shown in
% figure 20.

clear
% harmonics of interest
n=[5 7 11 13 17 19 23 25];
% frequency
w=377;
%Transformer Voltages
v1=4160;
v2=.450;
% Per unit reactances
xpctn=3;
xpcgen=20;
%calculation of transformer harmonic reactance
xtn=n.*(xpctn*v1^2/(100*1000*1000));
rtn=.2*(v1/v2)^2;
ztran=rtn+j*xtn;
% calculation of generator harmonic reactance
xgen=.00024482;
zgen=j.*xgen.*w.*n;
% Current drawn by the six pulse rectifier
Imag=[.2553 .1024 .0743 .0517 .0339 .0296 .0193 .0194];
%IEEE values of harmonic currents per unit for a six pulse recitier
Iee=[.192 .132 .073 .057 .035 .027 .020 .016];
%total system impedance
ztot=abs(zgen.*ztran./(zgen+ztran));
%predicted voltage harmonics using actual currents drawn
V=Imag.*ztot
% predicted voltage harmonics using IEEE estimates
V2=1.0567.*Iee.*ztot


%%%%%%%%%%%%%%%%%%%%%%%%%%%%%%%%%%%%%%%%%%%%%%%%%%%
%%%%%%%%%%%%%%%%%%%%%%%%%%%%%%%%%%%%%%%%%%%%%%%%%%%
%%%%%%%%%%%%%%%%%%%%%%%%%%%%%%%%%%%%%%%%%%%%%%%%%%%
%%%%%%%%%%%%%%%%%%%%%%%%%%%%%%%%%%%%%%%%%%%%%%%%%%%
%%%%%%%%%%%%%%%%%%%%%%%%%%%%%%%%%%%%%%%%%%%%%%%%%%%
```

```
% Edward West
% Thesis
% Calculation of short circuit current
% given per unit subtransient reactance
% bus voltage and total power available


clear
limit=[63000 63000 63000 63000 63000];
Vb=input('Enter line to line system voltage     ');
xdpp=[.2];
Pb=[40 50 60 70 80];
hold on
for i=1:length(xdpp);
    I=Pb./(.8*sqrt(3)*Vb*xdpp(i));
    plot(Pb,I*1000)
end
plot(Pb,limit/1000)
xlabel('Installed Power (MW)')
ylabel('Fault Current (kA)')
hold off

%%%%%%%%%%%%%%%%%%%%%%%%%%%%%%%%%%%%%%%%%%%%%%%%%%%%
%%%%%%%%%%%%%%%%%%%%%%%%%%%%%%%%%%%%%%%%%%%%%%%%%%%%
%%%%%%%%%%%%%%%%%%%%%%%%%%%%%%%%%%%%%%%%%%%%%%%%%%%%
%%%%%%%%%%%%%%%%%%%%%%%%%%%%%%%%%%%%%%%%%%%%%%%%%%%%
```

```
% Edward West
% Thesis
% Calculation of O/P filter inductance
% based on method outlined in
% Keller A W, Yadusky W F, "Rectifier Design for
% Minimum Line Current Harmonics and Maximum Power
% Factor" IEEE Transactions on Power Electronics, Vol
% 7. No 2 April 1992

clear

% Normalization References
Vref=input('Enter nominal rms line to neutral source voltage    ');
Pref=input('Enter nominal rectifier o/p power    ');
Fref=60;
Tref=2*pi/Fref;
Iref=Pref/Vref;
Zref=Vref^2/Pref;

% Inductance Calculation

Lon=.1;
Con=10;
Lo=Lon*(Vref/(Iref*Fref))
Co=Con*(Iref/(Vref*Fref))
```

```
% Edward West
% Thesis
% Calculation of Generator Fault Current



xd=2.2;
xq=2;
xdp=.45;
xdpp=.25;
xqpp=.22;
tdop=5;
tdopp=.2;
tqopp=.3;
t=0:.00001:.25;

tdp=xdp*tdop/xd;
tdpp=xdpp*tdopp/xdp;

ia1=(1/xd+(1/xdp-1/xd).*exp(-t./tdp)+(1/xdpp-1/xdp).*exp(-t./tdpp)).*cos(377*t)...
    -1./xdpp*exp(-t./ta);

hold
plot(t,-ia1,':')
%title('Generator Fault Current')
ylabel('Phase Current (pu)')
xdpp=.15;
tdp=xdp*tdop/xd;
tdpp=xdpp*tdopp/xdp;
ia1=(1/xd+(1/xdp-1/xd).*exp(-t./tdp)+(1/xdpp-1/xdp).*exp(-t./tdpp)).*cos(377*t)...
    -1./xdpp*exp(-t./ta);


plot(t,-ia1)
 h=legend('25% subtransient reactance','15% subtransient reactance')
% title('15% Subtransient Reactance')
% ylabel('Phase Current (pu)')
xlabel('time (sec)')
```

Appendix B.   LBES Comparison for Generator, Filter, and Voltage

Generator Current 10% Power

Generator Current 10% Power

Generator Current 50% Power

Generator Current 90% Power

Generator Current 90% Power

Line-Line Voltage 10% Power

Line-Line Voltage 10% Power

Line-Line Voltage 50% Power

Line-Line Voltage 50% Power

Line-Line Voltage 90% Power

Filter Current 50% Power

Filter Current 90% Power

Filter Current 90% Power
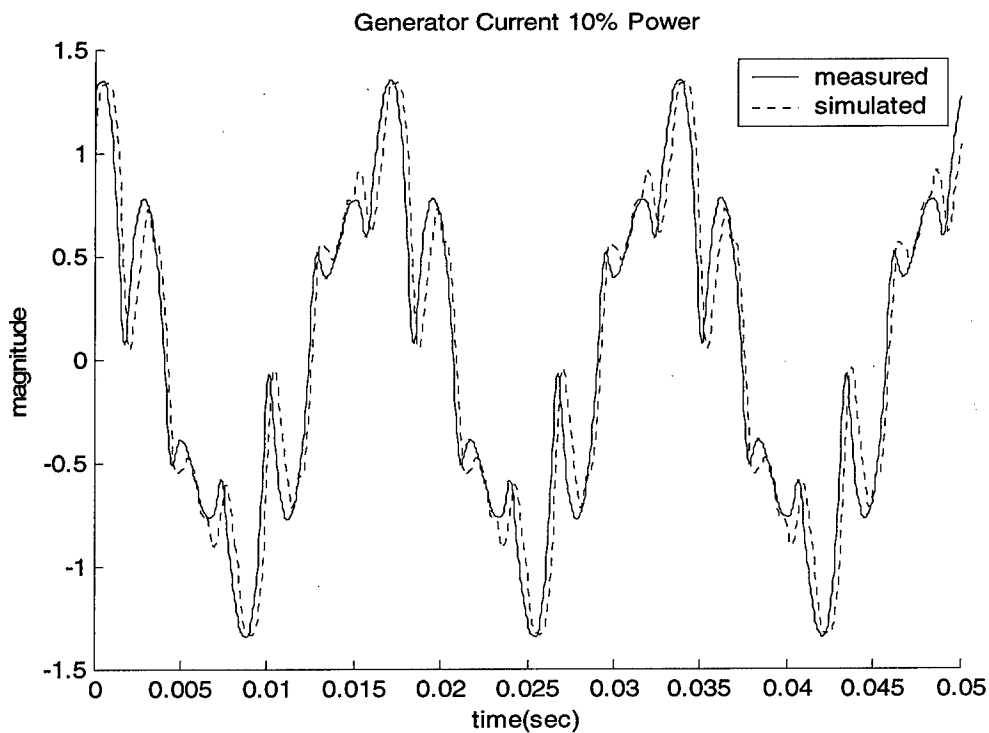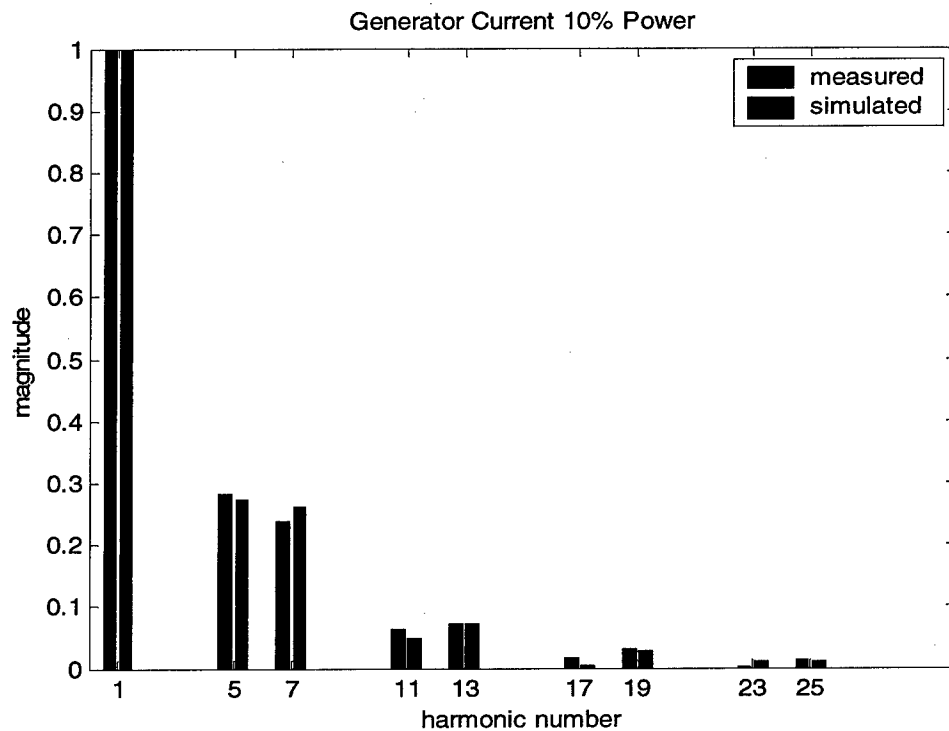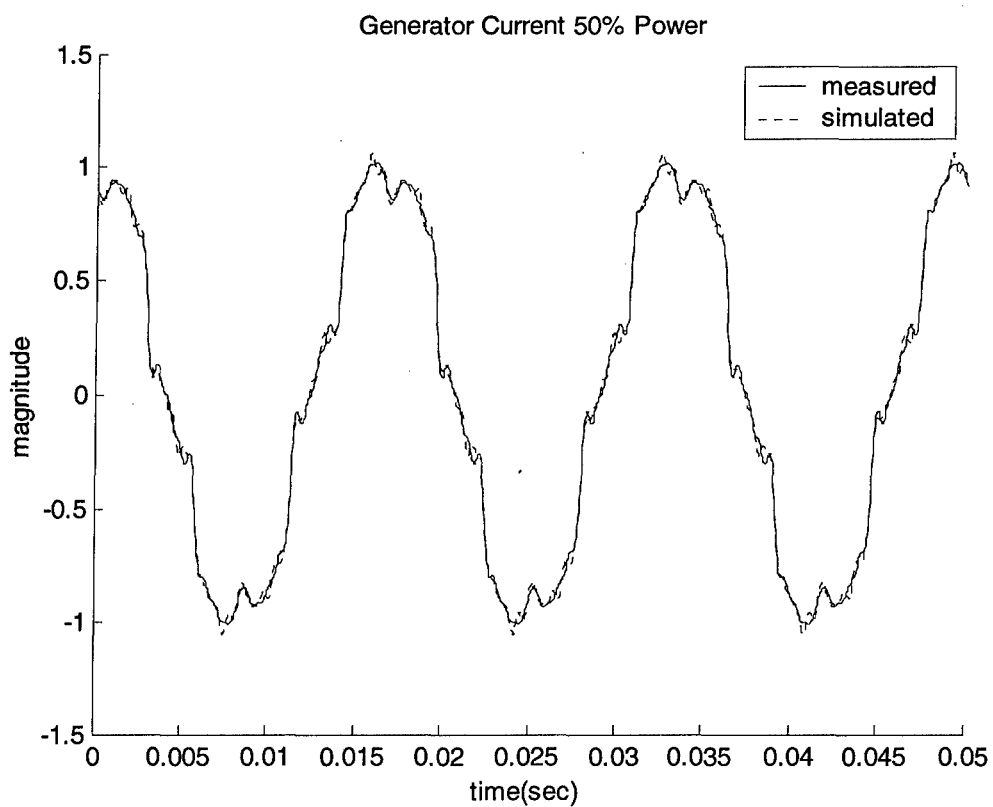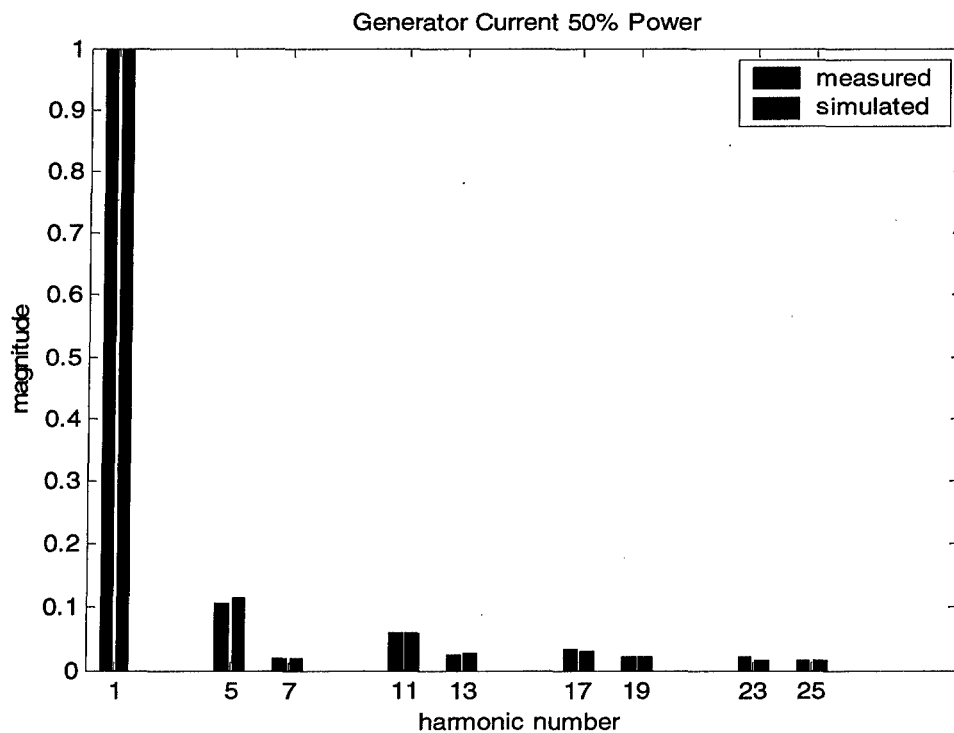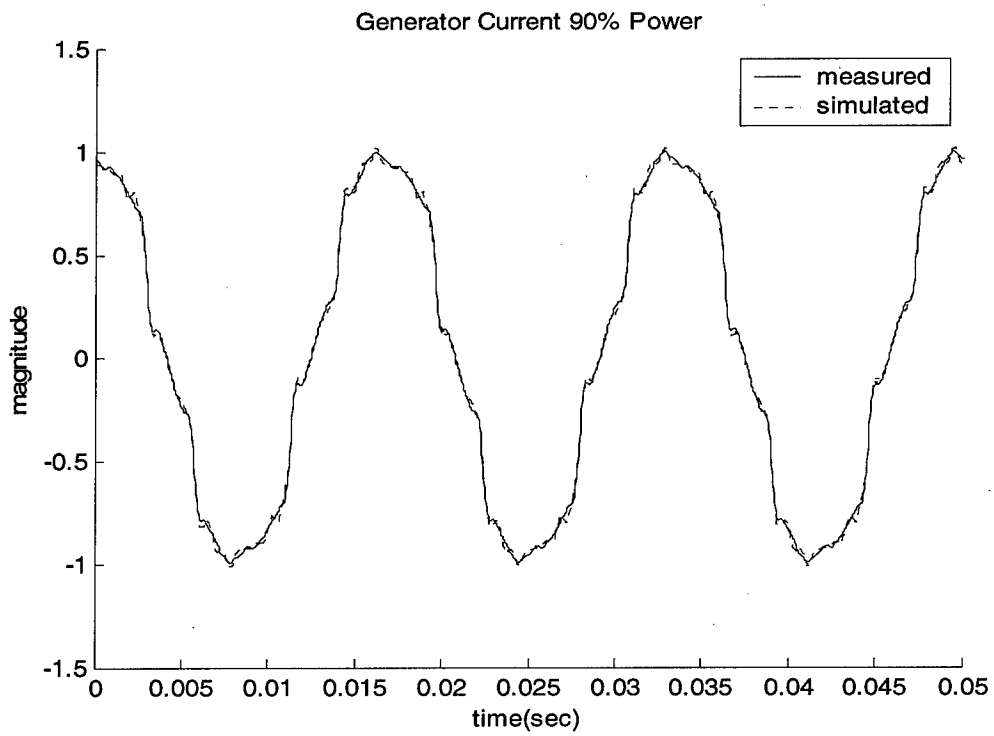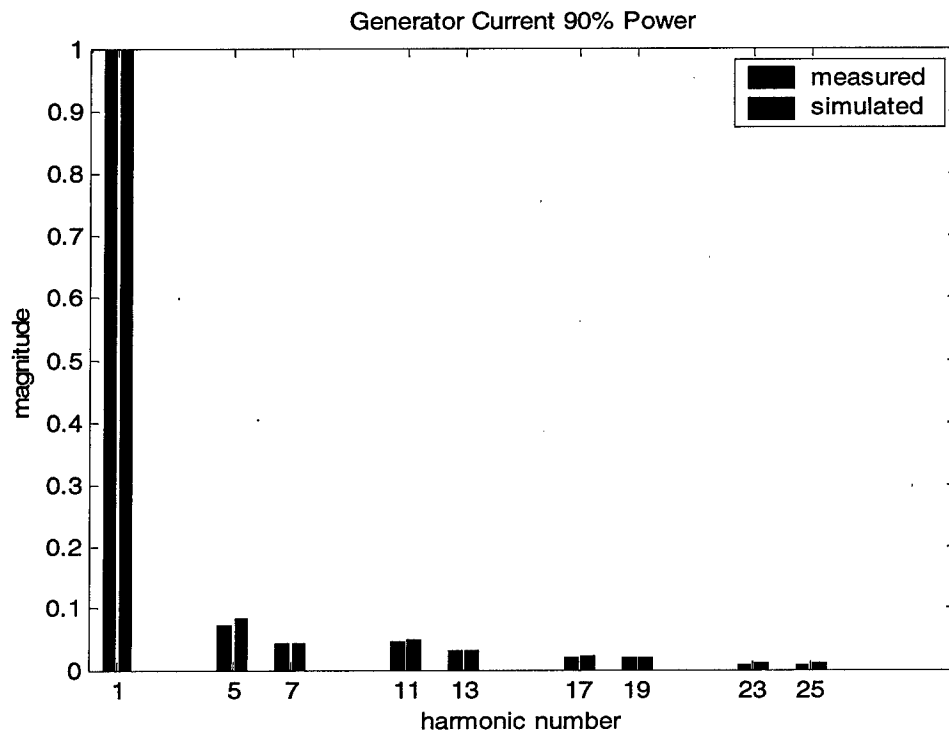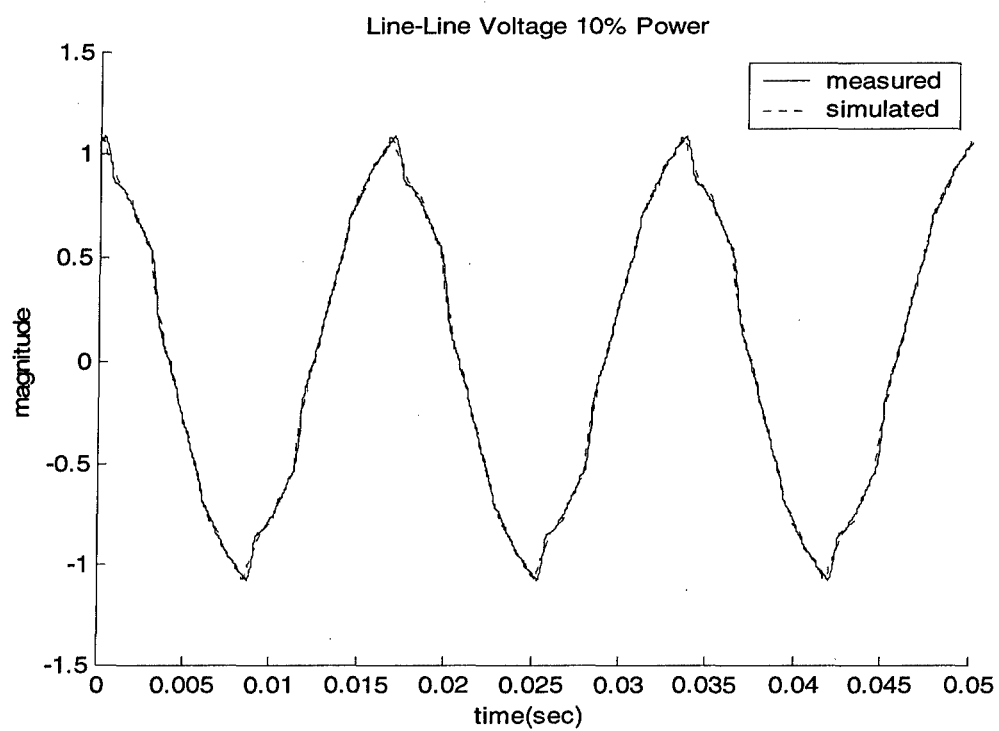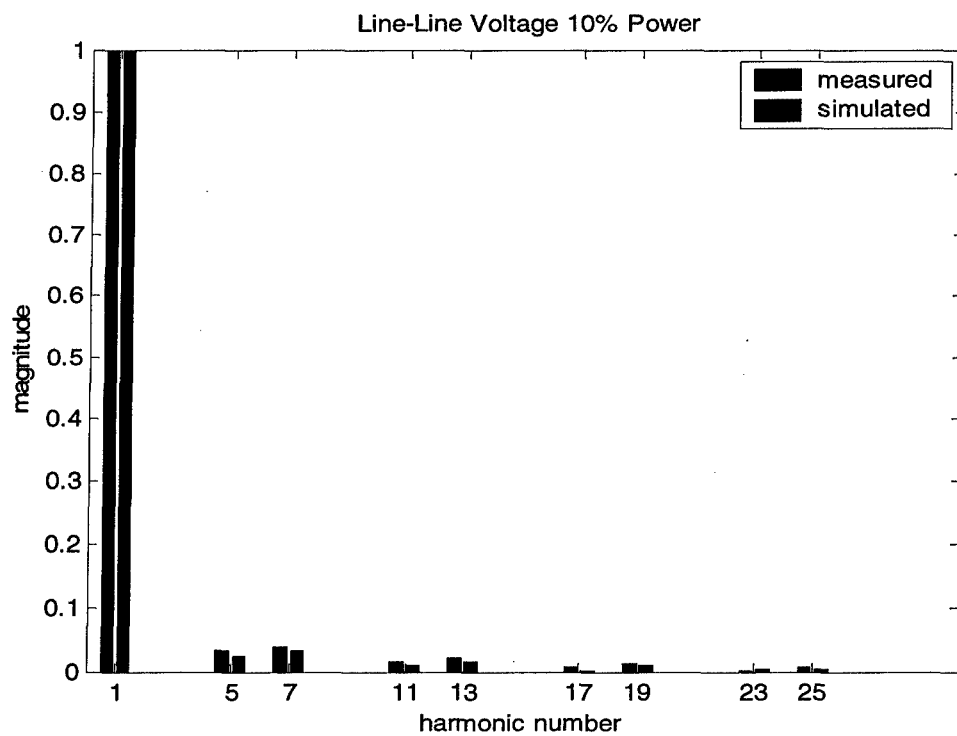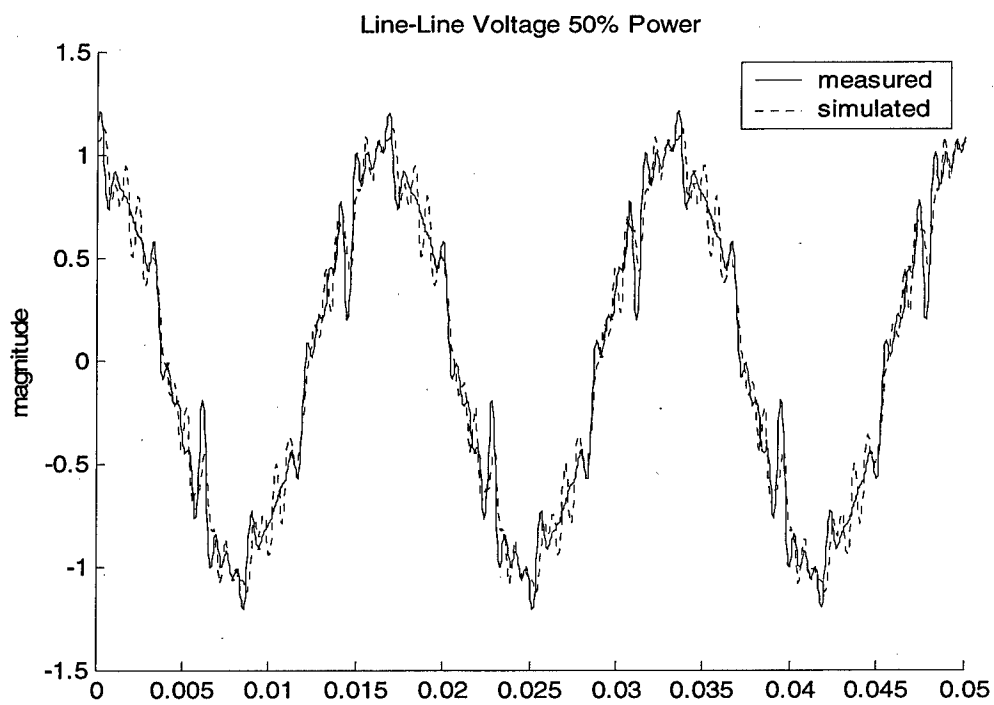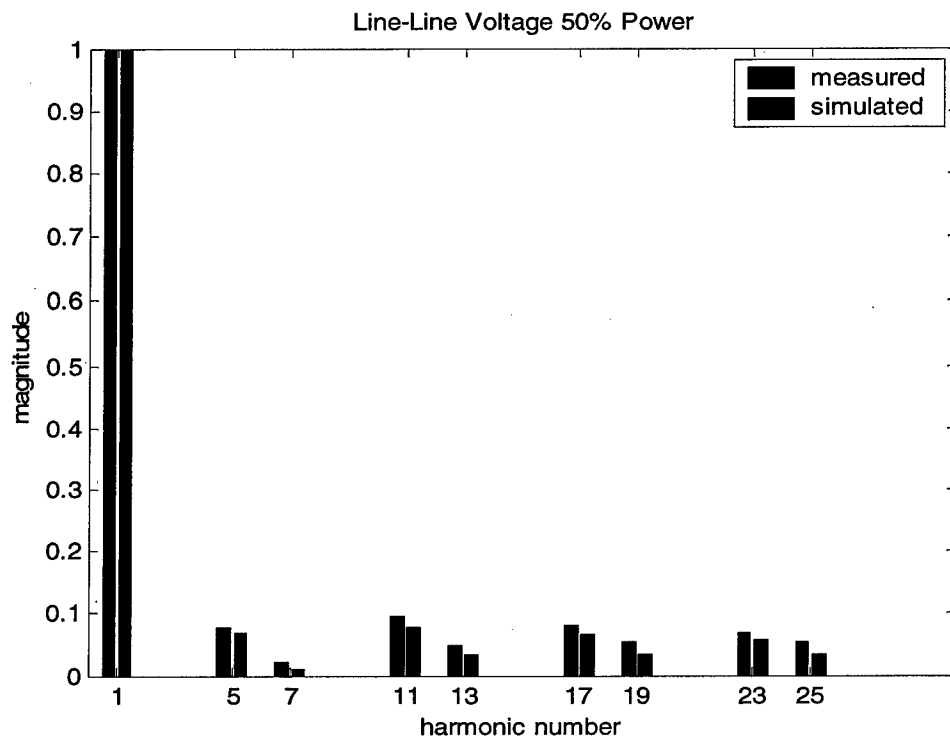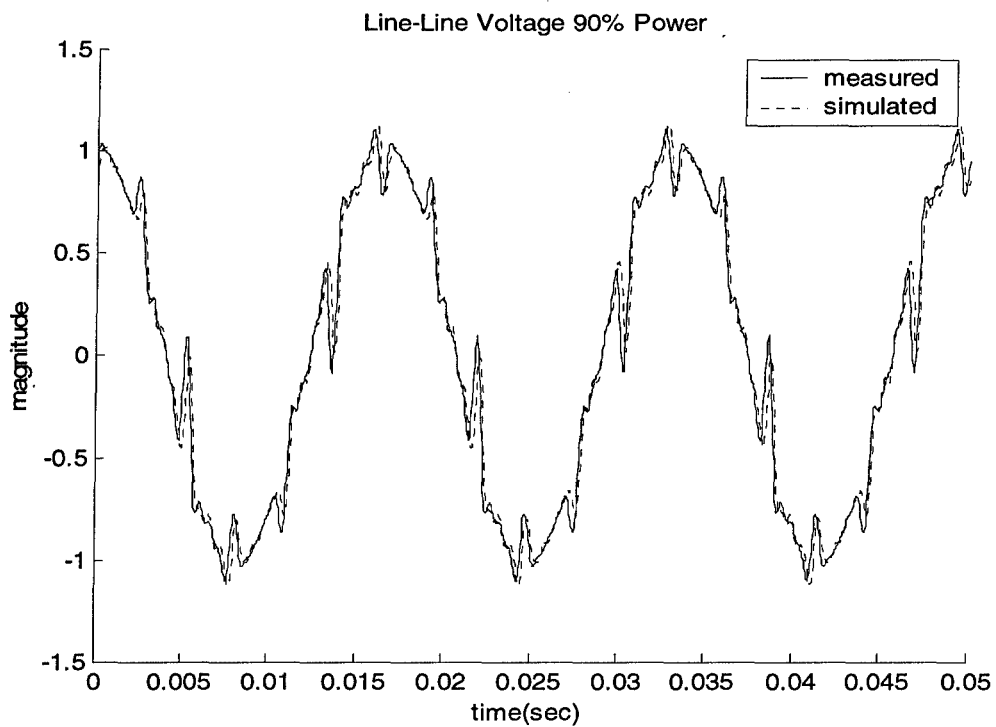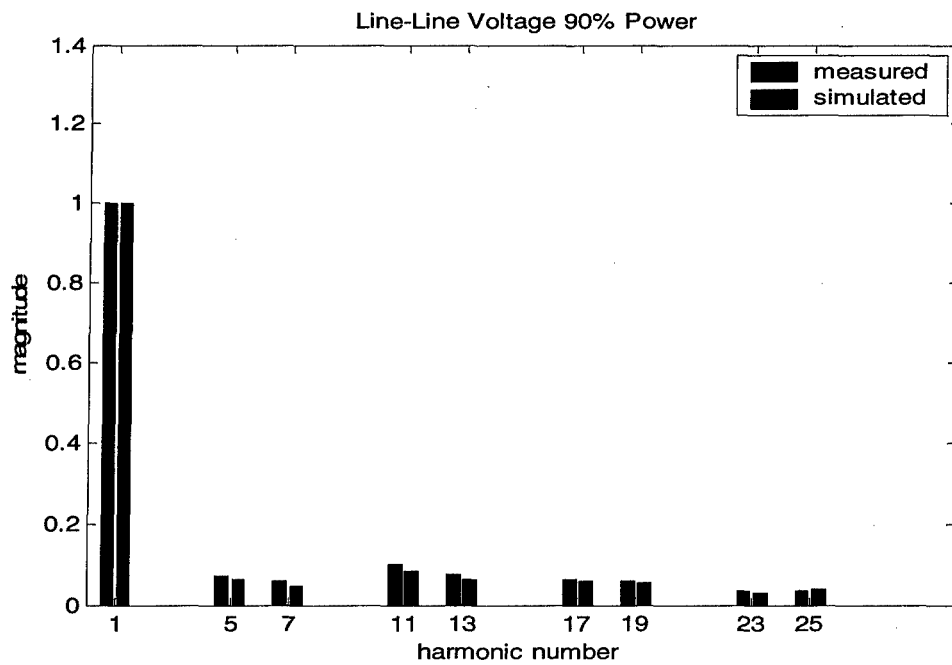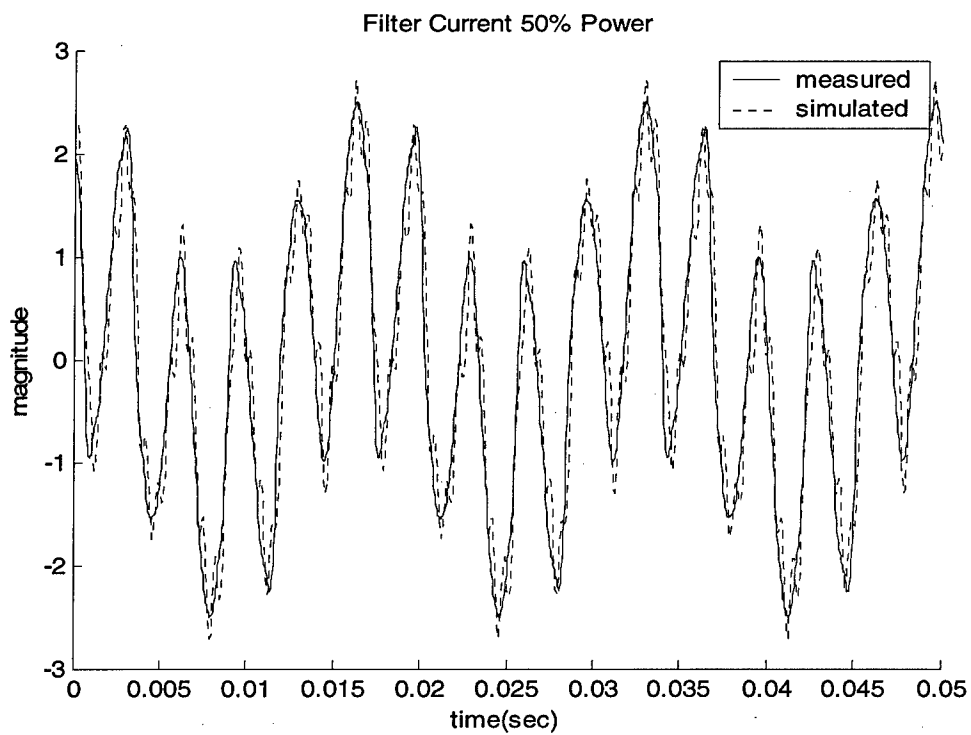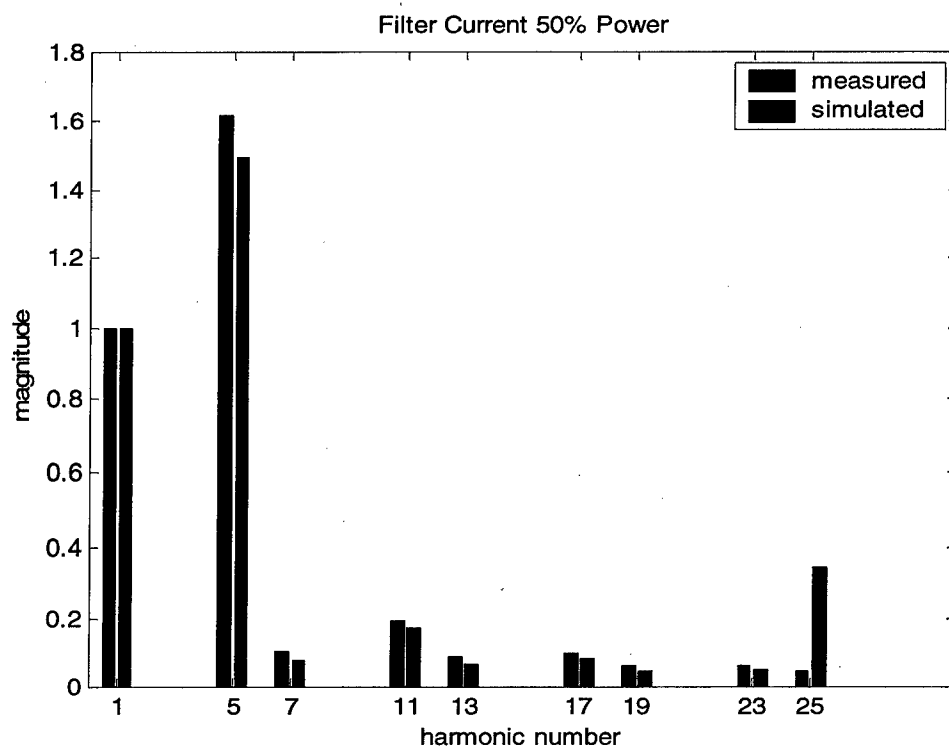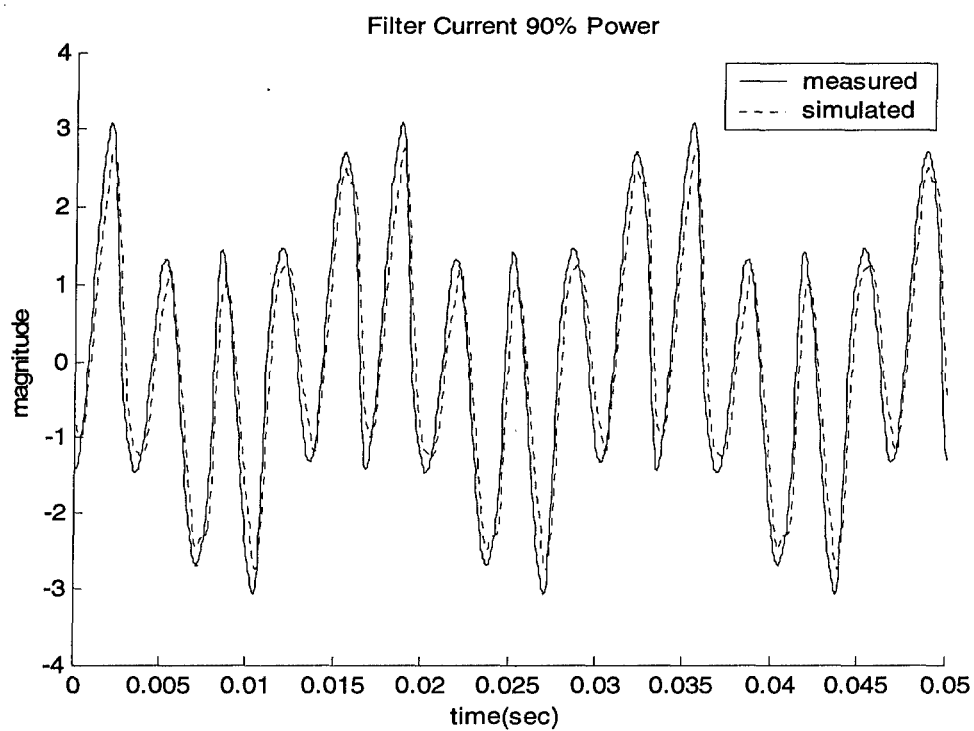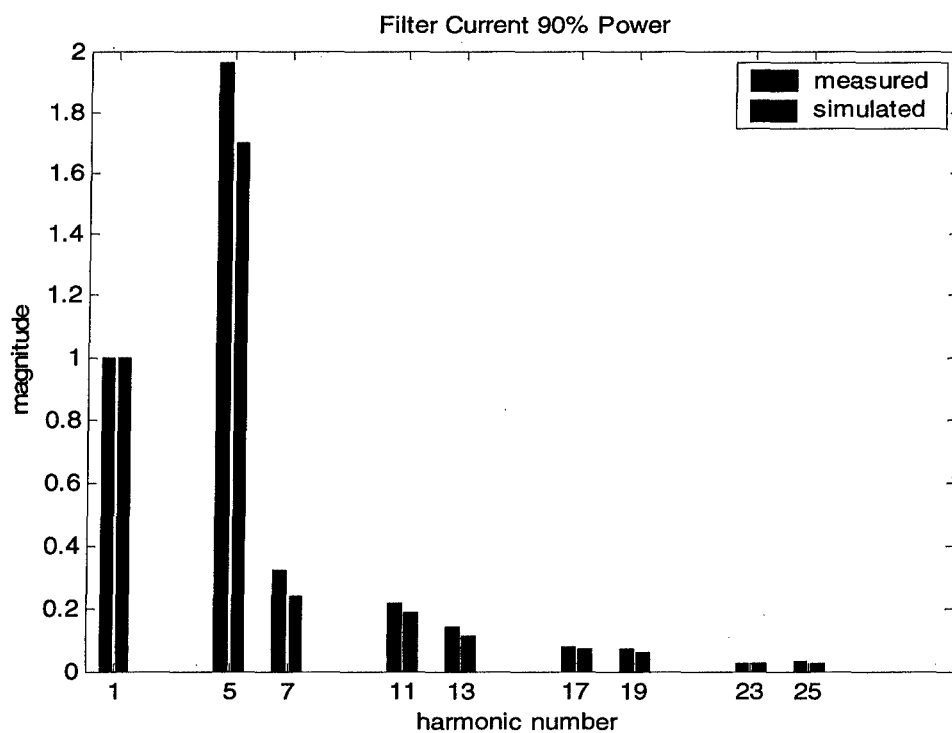
Appendix C. Tabulated Distortion Results

Table 8-2 Cruise Loading, 90 Degrees, Baseline System

Condition	Cruise
Temp	90
Speed	0

	Bus Voltage(Volts)	% of Fund	Gen Current (A)	% of Fund	Gen Current (kA)	% of Fund
1	436.56	100	753.28	100		
5	5.99	1.37209089	22.97	3.049331		
7	1.94	0.44438336	9.37	1.243893		
11	9.73	2.22878871	15.23	2.021825		
13	6.23	1.42706615	8.87	1.177517		
17	4.31	0.98726406	3.75	0.497823		
19	4.01	0.91854499	3.22	0.427464		
23	0.14	0.0320689	0.64	0.084962		
25	0.57	0.13056625	0.4	0.053101		
THD	3.30		4.09			

Condition	Cruise
Temp	90
Speed	15

	Bus Voltage(Volts)	% of Fund	Gen Current (A)	% of Fund	Gen Current (kA)	% of Fund
1	426.96	100	1376.27	100		
5	41.18	9.64493161	151.45	11.00438		
7	7.53	1.76363125	20.28	1.473548		
11	29.45	6.89760165	52.64	3.824831		
13	12.44	2.91362188	19.55	1.420506		
17	15.42	3.61157954	19.79	1.437945		
19	10.76	2.5201424	13.14	0.954755		
23	13.48	3.15720442	12.95	0.940949		
25	9.65	2.26016489	8.61	0.625604		
THD	13.54		11.92			

Condition	Cruise
Temp	90
Speed	25

	Bus Voltage(Volts)	% of Fund	Gen Current (A)	% of Fund	Gen Current (kA)	% of Fund
1	423.16	100	1369.92	100	3596.77	100
5	50.23	11.8702146	184.77	13.48765	539.54	15.00068
7	26.9	6.35693355	89.18	6.509869	264.77	7.361327
11	18.57	4.388411	39.58	2.88922	118.67	3.299349
13	11.44	2.70346914	30.91	2.256336	91.25	2.536998
17	6.99	1.65185745	12.52	0.913922	37.66	1.047051
19	14.26	3.36988373	8.02	0.585436	24.83	0.690342
23	0.75	0.17723792	1.09	0.079567	33.91	0.94279
25	0.11	0.0259949	2.11	0.154024	6.11	0.169875
THD	14.74		15.28		17.04	

Condition	Cruise
Temp	90
Speed	30

	Bus Voltage(Volts)	% of Fund	Gen Current (A)	% of Fund	Gen Current (kA)	% of Fund
1	433.84	100	1334.91	100	3723.09	100
5	46.43	10.9722091	182.49	13.32122	543.65	15.11495
7	33.98	8.03005955	96.05	7.011358	289	8.034987
11	12.22	2.88779658	28.2	2.058514	85.44	2.375465
13	10.28	2.42934115	18.83	1.374533	57.18	1.58976
17	2.48	0.58606674	1.89	0.137964	5.61	0.155973
19	5.57	1.31628698	4.72	0.344546	14.61	0.406198
23	6.85	1.61877304	7.72	0.563537	23.5	0.653364
25	7.25	1.71329993	7.17	0.523388	21.79	0.605821
THD	13.89		15.49		16.56	

Table 8-3 Cruise Loading, 10 Degree, Baseline System

Condition	Cruise
Temp	10
Speed	0

	Bus Voltage	% of Fund	Gen Current (A)	% of Fund	Gen Current (kA)	% of Fund
1	439.45	100	883.66	100		
5	7.06	1.60655365	28.03	3.17203449		
7	3.16	0.71908067	12.16	1.37609488		
11	8.71	1.98202298	14.16	1.60242627		
13	5.25	1.19467516	7.96	0.90079895		
17	4.57	1.03993628	4.17	0.47190096		
19	3.97	0.90340198	3.39	0.38363171		
23	1.11	0.25258846	0.75	0.08487427		
25	1.43	0.32540676	0.81	0.09166421		
THD	3.24		3.96			

Condition	Cruise
Temp	10
Speed	15

	Bus Voltage	% of Fund	Gen Current (A)	% of Fund	Gen Current (kA)	% of Fund
1	424.77	100	1506.89	100		
5	38.71	9.11316713	142.38	9.44859943		
7	5.58	1.31365209	15.58	1.03391754		
11	28.59	6.73070132	51.97	3.44882506		
13	12.39	2.91687266	19.85	1.31728262		
17	13.2	3.10756409	17.35	1.151378		
19	8.34	1.9634155	10.77	0.71471707		
23	12.59	2.96395696	12.48	0.82819582		
25	8.89	2.09289733	8.44	0.56009397		
THD	12.75		10.28			

Condition	Cruise
Temp	10
Speed	25

	Bus Voltage	% of Fund	Gen Current (A)	% of Fund	Gen Current (kA)	% of Fund
1	432.89	100	1374.29	100	3831.2	100
5	45.22	10.4460718	184.23	13.4054676	538.26	14.049384
7	30.48	7.04104969	88.11	6.41131057	261.26	6.81927333
11	17.29	3.99408626	38.49	2.80071892	114.98	3.00114847
13	16.92	3.9086142	28.89	2.1021764	86.34	2.253602
17	8.75	2.02129871	12.02	0.87463345	36.09	0.94200251
19	5.64	1.3028714	7.9	0.57484228	23.86	0.62278137
23	0.33	0.07623184	1.01	0.07349249	3.29	0.08587388
25	1.67	0.3857793	1.59	0.1156961	4.56	0.11902276
THD	13.86		15.13		15.90	

Condition	Cruise
Temp	10
Speed	30

	Bus Voltage	% of Fund	Gen Current (A)	% of Fund	Gen Current (kA)	% of Fund
1	431.1	100	1343.14	100	4083.56	100
5	45.93	10.6100857	181.36	13.1966324	543.38	14.1830236
7	32.47	7.50075077	95.34	6.9374004	284.72	7.43161412
11	11.75	2.71431542	26.78	1.94864257	82.28	2.14762999
13	9.74	2.24999422	18.16	1.3214096	54.38	1.41939862
17	2.19	0.50590219	2.42	0.17609093	7.38	0.19262894
19	5.1	1.17812839	4.66	0.33908418	13.72	0.35811234
23	6.37	1.47150546	7.31	0.53191102	22.79	0.59485279
25	6.42	1.48305574	6.67	0.48534152	19.59	0.51132804
THD	13.61		15.28		15.06	

Table 8-4 Battle Loading, 90 Degree, Baseline System

Condition	Battle					
Temp	90					
Speed	0					
	Bus Voltage(Volts)	% of Fund	Gen Current (A)	% of Fund	Gen Current (kA)	% of Fund
1	430.01	100	1120.02	100		
5	11.39	2.64877561	45.77	4.086534		
7	6.86	1.59531174	21.39	1.909787		
11	5.78	1.34415479	10.51	0.938376		
13	2.38	0.5534755	5.09	0.454456		
17	5.54	1.28834213	4.94	0.441064		
19	3.11	0.72323899	3.58	0.319637		
23	2.92	0.67905398	2.13	0.190175		
25	2.57	0.59766052	1.83	0.16339		
THD	3.83		4.66			

Condition	Battle					
Temp	90					
Speed	15					
	Bus Voltage(Volts)	% of Fund	Gen Current (A)	% of Fund	Gen Current (kA)	% of Fund
1	422.02	100	1743.29	100		
5	35.02	8.29818492	129.19	7.4107		
7	2.11	0.4999763	3.74	0.214537		
11	27.17	6.4380835	50.49	2.896248		
13	12.42	2.94298848	21.55	1.236168		
17	13.38	3.17046585	18.24	1.046298		
19	6.98	1.65395005	9.32	0.534621		
23	8.66	2.05203545	9.26	0.53118		
25	7.64	1.81034074	7.77	0.445709		
THD	11.73		8.14			

Condition	Battle					
Temp	90					
Speed	25					
	Bus Voltage(Volts)	% of Fund	Gen Current (A)	% of Fund	Gen Current (kA)	% of Fund
1	429.68	100	1425.58	100	4205.67	100
5	45.96	10.6963322	190.74	13.37982	545.06	12.96012288
7	30.58	7.11692422	90.27	6.33216	262.62	6.244427166
11	16.46	3.83075777	37.56	2.634717	110.47	2.626692061
13	15.41	3.58638987	27.92	1.958501	79.16	1.882220907
17	7.49	1.7431577	10.39	0.728826	30.56	0.726638086
19	4.33	1.00772668	6.34	0.444731	18.89	0.449155545
23	1.03	0.23971327	2.19	0.153622	6.57	0.156217678
25	1.68	0.39098864	2.17	0.152219	6.51	0.154791032
THD	13.89		15.02		14.61	

Condition	Battle					
Temp	90					
Speed	30					
	Bus Voltage(Volts)	% of Fund	Gen Current (A)	% of Fund	Gen Current (kA)	% of Fund
1	427.95	100	1430.28	100	3972.9	100
5	45.83	10.6660771	185.86	13.0375	553.42	13.15890215
7	31.94	7.43343884	95.05	6.667462	285.9	6.797965604
11	11.15	2.59495438	27.34	1.917816	82.6	1.964015246
13	8.77	2.04105381	16.46	1.154618	49.98	1.188395666
17	2.28	0.53062744	2.75	0.192904	8.36	0.198779267
19	5.14	1.19623906	5.45	0.382301	16.52	0.392803049
23	6.22	1.4475889	8.28	0.580816	25.11	0.597051124
25	5.88	1.36846025	6.56	0.460164	19.98	0.475072937
THD	13.55		14.63		15.70	

Table 8-5 Battle Loading, 10 Degrees, Baseline System

Condition	Battle					
Temp	90					
Speed	0					
	Bus Voltage(Volts)	% of Fund	Gen Current (A)	% of Fund	Gen Current (kA)	% of Fund
1	436.25	100	805.93	100		
5	7.34	1.682521	28.99	3.597087		
7	3.29	0.754155	12.48	1.548522		
11	9.2	2.108883	14.76	1.831425		
13	5.57	1.276791	8.25	1.023662		
17	4.97	1.139255	4.56	0.565806		
19	4.38	1.004011	3.73	0.462819		
23	1.25	0.286533	0.88	0.109191		
25	1.67	0.382808	0.96	0.119117		
THD	3.46		4.50			

Condition	Battle					
Temp	90					
Speed	15					
	Bus Voltage(Volts)	% of Fund	Gen Current (A)	% of Fund	Gen Current (kA)	% of Fund
1	426.54	100	1426.47	100		
5	39.94	9.363717	145.61	10.20772		
7	5.92	1.387912	15.78	1.106227		
11	30.18	7.075538	53.66	3.761734		
13	13.04	3.057158	20.09	1.408372		
17	14.52	3.404136	18.47	1.294805		
19	9.35	2.192057	11.53	0.808289		
23	13.99	3.27988	13.18	0.923959		
25	10.09	2.365546	9.08	0.636536		
THD	13.36		11.12			

Condition	Battle					
Temp	90					
Speed	25					
	Bus Voltage(Volts)	% of Fund	Gen Current (A)	% of Fund	Gen Current (kA)	% of Fund
1	435.14	100	1376.41	100	3684.71	100
5	45.98	10.56671	185.86	13.50324	542.87	14.73305
7	30.93	7.108057	89.21	6.481354	264.75	7.185097
11	17.77	4.083743	38.64	2.807303	115.81	3.142988
13	17.55	4.033185	29.36	2.133085	88.19	2.393404
17	8.81	2.024636	11.89	0.863841	35.74	0.969954
19	5.79	1.330606	7.92	0.57541	23.82	0.646455
23	0.18	0.041366	1.17	0.085004	3.59	0.09743
25	0.24	0.055155	1.71	0.124236	5.21	0.141395
THD	14.04		15.24		16.67	

Condition	Battle					
Temp	90					
Speed	30					
	Bus Voltage(Volts)	% of Fund	Gen Current (A)	% of Fund	Gen Current (kA)	% of Fund
1	433.42	100	1416.16	100	3668.44	100
5	46.36	10.65404	183.86	13.35794	547.19	14.85029
7	32.89	7.558487	95.19	6.915817	286.15	7.765876
11	11.86	2.72556	27.85	2.02338	84.33	2.288647
13	10.06	2.3119	17.81	1.293946	54.13	1.469044
17	2.24	0.514777	23.23	1.687724	7.01	0.190246
19	5.32	1.222595	5.13	0.372709	15.43	0.418758
23	6.16	1.415636	8.08	0.587034	24.45	0.663553
25	6.66	1.530542	6.65	0.483141	20.23	0.549026
THD	13.69		14.76		16.84	

Table 8-6 Anchor Loading, Baseline System

Condition	Anchor
Temp	90
Speed	0

	Bus Voltage(Volts)	% of Fund	Gen Current (A)	% of Fund	Gen Current (kA)	% of Fund
1	442.88	100	835.95	100		
5	7.35	1.659592	27.83	3.32914648		
7	3.61	0.815119	10.42	1.246486034		
11	10.16	2.294075	16.67	1.994138405		
13	5.34	1.205744	7.9	0.945032598		
17	2.89	0.652547	2.75	0.328967043		
19	2.82	0.636741	2.57	0.307434655		
23	1.95	0.4403	1.78	0.212931395		
25	1.43	0.322887	1.39	0.166277887		
THD	3.35		4.21			

Condition	Anchor
Temp	10
Speed	0

	Bus Voltage(Volts)	% of Fund	Gen Current (A)	% of Fund	Gen Current (kA)	% of Fund
1	439.98	100	843.69	100		
5	7.59	1.725078	28.59	3.388685418		
7	3.53	0.802309	10.34	1.225568633		
11	10.01	2.275103	16.63	1.97110313		
13	5.31	1.206873	7.82	0.926880726		
17	2.86	0.65003	2.76	0.327134374		
19	2.85	0.647757	2.58	0.305799524		
23	1.88	0.427292	1.73	0.205051618		
25	1.35	0.306832	1.28	0.151714492		
THD	3.37		4.24			

Table 8-7 Line Commutated System, 90 Degree Day, Cruise Loading

Condition	Cruise
Temp	90
Speed	15

	Bus Voltage(Volts)	% of Fund	Gen Current (A)	% of Fund	Gen Current (A)	% of Fund
1	442.22	100	1189.59	100		
5	21.93	4.95907	96.12	8.080095		
7	11.72	2.650265	37.61	3.161593		
11	14.88	3.364841	24.58	2.066258		
13	9.98	2.256795	14.93	1.255054		
17	1.83	0.413821	0.74	0.062206		
19	1.27	0.287187	0.25	0.021016		
23	3.63	0.820858	2.76	0.232013		
25	3.56	0.805029	2.53	0.212678		
THD	7.03		8.98			

Condition	Cruise
Temp	90
Speed	25

	Bus Voltage(Volts)	% of Fund	Gen Current (A)	% of Fund	Gen Current (A)	% of Fund
1	441.32	100	1378.92	100	2886.83	100
5	36.52	8.275174	140.28	10.17318	409.58	14.18788
7	21.06	4.772047	71.04	5.151858	210.75	7.300395
11	8.64	1.957763	19.17	1.390218	57.42	1.989033
13	1.91	0.432793	11.03	0.799901	33.2	1.15005
17	6.81	1.543098	9.52	0.690395	28.81	0.99798
19	2.82	0.638992	7.99	0.579439	24.15	0.836558
23	2.79	0.632194	5.17	0.374931	15.62	0.541078
25	1.13	0.25605	3.96	0.287181	11.91	0.412563
THD	9.88		11.48		15.98	

Condition	Cruise
Temp	90
Speed	30

	Bus Voltage(Volts)	% of Fund	Gen Current (A)	% of Fund	Gen Current (A)	% of Fund
1	443.14	100	1366.22	100	3198.88	100
5	33.95	7.661236	141.01	10.32118	419.92	13.12709
7	22.76	5.136074	68.05	4.980896	204.78	6.401616
11	2.82	0.636368	9.92	0.726091	30.16	0.94283
13	5.21	1.175701	8.82	0.645577	26.83	0.838731
17	6.74	1.520964	9.56	0.699741	29.87	0.933764
19	4.35	0.981631	6.34	0.464054	19.2	0.60021
23	3.01	0.679244	2.78	0.203481	8.45	0.264155
25	2.35	0.530306	2.81	0.205677	8.55	0.267281
THD	9.49		11.46		14.55	

Table 8-8 Filter System Tabulated Results

Condition	Cruise
Temp	90
Speed	15

	Bus Voltage(Volts)	% of Fund	Gen Current (A)	% of Fund	Gen Current (A)	% of Fund
1	435.97	100	1283.73	100		
5	2.52	0.578021	1.29	0.100488		
7	2.49	0.57114	5.53	0.430776		
11	18.22	4.179187	31.85	2.481051		
13	6.88	1.57809	10.7	0.833509		
17	8.67	1.988669	11.6	0.903617		
19	2.6	0.596371	4.09	0.318603		
23	8.2	1.880863	8.56	0.666807		
25	6	1.376241	5.55	0.432334		
THD	5.50		2.93			

Condition	Cruise
Temp	90
Speed	25

	Bus Voltage(Volts)	% of Fund	Gen Current (A)	% of Fund	Gen Current (A)	% of Fund
1	436	100	1378.92	100	2886.83	100
5	5.98	1.37156	140.28	10.17318	409.58	14.18788
7	20.12	4.614679	71.04	5.151858	210.75	7.300395
11	17.29	3.965596	19.17	1.390218	57.42	1.989033
13	26.47	6.071101	11.03	0.799901	33.2	1.15005
17	11.25	2.580275	9.52	0.690395	28.81	0.99798
19	9.07	2.080275	7.99	0.579439	24.15	0.836558
23	6.56	1.504587	5.17	0.374931	15.62	0.541078
25	4.88	1.119266	3.96	0.287181	11.91	0.412563
THD	9.46		11.48		15.98	

Condition	Cruise
Temp	90
Speed	30

	Bus Voltage(Volts)	% of Fund	Gen Current (A)	% of Fund	Gen Current (A)	% of Fund
1	432.14	100	1366.22	100	3198.88	100
5	5.99	1.386125	141.01	10.32118	419.92	13.12709
7	28.45	6.583515	68.05	4.980896	204.78	6.401616
11	14.56	3.369278	9.92	0.726091	30.16	0.94283
13	11.25	2.603323	8.82	0.645577	26.83	0.838731
17	14.37	3.325311	9.56	0.699741	29.87	0.933764
19	3.21	0.742815	6.34	0.464054	19.2	0.60021
23	5.22	1.207942	2.78	0.203481	8.45	0.264155
25	5.9	1.365298	2.81	0.205677	8.55	0.267281
THD	8.82		11.46		14.55	

Table 8-9 12 Pulse System Tabulated Results

Condition	Cruise
Temp	90
Speed	15

	Bus Voltage(Volts)	% of Fund	Gen Current (A)	% of Fund	Gen Current (A)	% of Fund
1	443.98	100	1254.38	100		
5	5.47	1.232037	22.45	1.789729		
7	1.55	0.349115	8.95	0.7135		
11	19.54	4.401099	32.98	2.629187		
13	13.64	3.07221	19.98	1.592819		
17	4.02	0.905446	3.93	0.313302		
19	4.22	0.950493	3.64	0.290183		
23	4.66	1.049597	5.17	0.412156		
25	4.42	0.99554	4.36	0.347582		
THD	5.84		3.69			

Condition	Cruise
Temp	90
Speed	25

	Bus Voltage(Volts)	% of Fund	Gen Current (A)	% of Fund	Gen Current (A)	% of Fund
1	429.4	100	1019.66	100	3734.27	100
5	3.97	0.924546	13.24	1.298472	25.53	0.683668
7	0.4	0.093153	5.58	0.547241	7.08	0.189595
11	26.2	6.101537	44.03	4.318106	137.67	3.686664
13	20.45	4.762459	30.39	2.980405	92.63	2.480538
17	2.07	0.482068	2.67	0.261852	4.15	0.111133
19	2.52	0.586865	2.55	0.250083	3.96	0.106045
23	4.18	0.973451	3.37	0.330502	12.24	0.327775
25	4.15	0.966465	4.12	0.404056	11.04	0.29564
THD	7.93		5.46		4.52	

Condition	Cruise
Temp	90
Speed	30

	Bus Voltage(Volts)	% of Fund	Gen Current (A)	% of Fund	Gen Current (A)	% of Fund
1	440.87	100	1302.76	100	3515.63	100
5	3.38	0.766666	8.04	0.617151	19.87	0.56519
7	0.78	0.176923	2.8	0.214928	5.77	0.164124
11	24.75	5.6139	42.36	3.251558	13.02	0.370346
13	17.26	3.914986	26.75	2.053333	78.87	2.24341
17	1.96	0.444575	1.69	0.129725	2.97	0.08448
19	2.25	0.510355	0.53	0.040683	3.52	0.100124
23	8.23	1.866763	8.94	0.686235	2.57	0.073102
25	7.65	1.735205	6.88	0.52811	2.22	0.063147
THD	7.36		3.99		2.35	